SOLID STATE ABSTRACTS

an abstract journal devoted to the theory, production and use of solid state materials and devices

VOLUME 1 NUMBER 5

PHYSICS

METALLURGY

ELECTRONICS

METALS

SEMICONDUCTORS

SUPERCONDUCTORS

PHOSPHORS

MAGNETICS

DIELECTRICS

SOLID STATE ABSTRACTS

VOLUME 1, NUMBER 5

February, 1961

Abstracts 7226–7544

TABLE OF CONTENTS

Abstracts of the Solid State Literature

Conference Programs Abstracted in Solid State Abstracts, Vol. 1, No. 5; see page 271

Editor: GEOFFREY KNIGHT, JR.

Assistant Editor: MYRON A. COHEN

PUBLISHED MONTHLY BY

Cambridge Communications Corporation, 238 Main Street, Cambridge 42, Massachusetts, Tel. Klrkland 7-1997

Subscription Rate: $25.00 per year. Single Copies and Back Issues: $2.50. Advertising Rates on Request.

Cambridge Communications Corp. is not prepared to furnish copies of the articles abstracted. However, there are many libraries throughout the country which maintain photocopying services.

SYMBOLS USED IN THE ABSTRACTS

L: Letter to the Editor. A: Only an abstract is given in the reference. R: Only a review is given in the reference. E: Erratum.

The reference numbers in the indices are the abstract numbers, not the page numbers.

Second-class mail privileges applied for at Boston, Massachusetts.

ABSTRACTS OF THE SOLID STATE LITERATURE

METALLURGY AND CHEMISTRY OF SOLIDS

SOLID STATE REACTIONS

226 SOLID STATE REACTIONS OF OXYGEN IN SILICON H. Reiss and W. Kaiser (Bell Labs.); Properties of Elemental and Compound Semiconductors, (Interscience), pp. 103-119, 960

me reactions of oxygen in silicon are reviewed. The discus-on is mainly concerned with three well-investigated subjects: e precipitation of lithium in oxygen containing silicon, the lymerization reaction of oxygen during a heat treatment at veral hundred degrees centigrade, and the effect of group III purities on this reaction.

227 REACTIONS OF LITHIUM AS A DONOR AND AN AC-EPTOR IN ZnO by J. J. Lander (Bell Labs.); J. Phys. Chem. lids, Vol. 15, pp. 324-334, Oct. 1960

actions of oxidized lithium with ZnO have been investigated means of conductivity measurements. Donors are formed in nO if the atmosphere surrounding the crystal is reducing. The nor center is probably the molecular ion $LiO^{=}$. Oxidizing nditions favor an acceptor center presumably obtained by splacement of a lattice zinc atom by lithium. Solubilities d diffusion coefficients have been measured and some results e reported for the kinetics and equilibria of the displacement action. High temperatures favor displacement. In one atmos-ere of oxygen the Fermi level, which is normally near the p of the 3.0 ev band gap, can be pushed down to the center the band gap. Impractically high oxygen pressures would be quired to produce strongly p-type material. The precipita-on of lithium on dislocations and their decoration were also udied.

ALLOYS

228 USE OF THE ELECTRON PROBE X-RAY MICROANALY-ER IN THE STUDY OF SEMICONDUCTOR ALLOYS by D. B. ttry (California Inst. Tech.); J. M. Axelrod and J. O. Mc-ldin (Hughes Semicon.); Properties of Elemental and Compound Semiconductors (Interscience), pp. 89-100, 1960

The electron probe microanalyzer permits a quantitative chemical analysis of a few cubic microns of volume by means of x-ray emission spectra excited by a focused electron beam. Use of this new analytical tool to study semiconductor alloys is reported. Applications for which the concentrations are sufficiently high to permit accurate quantitative analysis include determination of diffusion coefficients, measurement of solubility limits, investigation of the interactions of dopants, and identification of phases. The following investigations are described: (a) diffusion of zinc in gallium arsenide, (b) diffusion of arsenic in germanium and in germanium regrown from solution in aluminum, (c) determination of the solubility of gallium in germanium, and (d) identification of phases formed during attachment of leads to silicon transistors. In these investigations, the electron probe microanalyzer was found to give a precision comparable to that of less convenient methods of analysis and a sensitivity of about two parts in 10^4.

7229 METALLURGY OF SOME TERNARY SEMICONDUCTORS AND CONSTITUTION OF THE $AgSbSe_2$-$AgSbTe_2$-$AgBiSe_2$-PbSe-PbTe SYSTEM by J. H. Wernick (Bell Labs.); Properties of Elemental and Compound Semiconductors, (Interscience), pp. 69-88, 1960

Metallurgical techniques employed in the preparation of some semiconducting ternary compounds are discussed. Some electrical and thermal properties are presented. In addition, six pseudo-binary phase diagrams in the semiconducting pseudo-quinary system, $AgSbSe_2$-$AgSbTe_2$-$AgBiSe_2$-PbSe-PbTe, have been determined. A complete series of solid solutions with the disordered NaCl-type structure exists in this system. The locus of temperatures and compositions for the order-disorder transition has been determined. Lattice constants as a function of composition for the cubic phase are also presented. The valence electron to atom ratio increases from 4-1/2 to 5 in going from the ternary to the binary compound, and large negative deviations from Vegard's law occur in all but the $AgSbTe_2$-PbSe system. A positive deviation occurs in the $AgSbTe_2$-PbSe system. Possible reasons for these deviations are discussed.

Phase Diagrams of $I^bInVI_2^b$ and $II^bIn_2VI_4^b$ Alloys - See 7274

7230 EFFECTS OF SOLID SOLUTION OF Ga_2Te_3 WITH $A^{II}B^{VI}$ TELLURIDES by J. C. Woolley and B. Ray (U. Nottingham); J. Phys. Chem. Solids, Vol. 16, pp. 102-106, Nov. 1960

Alloys have been produced for the three systems Ga_2Te_3-ZnTe, Ga_2Te_3-CdTe and Ga_2Te_3-HgTe and annealed to obtain equilibrium conditions. The ranges of solid solution, the variation

of lattice parameter with composition and the ranges and types of ordering which occur are discussed. For the system Ga_2Te_3-ZnTe, the variation of optical energy gap E_g with composition has been determined by infrared transmission measurements.

7231 SOLID SOLUTIONS OF InTe AND CdTe IN PbTe AND SnTe by A. J. Rosenberg (Lincoln Lab.); J. Electrochem. Soc., Vol. 107, p. 269C (A), Dec. 1960

Preparation of single crystals of the compositions $Pb_{.97}In_{.03}Te$, $Pb_{.91}Cd_{.09}Te$, $Sn_{.97}In_{.03}Te$, and $Sn_{.92}Cd_{.08}Te$ is reported. The crystals have the rock-salt structure type characteristic of PbTe and SnTe, but with smaller lattice parameters than the pure compounds. The macroscopic densities agree with the values calculated on the assumption that Cd and In replace Pb and Sn. Despite the fact that the concentrations of valence electrons in PbTe and SnTe are reduced by as much as $3 \times 10^{22}/cm^3$ by these substitutions, the magnitude of the free charge carrier concentration remains unaffected in every case. The general significance of these results is discussed.

Solid Solutions of InSb and In_2Te_3 - See 7323

Solid Solutions of $NaNbO_3$ and $PbZrO_3$ - See 7293

Solid Solutions of Semiconductors with Deviations from Stoichiometry - See 7401

Solubility of Li in ZnO - See 7227

7232 DISTRIBUTION COEFFICIENTS OF IMPURITIES DISTRIBUTED BETWEEN Ge OR Si CRYSTALS AND TERNARY ALLOYS OR SURFACE OXIDES by C. D. Thurmond (Bell Labs.); Properties of Elemental and Compound Semiconductors, (Interscience); pp. 121-140, 1960

The binary distribution coefficients of a number of elements in Ge and Si as a function of temperature are used to estimate the distribution coefficients of these elements in ternary alloys and in semiconductor-oxide systems. A number of group III-V elements are sufficiently soluble in Ge and Si to make the semiconductor extrinsic at the saturation temperature over a wide temperature range. As a consequence of this fact, the ternary distribution coefficient of such an element, diluted by a third component, will be substantially larger than would have otherwise been expected.

7233 DISTRIBUTION COEFFICIENTS OF VARIOUS IMPURITIES IN GALLIUM ARSENIDE by J. M. Whelan, J. D. Struthers, and J. A. Ditzenberger (Bell Labs.); Properties of Elemental and Compound Semiconductors, (Interscience); pp. 141-154, 1960

The distribution coefficient, k, of Fe, Cu, Ge, Si, S, Se, Te, Zn, and Cd in GaAs is discussed. Impurities were distributed by floating zone refining and their concentrations measured with the aid of radioactive tracer techniques. The following values were obtained: Fe, 0.003; Cu, <0.002; Ge, 0.01_8; Si, 0.1_4; S, $1.0>k>0.5$; Se, $0.5_5>k>0.4_4$; Te, $0.1_6>k>0.05_4$; Zn, $0.9>k>0.2_7$; and Cd, <0.2. Germanium and silicon are self-compensating donors in GaAs. The ratio of electron concentration to Ge concentration, n/Ge, is 0.2 for a Ge concentration of $1.5 \times 10^{18} cm^{-3}$. The ratio, n/Si, is 0.7 and 0.2 for Si concentrations of 9.4×10^{17} and $1.6 \times 10^{19} cm^{-3}$, respectively.

Changes in Lattice Parameters Due to Crystal Imperfections - See 7237, 7238, 7241

7234 COLOUR CENTRES IN X-IRRADIATED ALKALI METAL AZIDES by H. G. Heal and J. P. S. Pringle (U. Brit. Columbia); J. Phys. Chem. Solids, Vol. 15, pp. 261-269, Oct. 19

Absorption bands produced in the alkali metal azides by x-irradiation at liquid nitrogen and room temperatures are discussed. Sodium, potassium, rubidium and cesium azides x-irradiated at liquid nitrogen temperature develop F bands, oth absorption bands at longer wavelength, ascribed to electron surplus centers, and V bands in the ultraviolet. At room temperature, sodium azide gives a broad band in the ultraviolet ascribed to photo-emission by sodium metal and potassium develops two bands in the red ascribed to R centers. Cesium and rubidium azides develop broad structured bands in the ultraviolet of undetermined origin.

7235 SPONTANEOUS GENERATION OF COLOR CENTERS IN IRRADIATED ALKALI HALIDE CRYSTALS AFTER ANNEALING by A. A. Vorob'ev and B. V. Budylin; Soviet Phys.-Solid State, Vol. 2, pp. 615-616, Oct. 1960

Color centers spontaneously created in NaCl, KCl, KBr, and KI crystals by irradiating the crystals in a reactor and then annealing them until they were again transparent to visible light are discussed. The creation of the color centers is caused by interaction between radioactive sources created within the crystal due to irradiation in the reactor and the crystal materi A method of bulk irradiation of the above-mentioned material by non-penetrating types of radiation is proposed.

7236 LOW-TEMPERATURE BLEACHING OF F CENTERS IN KCl by A. R. Reinberg and L. I. Grossweiner (Illinois Inst. Tech.); Bull. Am. Phys. Soc., Ser. II, Vol. 5, p. 423 (A), Nov. 25, 1960

Bleaching of F centers in x-rayed and additively colored KCl crystals at 77°K was discussed. Steady "F light" incident on the crystal establishes a photostationary equilibrium between F and F' centers. The application of additional light in the form of a 20-μsec pulse of high intensity displaces the system from equilibrium, to which it returns in a time varying with th steady light intensity. This displacement may be to higher F or F' center concentration depending on the spectral distribution of the light pulse. The quantum efficiency for the initial flash-induced change depends on the method of coloration and previous sample history. The lowest values are obtained for additively colored crystals and crystals which have been previously bleached with "F light" at room temperature. The return to equilibrium follows first-order kinetics, where the rate constant is independent of all factors except previous room temperature bleaching.

7237 VOLUME CHANGES AND COLOR CENTERS PRODUCED BY X-RAYS IN NaCl AT LOW TEMPERATURES by S. Mascarenhas, D. A. Wiegand (Carnegie Inst. Tech.), and R. Smolucho ski (Princeton U.); Bull. Am. Phys. Soc., Ser. II, Vol. 5, p. 422 (A), Nov. 25, 1960

Measurements of the volume expansion of x-ray irradiated NaC from 15° to 90°K and the optical behavior of the irradiated

rystal from 15° to 300°K was discussed. An improved photo-lastic method was used and the strain profiles obtained agree vith the shape predicted by the linear theory. Slow cooling 10°C per hr) is essential to minimize background strain. wenty-four hours of irradiation by 45 kv, 30 mA x-rays at 15°K roduces $\Delta V/V$ of the order of 10^{-5}. This volume increase does ot anneal up to 80°K. In contrast, the F band shows in this ange three stages of annealing and three more between 80°K nd 300°K. Growth curves of the F band and of the 343 mμ and were made at 15°K. Annealing at 80°K followed by re-rradiation at 15°K indicates that these bands recover quickly. Comparison with results on KCl and KBr indicate that the F enters are annihilated by hole capture. It follows also that in he range 15° to 80°K electronic changes do not lead to volume hanges greater than the experimental error, $\Delta V/V \sim 10^{-6}$.

7238 ANNEALING OF VOLUME EXPANSION AND OF THE BAND IN X-RAY IRRADIATED LiF by D. A. Wiegand, S. Mascarenhas (Carnegie Inst. Tech.), and R. Smolochowski Princeton U.); Bull. Am. Phys. Soc., Ser. II, Vol. 5, pp. 422-23 (A), Nov. 25, 1960

t has been shown previously that the $\Delta V/V$ and F-center rowth curves in LiF obtained at 80°K anneal out partially ear 130°K. Upon re-irradiation at 80°K the F-center curve ecovers quickly while the $\Delta V/V$ curve does not recover. In he present study a second annealing stage of $\Delta V/V$ and of the band was found near room temperature. In contrast to the 30°K stage upon re-irradiation at 80°K neither the growth urve of $\Delta V/V$ or of the F band recovers. The low-temperature nnealing was found to be smaller than in the previous work, resumably because of different crystal purity. The irreversi-ility of the room-temperature annealing indicates the presence f defect recombination in contrast to the low-temperature stage.

7239 COLOR CENTERS IN CESIUM HALIDE SINGLE CRYS-ALS by P. Avakian and A. Smakula (MIT); Phys. Rev., Vol. 20, pp. 2007-2014, Dec. 15, 1960

Color centers in cesium chloride, bromide, and iodide single rystals grown from the melt and in cesium chloride crystals rown from solution are discussed. Coloration was produced by 30-kv x-rays, 3.0-Mev electrons, and by electrolysis. In CsI oloration resulted from electrolysis only. The absorption of ncolored and colored crystals was measured from 0.175 to 3.5μ t 25°, −78°, and −190°C. After coloration all three crystals how one strong band in the visible (near infrared for CsI) and everal weaker bands at shorter and longer wavelengths, which hift with temperature change. The spectral positions for a num-er of the bands at −190°C are given. The strongest band (λ_6) ehaves similarly to the F band in the NaCl-type alkali halides. he half-width of the band (0.20 to 0.23 ev at −190°C) and its ncrease with temperature, the shifting of the band maximum oward longer wavelengths upon warming to room temperature by ~0.08 ev), and the conversion by bleaching with light into ther bands support the assignment of this band as the F band. he spectral position of the band maximum approximately fol-ows the Mollwo relation ($\lambda_{max} = \text{const } d^n$, where d = interionic istance and n = 2.5). Bleaching experiments suggest the as-gnment of the band λ_{10} as the M band and the bands between he F and M bands as R bands. The origin of the ultraviolet ands is still uncertain.

7240 THEORY OF VACANCY ANNEALING IN IMPURE METALS by A. C. Damask and G. J. Dienes (Brookhaven Nat'l Lab.); Phys. Rev., Vol. 120, pp. 99-104, Oct. 1, 1960

Analog computer solutions of the general equations for the annealing of vacancies in metals containing impurities to which the vacancies can be attached are presented. The computer results show that some simplifying assumptions may be made which permit the general equations to be solved analytically. It is shown that for many physically interesting cases of vacancy migration the decay curve is exponential, and the decay constant is related to, but not equal to, the rate constant for vacancy migration. It is further shown that only experiments performed on zone-refined metals can give the correct vacancy migration energy, and that impurity contents as low as 10^{-5} can seriously affect the results. Experimental methods and calculations which can be used to measure the binding energy of vacancies to impurities in metals prepared by controlled doping are discussed.

7241 CHANGES IN MACROSCOPIC SHAPE, LATTICE PARAMETER, AND DENSITY IN CRYSTALS DUE TO POINT DEFECTS by R. W. Balluffi and R. O. Simmons (U. Illinois); J. Appl. Phys., Vol. 31, pp. 2284-2288, Dec. 1960

It is shown that a crystal of arbitrary shape filled with a fine random distribution of centers of dilatation will dilate homogeneously. No elastic approximations are made, and the results should hold for strains of any magnitude. By use of an average and perfect reference lattice embedded in the strained crystal, it is then shown that the lattice dilatation as measured by x-ray lattice parameter measurements and by macroscopic dimensional measuremements should be the same along any direction when the number of substitutional atomic sites remains constant. Perturbing effects due to x-ray diffuse scattering should cause negligible error in determining the positions of the Laue-Bragg maxima under usual conditions. All results should apply also to the case of thermal dilatation at temperatures up to the melting point. The use of density measurements in the determination of point defect concentrations is discussed and experimental data are reviewed.

Correlation Between Etch Pits and Edge Dislocations in GaAs - See 7244

Precipitation of Li on Dislocations in ZnO - See 7227

7242 GOLD-INDUCED CLIMB OF DISLOCATIONS IN SILICON by W. C. Dash (GE); J. Appl. Phys., Vol. 31, pp. 2275-2283, Dec. 1960

Studies made of the climb of dislocations in silicon crystals induced by the diffusion of gold in the temperature range from 1000°C to 1300°C are discussed. For some studies, dislocations were introduced into previously dislocation-free crystals by indentation at room temperature and deformation at about 900°C in order to predetermine both Burgers vector and the direction of deformation. It was possible in this way to introduce left-handed screw dislocations in small concentrations. The left-handed screw dislocations were found to form right-handed helices upon the diffusion of gold during subsequent heat treatment at temperatures above 1000°C. This observation is shown to be consistent with the idea that gold diffuses as an interstitial atom and causes a vacancy deficiency in the neighborhood of dislocations. Further evidence of the structure sensitivity of the diffusion of gold is shown by autoradiographic techniques. Studies were made of the effect of heat-treatment times and quenching rates upon the diameter of helices. The diameter of the helices increases with time at a given temperature, and

increases with temperature during a given time of heat treatment. Variation of the cooling time by a factor of 10^3 has no apparent effect on the diameter. Therefore, the helices form as a result of a gradient in the concentration of gold rather than by a quenching process. Impurities introduced by heat treatment at 900°C strongly modify climb in crystals which are relatively free from oxygen. Precipitates believed to be formed during this heat treatment act as nucleation sites for the formation of prismatic loops. Crystals grown from quartz crucibles and thus containing about 10^{+5} atom fraction of oxygen have complicated climb mechanisms believed to be associated with the pinning effect of the oxygen on the dislocations. Modified Bardeen-Herring sources have been found in these cases.

7243 DISLOCATIONS IN SILICON AND GERMANIUM CRYSTALS by W. C. Dash (GE); Properties of Elemental and Compound Semiconductors, (Interscience), pp. 195-209, 1960

The use of combined etching, decoration, and x-ray techniques for studying dislocations in silicon and in germanium crystals is discussed. Spiral etch pits do not appear to be associated with dislocations except in special circumstances. The considerations involved in the growth of dislocation-free crystals of silicon and germanium are reviewed. Unless considerable care is taken to eliminate surface damage introduced in cutting and handling, serious degradation of perfection can occur when a specimen is heated to a temperature at which dislocations can move.

7244 ETCH PITS, DEFORMATION, AND DISLOCATIONS IN GaAs by M. S. Abrahams and L. Ekstrom (RCA); Properties of Elemental and Compound Semiconductors, (Interscience), pp. 225-241, 1960

An etchant composed of 1 part HNO_3 and 2 parts H_2O which produces in GaAs etch pits which are crystallographically unique and reproducible on a given {111} face is discussed. The pits are produced on any {111} faces terminating with Ga atoms but not on those terminating with As atoms. A quantitative correlation between these etch pits and edge dislocations has been established by a series of bending and annealing experiments. The etchant has been used to study the dislocation morphology in crystals grown by the Czochralski and floating zone methods. The dislocation densities in Czochralski grown crystals vary from about $4 \times 10^3 cm^{-2}$ to $3 \times 10^4 cm^{-2}$ while the densities in crystals grown by the floating zone method are about an order of magnitude larger. The observation of dislocations arrayed along slip lines or in lineage boundaries in single, untwinned crystals is rare.

7245 NEW METHOD OF DETERMINING THE MOSAIC STRUCTURE OF CRYSTALS by R. H. Bragg (Armour Res. Found.) and L. V. Azaroff (Illinois Inst. Tech.); Bull. Am. Phys. Soc., Ser. II, Vol. 5, p. 421 (A), Nov. 25, 1960

The integrated intensity of reflections from mosaic crystals depends upon the crystallite tilt parameter η and the mean crystallite size t_0. A method of analyzing the mosaic structure which depends upon variation of the coefficient of reflection Q and the primary extinction function $f(A_0)$ by varying the wavelength of the diffracted x-rays λ is described. This variation is achieved by orienting the crystal so that a selected set of lattice planes of spacing d is inclined at angle θ relative to the direct beam which causes the desired wavelength to be reflected in accordance with Bragg's law. In order to place the intensities on an absolute basis, the intensity distribution in the incident beam $I_0(\lambda)$ is measured with a scintillation counter. Measurements have been made on a (111) plate of silico using x-ray wavelengths in the range 0.37 to 1.18 A. Etch pit counts at the edge and center portions of the plate were 3×10^6 and $5 \times 10^5/cm^2$, respectively. Corresponding crystalli sizes were found to be 9 and 3 μ, and the corresponding tilt parameters were 15 and 3 sec of arc. The latter results were in satisfactory agreement with direct measurements using the focusing Laue case method of Guinier and Tennevin.

7246 INTERSTITIAL VERSUS SUBSTITUTIONAL OXYGEN IN SILICON by W. L. Bond and W. Kaiser (Bell Labs.); J. Phys Chem. Solids, Vol. 16, pp. 44-45, Nov. 1960

Lattice constant and density studies on oxygen free and oxyge doped silicon single crystals which suggest that oxygen occupies an interstitial lattice site are reported.

Interstitial Oxygen in Si - See 7378

7247 INHOMOGENEOUS IMPURITY DISTRIBUTIONS IN InS CRYSTALS by A. J. Strauss and T. C. Harman (Lincoln Lab.); J. Electrochem. Soc., Vol. 107, p. 268C (A), Dec. 1960

The use of four-point resistivity measurements and differential chemical etching to investigate transverse and longitudinal in homogeneities in the distribution of various impurities in pulle crystals of InSb was discussed. The data indicate that in the case of Zn, at least, the increase in impurity concentration due to the presence of a <111> facet at the growth interface i associated with impurity "adsorption" at the interface. The mechanism of facet growth was discussed.

7248 THE EFFICIENCY OF ZONE-REFINING PROCESSES b L. W. Davies (Bell Labs.); Properties of Elemental and Compound Semiconductors, (Interscience); pp. 11-16, 1960

A theoretical investigation of refining processes which depend on the segregation of one material with respect to the liquid and solid states of another is discussed. For a given monotonic distribution of solute in an ingot, figures of merit which are relevant to discussions of solvent purification and of the concentration of the solute toward one end of the ingot in the cas that the solute is a desirable impurity are defined. It is shown that the optimum conditions for solvent purification and solute concentration are identical. In the zone-refining process, if the solute is initially distributed uniformly, a determination of the optimum ratio of the lengths of zone and ingot yields the values unity and $\lesssim 0.3$, respectively, for most efficient passage of the first two zones. Variation of the effective distribution coefficient is also discussed.

Purification of As, P, and Ga to 99.9999% - See 7271

7249 EVALUATION AND CONTROL OF DIFFUSED IMPURIT LAYERS IN GERMANIUM by H. S. Veloric and W. J. Greig (RCA); RCA Rev., Vol. 21, pp. 437-456, Sept. 1960

Methods for the evaluation of diffused impurity layers in germanium are presented. The calculations reported are for n- and p-type impurities with a complementary-error-function (erfc) distribution in uniformly doped germanium of the opposite conductivity. These methods are then used to evaluate a new solid-phase diffusion process employing a powdered-germanium alloy doped with a known impurity concentration

as the diffusant. The surface concentration of a diffused layer is shown to be approximately equal to the concentration in the source powder at high temperature and to decrease with decreasing temperature. Diffusion constants for arsenic and antimony are determined by use of "sheet-resistance" and junction-penetration measurements. Because the surface concentration can be predicted within a factor of two, and the penetration within ten per cent, the present experiments show that the powder diffusion method is suitable for the fabrication of carefully controlled impurity layers.

7250 THE DIFFUSION OF HYDROGEN IN SINGLE-CRYSTAL GERMANIUM by R. C. Frank (GM) and J. E. Thomas, Jr. (Wayne State U.); J. Phys. Chem. Solids, Vol. 16, pp. 144-151, Nov. 1960

Measurements of the permeation rate and diffusion coefficient of hydrogen in single crystal germanium from 800° to 910°C are discussed. A thin, hollow, cylindrical specimen sealed at one end and attached to a mass spectrometer at the other is surrounded with hydrogen gas. The diffused gas is then observed in the mass spectrometer. The excellent agreement between diffusion coefficients measured by the "time lag" and decay curve methods indicates that trapping effects by lattice defects were small or nonexistent. The activation energy for diffusion is 8.7 ± 0.8 kcal/g atom and the heat of solution is 52.8 ± 1.4 kcal/g atom. The permeation rate was found to vary as the square root of the gas pressure, which indicates that the hydrogen exists in the germanium lattice as hydrogen atoms or ions.

Electron Probe Method of Measuring Diffusion Coefficients - See 7228

7251 SELF-DIFFUSION OF THE CHLORIDE ION IN SODIUM CHLORIDE by N. Laurance (Ford Motor); Phys. Rev., Vol. 120, pp. 57-62, Oct. 1, 1960

The measurement of the diffusion coefficient of Cl^{36} in NaCl in the temperature range from 520° to 740°C is discussed. Diffusion was measured in pure Harshaw crystals and in crystals containing from 0.01 to 0.1 mole percent calcium. The diffusion coefficient in pure crystals is represented by the equation $D = 56 \exp(2.12 \text{ ev}/kT) \text{ cm}^2/\text{sec}$. The diffusion coefficient in crystals containing calcium was smaller than that measured in pure crystals by a factor of from 5 to 10, and had an activation energy of 2.5 ev. Over the range of impurity concentration employed the diffusion coefficient was insensitive to differences in calcium concentration. The results are discussed in terms of motion of free negative ion vacancies and of vacancy pairs. Possible complicating effects of dislocation lines on the diffusion coefficient are also considered.

7252 THE DIFFUSION OF Zn IN InSb by B. Goldstein (RCA Labs.); Properties of Elemental and Compound Semiconductors, (Interscience), pp. 155-161, 1960

Measurement of the diffusion of zinc in single crystal indium antimonide in the temperature range from 362 to 508°C using radio-active Zn^{65} is discussed. Standard sectioning and counting techniques were employed. The diffusion was found to follow the customary relation, $D = D_0 \exp\{-E/kT\}$, where D_0 is 0.5 cm^2/sec and E, the activation energy, is 1.35 ev. The mechanism of this diffusion is discussed in terms of the results reported here and the work of others.

Diffusion of Li in ZnO - See 7227

Precipitation of Lithium in Silicon Containing Oxygen - See 7226

7253 BEHAVIOR OF CARBON IN GaAs by B. Goldstein and L. R. Weisberg (RCA); Bull. Am. Phys. Soc., Ser. II, Vol. 5, p. 407 (A), Nov. 25, 1960

Measurements made in a crystal of GaAs grown by the horizontal Bridgman technique in a quartz boat coated with a radioactive carbon film were discussed. The carbon was found to be homogeneously distributed throughout the bulk in the range of 3 to $8 \times 10^{16} \text{ cm}^{-3}$. No segregation was observed at the grain boundaries. Occluded carbon, however, was observed at the surface of the crystal. The effective distribution coefficient of the carbon was found to be about 0.8. It was found that silicon was the major detectable impurity in the crystal, with a concentration varying from the front to the tail from 1 to 30 ppm atomic. The electron concentration varied from 3×10^{16} to $1.5 \times 10^{18} \text{ cm}^{-3}$, and the mobility was below $3500 \text{ cm}^2\text{v}^{-1}\text{sec}^{-1}$. This low mobility is characteristic of crystals grown in contact with carbon.

7254 STOICHIOMETRY IN COMPOUND SEMICONDUCTORS by W. W. Scanlon (U.S. Naval Ord. Lab.); Properties of Elemental and Compound Semiconductors, (Interscience), pp. 185-194, 1960

In principle all crystals of compound solids should show deviations from the stoichiometric proportions of the elements. Generally these deviations are small, but they may have an important effect on the electrical properties of the solid. Some of the basic principles governing deviations from stoichiometry are discussed. Methods for controlling the amount of deviation in a semiconductor are illustrated for the case of the polar semiconductor PbS.

7255 DIELECTRIC BREAKDOWN DENDRITES ON LiF CLEAVAGE FACES by J. Pasternak and J. W. Davisson (U. S. Naval Res. Lab.); Bull. Am. Phys. Soc., Ser. II, Vol. 5, p. 421 (A), Nov. 25, 1960

An investigation of the nature of surface dielectric breakdown paths on cleavage faces of LiF crystals which utilized the short-time etching, or Flash etching, technique was discussed. It was observed that all the <100> paths, some of the <110> branches, and the scratches which were caused by rubbing with soft tissue paper appeared on the first flash etch while more etching was required to reveal dislocation etch pits which accompanied plastic deformation. Other samples which were annealed after breakdown and rubbing also showed <100> paths and scratches following the first flash etch without showing any of the aged dislocations. When the dislocation etch pits did appear on the unannealed samples, it was observed that <110> branches which consisted of double rows of dislocation-type etch pits were revealed on the ends of the <100> dendrites. It was suggested that the <100> dendrites are formed by electronic currents which caused local melting on the surface.

7256 DEEP ETCH STUDY OF DIELECTRIC BREAKDOWN DENDRITES ON LiF CLEAVAGE FACES by J. W. Davisson, J. Pasternak, and W. H. Vaughan (U.S. Naval Res. Lab.); Bull. Am. Phys. Soc., Ser. II, Vol. 5, p. 421 (A), Nov. 25, 1960

Deep etch studies of dielectric breakdown dendrites having <100> stems and arms with terminating <110> Y branches formed on LiF cleavage faces which show that the Y branches disappear

first and the dendrite stems last were discussed. The two parallel rows of etch pits constituting a branch of a Y converge as etching proceeds and terminate on a surface parallel <110> line. The deepest portion of the arms is the apex of the Y's. Double rows of steep conical etch pits paralleling the <100> stems are the last features to disappear. Since conical pits are not characteristic of new dislocations (square based pits are also observed), they may be following hollow <110> breakdown channels. The basic structure of the dendrite is observed at "Random Sites" which etch at the same rate as the dendrites. Each Site yields a giant etch pit showing four centers corresponding to steep <110> breakdown paths and also yields Y branches formed from submerged, surface parallel, <110> breakdown paths.

7257 TEXTURE IN EVAPORATED GERMANIUM FILMS by J. E. Davey and A. J. McAlister (U.S. Naval Res. Lab.); Bull. Am. Phys. Soc., Ser. II, Vol. 5, p. 408 (A), Nov. 25, 1960

An investigation of structure in vacuum evaporated thin germanium films deposited on neutral substrates between temperatures characteristic of the amorphous state up to the melting point of germanium was discussed. Both hot deposition and annealing have been employed to determine possible structural changes. Deposited hot or annealed films between 375° and 475°C yield the standard crystalline powder pattern in reflection electron diffraction. Depositing hot between 150° and 350°C yields a weak to strong 110 fiber structure depending on the temperature extrema. Films deposited near the lower temperature range of observable 110 structure also yield a 111 orientation in coexistence with the superficial 110. Hot deposition at near 600°C yields the single 111 fiber orientation. Treatment above 650°C results in mild to strong random crystal growth out of the plane of the film; in the vicinity of 800° to 900°C whiskers and facets up to 0.05 mm in extent have been observed.

7258 PREPARATION AND STRUCTURE OF COMPOUNDS IN THE SAMARIUM-SULFUR SYSTEM by M. D. Houston (Westinghouse); J. Electrochem. Soc., Vol. 107, p. 268C (A), Dec. 1960

The preparation of samarium sulfides was discussed on the basis of the chemistry of the reactants and the reaction. X-ray diffraction data for compound and structure identification were presented and physical properties of polycrystalline compacts were given.

7259 INTERMETALLIC COMPOUNDS BETWEEN LANTHANONS AND TRANSITION METALS OF THE FIRST LONG PERIOD I. PREPARATION, EXISTENCE AND STRUCTURAL STUDIES by K. Nassau, L. V. Cherry and W. E. Wallace (U. Pittsburgh); J. Phys. Chem. Solids, Vol. 16, pp. 123-130, Nov. 1960

Alloys with compositions corresponding to the formulas AB_5, AB_2, AB and A_3B, in which A is Y, La, Ce, Sm, Gd, Dy or Ho and B is Mn, Fe, Co or Ni are discussed. Samples were prepared by the technique of levitation melting and powder diffraction patterns were obtained to establish whether or not the various alloys existed in the form of intermetallic compounds. Extensive compound formation tendency was exhibited by all the lanthanons except La. All AB_2 type compounds were found to exist in the $MgCu_2$ structure. The AB_5 type compounds occurred either in the $CaCu_5$ structure or in an unsolved orthorhombic structure. Some AB and A_3B compounds may exist. Confirmation awaits interpretation of their diffraction patterns. Factors affecting the existence of these compounds and their structural parameters are discussed.

7260 A METHOD OF GROWING DISLOCATION-FREE GERMANIUM CRYSTALS by B. Okkerse (N. V. Philips); Philips Tech. Rev., Vol. 21, No. 11, pp. 340-345, 1959/1960

The growth of dislocation-free germanium crystals by the pulli method is discussed. The diameter of the crystal grown from th seed is initially reduced to 1 or 2 mm, is maintained at that va ue over a length of about 20 mm, and is then gradually raised the desired value. In the thin neck of the crystal thus produc the dislocations present tend to intersect the surface somewher where they end; thermal stresses are too small to generate fres dislocations. The thermal stresses generally increase as the crystal diameter is increased but no dislocations are created because of the absence of sources. However, should a piece of solid material floating on the melt come into contact with the growing crystal, dislocation sources are produced in the surface. Freedom from dislocations is demonstrated by the etch-pit method. Dislocation-free single crystals still contain point defects.

Growth of Dislocation-Free Si and Ge - See 7243

7261 SEGREGATION AND DISTRIBUTION OF IMPURITIES IN THE PREPARATION OF GERMANIUM AND SILICON by J. Goorissen (N. V. Philips); Philips Tech. Rev., Vol. 21, No. 7, pp. 185-195, 1959/1960

Two techniques for growing silicon and germanium crystals wit uniform resistivity are described. Uniform distribution is achieved by adding as much impurity from outside to a molten zone per second as leaves it via the solid-liquid interface to enter the growing crystal. For doping silicon crystals grown b zone melting a trace of PH_3, which decomposes at the molten zone, is added to the inert gas flowing over the pure silicon charge. Homogeneously doped germanium is obtained by pulling the crystal from a "floating crucible", which is equivalent to a zone whose concentration is kept constant. Both methods have a high effectiveness as regards homogeneity of the product.

Growth of GaAs Single Crystals by Zone Melting - See 7431

7262 EXPERIMENTAL RESULTS WITH "LARGE-AREA FLOATING ZONES" by K. E. Benson (Bell Labs.); Properties of Elemental and Compound Semiconductors, (Interscience), pp. 17-23, 1960

An experimental investigation of floating zones in solid members other than round rods by simulated zones formed with wate and by actual liquid zones in metals is discussed. Zone shapes studied include: (a) strip, a zone melted through the thickness and across part or the entire width of a vertical plate; (b) disk a round zone in a horizontal plate (which may be pressurized o the under side to support the zone); (c) annular, a zone melte through the cross section of a vertical pipe. Using these zone shapes, it is feasible to zone melt larger and also smaller cross sections than are feasible for round rods.

7263 SILICON MONOCRYSTALS FOR POWER RECTIFIERS [in Czech.] by S. Kosler and E. Uher (CKD); Elektrotech. Obzor., Vol. 49, pp. 575-578, Nov. 1960

The parameters of silicon single crystals for use in the manufacture of power rectifiers are discussed. Equipment for the

preparation of silicon single crystals by the floating zone method is described. The technological principles of the preparation and the results obtained in the national enterprise CKD Prague are given.

7264 A MODIFIED RF COIL TO FACILITATE FLOATING ZONE TECHNIQUES by S. J. Silverman (GE); J. Electrochem. Soc., Vol. 107, p. 268C(A), Dec. 1960

A modified rf work coil which can produce stable molten zones with length to diameter ratios less than unity in crystals grown by floating zone techniques was described. It is believed that these results are achieved because the coil concentrates the rf power in a limited region rather than because of enhanced electromagnetic levitation forces. The concentration of power promotes the formation of a flatter liquid-solid interface, and in practice permits the growth of crystals of larger diameter than have otherwise been obtained by a floating zone procedure using Ge or GaAs.

7265 FLOATING ZONE CRYSTALS USING AN ARC IMAGE FURNACE by R. P. Poplawsky and J. E. Thomas, Jr. (Wayne State U.); Rev. Sci. Instr., Vol. 31, pp. 1303-1308, Dec. 1960

A floating zone technique for growing crystals of medium high melting point materials with an arc image furnace is presented. This technique has been successfully applied to silicon. The oxygen concentration, resistivities, and dislocation densities of resulting crystals were determined to make possible a comparison with crystals obtained by standard methods. In general this comparison is favorable. Considerations of floating zones, maximum power, and flux distribution indicate that floating zone techniques combined with an arc image furnace are promising in connection with the growth of good quality crystals of a variety of high melting point materials.

7266 THE ARC IMAGE FURNACE FOR GROWING SEMICONDUCTOR CRYSTALS by R. P. Poplawsky and J. E. Thomas, Jr. (Wayne State U.); U.S. Gov. Res. Rep., Vol. 34, p. 500(A), Oct. 14, 1960 PB 161 868

The optical, mechanical, and electrical details of an arc image furnace are given. The furnace uses two 60-inch paraboloidal reflectors in vertical arrangement with a high intensity carbon arc as the source and was designed to study "arc image" crystal growing techniques. Two crucible-free techniques, "pushing" and "pulling", which resulted in the growth of several arc image silicon crystals are discussed. Pushing a silicon crystal consists of melting the top surface of a single crystal seed disk, which is positioned at the image point of the furnace, and then feeding a long, small diameter, polycrystalline rod into this melt. Pulling a silicon crystal is accomplished by first dipping a small rectangular seed crystal into a melt produced on the top surface of a relatively large, polycrystalline, silicon cylinder. The seed is then slowly withdrawn and liquid material solidifies onto it. The results of measurements made on pushed and pulled silicon crystals show that they are essentially free of oxygen, have high resistivities when a good grade of bulk material is used, and have a dislocation density of the order of $10^4 cm^{-2}$. The factors which influence the growth and quality of arc image crystals are discussed. These include: maximum useful furnace power, shapes of floating zones, and radiant flux considerations.

Growth of GaAs Crystals by the Horizontal Bridgman Method - See 7253

Preparation of Vacuum Evaporated Ge Films - See 7257

7267 SURFACE PHENOMENA IN SEMICONDUCTORS AND GROWTH OF SEMICONDUCTOR CRYSTALS by W. A. Albers, V. E. Noble (Wayne State U.); U.S. Gov. Res. Rep., Vol. 34, p. 500(A), Oct. 14, 1960 PB 161 867

A photo-electric etching technique for the preparation of thin filaments of single crystal germanium is described. Magnetoresistance measurements made on these thin samples have yielded one of the first direct observations of the mobility of electrical carriers near the surface of a semiconductor. 1/f noise measurements have been made upon the thin filaments in order to relate the semiconductor surface properties to the process of carrier trapping by surface energy states. The problem of preparing hyper-pure crystals of semiconducting materials was attacked by employing a high intensity carbon arc. An interpretation of the results of vertical liquid zone and irradiance profile calculations has indicated the feasibility of growing large, good quality crystals of the medium high melting point semiconductors using arc image techniques.

7268 EPITAXIAL FILMS OF SILICON AND GERMANIUM BY HALIDE REDUCTION by H. C. Theurer and H. Christensen (Bell Labs.); J. Electrochem. Soc., Vol. 107, p. 268C(A), Dec. 1960

The preparation of epitaxial films of silicon and germanium with controlled thickness and conductivity type on low-resistivity substrates by the hydrogen reduction of either $SiCl_4$ or $GeCl_4$ was discussed. The reduction apparatus consists essentially of a source of pure hydrogen, a halide saturator, and a water-cooled quartz reaction vessel. The substrate wafer to be coated rests in a silicon or graphite heating pedestal within the reactor and is heated externally by a radio frequency generator. In the case of silicon, the substrate is first heated at 1295°C for 1/2 hr in dry hydrogen to remove surface oxygen. For film deposition, treatment in hydrogen containing 2 mole percent $SiCl_4$ at a flow of 1 l/min for 5 min at 1270° C results in an epitaxial layer 6-8 μ thick. For germanium, the hydrogen pretreatment is carried out at 830°C for 10 min. Subsequent treatment in hydrogen containing 0.2 mole percent $GeCl_4$ with a hydrogen flow of 1 l/min for 10 min at 830°C results in a film approximately 5 μ thick. The kinetics of the two reduction processes are quite similar. The chemistry of the silicon process, including the doping of $SiCl_4$ with BBr_3 and PCl_3 for p- and n-type films of controlled resistivity, was discussed in some detail. Films prepared by the halide reduction method are good single crystals with the orientation of the substrate as determined from electron diffraction patterns which show Kukuchi lines.

7269 PREPARATION OF UNSUPPORTED CARBON FILMS AND THEIR ABSORPTION AT 180 A by D. J. Baker, D. E. Bedo, and D. H. Tomboulian (Cornell U.); Bull. Am. Phys. Soc., Ser. II, Vol. 5, pp. 415-416(A), Nov. 25, 1960

Unsupported carbon films for use as windows in the soft x-ray region were discussed. The films were prepared by depositing the material on a glass slide treated with a wetting agent. The carbon was vaporized from a high-current vacuum arc operated intermittently between pure carbon electrodes one of which was pointed while the other was flat. The deposited layer was "floated off" by immersing the slide in distilled water. Unusually large unsupported films, with areas up to 1.6 cm^2, have been made by this process. Such films have a surface density of 48 $\mu g/cm^2$, and a corresponding thickness of 2000 A if a

density of 2.4g/cc is assumed. It is possible to make much thinner specimens, but the largest possible unsupported size decreases rapidly with diminishing thickness. The attenuation was measured by means of a photon counting spectrometer previously described. The value of the linear absorption coefficient (at 180 A) depends somewhat on the age of the film and is found to approach the constant value of $(1.25 \pm 0.1) \times 10^5 \text{ cm}^{-1}$.

7270 SIMPLE APPARATUS FOR THE GROWTH OF GERMANIUM DENDRITES by R. F. Lever, J. K. Powers, J. L. Richards, and H. V. Sirgo (Philco); Rev. Sci. Instr., Vol. 31, pp. 1334-1335, Dec. 1960

A simple resistance-heated apparatus for pulling germanium dendrites is discussed. Two distinct types of growth are obtainable. When the correct conditions are achieved, growth may continue indefinitely. A typical product is a 2 m length of essentially uniform ribbon 1.5 to 3 mm in width, and 0.1 mm thick.

7271 MATERIALS RESEARCH ON GaAs AND InP by L. R. Weisberg, F. D. Rosi, and P. G. Herkart (RCA Labs.); Properties of Elemental and Compound Semiconductors, (Interscience), pp. 25-67, 1960

Methods of producing GaAs and InP single crystals with low dislocation densities and measurements made on impurities in these crystals are reviewed. Techniques have been developed for the preparation of arsenic, phosphorus, and gallium with a purity of about 99.9999%. These include the single crystal growth of arsenic from the melt, the distillation of arsenic from lead-arsenic alloys, the vacuum annealing of gallium with a cold "finger", single crystal growth of gallium, and chemical and physical treatments of phosphorus. It has been shown that the main donor in GaAs is silicon, and the main acceptor is copper. Both the electrical types of 24 impurities and the segregation coefficients of 18 impurities have been determined in GaAs. In addition, various impurity energy levels were detected, and those of copper, zinc, and oxygen were identified. Energy levels at 0.2 ev above the valence band and 0.55 below the conduction band are found in most of the high resistivity GaAs. In a study of thermal effects, it was shown that thermal conversion in GaAs is caused by the inward diffusion of copper which does not precipitate out upon annealing at lower temperatures. Both the lattice mobilities and their temperature variation were determined for n- and p-type GaAs and InP. At 78°K, the highest mobilities measured in n- and p-type GaAs were 14,600 and $4{,}200 \text{ cm}^2\text{v}^{-1}\text{sec}^{-1}$, and in n- and p-type InP were 24,900 and $1{,}200 \text{ cm}^2\text{v}^{-1}\text{sec}^{-1}$.

7272 MEASUREMENTS ON GaAs-GaP ALLOYS by H. Flicker and P. G. Herkart (RCA Labs.); Bull. Am. Phys. Soc., Ser. II, Vol. 5, p. 407 (A), Nov. 25, 1960

A series of $GaAs_{1-x}P_x$ alloys prepared with $0 \leq x \leq 1$ was discussed. Measurements of lattice constant and chemical composition have been carried out by x-ray and spectrochemical analysis in the range of $0 \leq x \leq 0.5$. The results indicate that Vegard's law is obeyed. The optical band gap has been measured and is in agreement with previous results. Hall measurements on a sample of $x = 0.15$ having a 1.6-ev band gap showed an electron Hall mobility of $1700 \text{ cm}^2\text{v}^{-1}\text{sec}^{-1}$. In the range $0 \leq x \leq 0.5$ the absorption curve is similar to that observed in GaAs, and in samples of $x \geq 0.7$ the absorption curve is similar to that observed in GaP. This would indicate that the absorption process changes from a direct transition, as in GaAs, to an indirect transition as in GaP.

7273 THE PREPARATION AND THE ELECTRICAL AND OPTICAL PROPERTIES OF SnS CRYSTALS by W. Albers, C. Haas and F. van der Maesen (N. V. Philips); J. Phys. Chem. Solids, Vol. 15, pp. 306-310, Oct. 1960

SnS crystals prepared by melting the components in an evacuated quartz tube at about 900°C are discussed. The observed melting point is 880 ± 5°C. The crystals were p-type with a hole density between 10^{17} and 10^{18} cm^{-3} and $\mu_p = 65 \text{ cm}^2/\text{v sec}$ at room temperature. One of the crystals showed an anomalous behavior of the Hall coefficient with temperature similar to what was found recently in SnSe. Preliminary measurements show that the conductivity in the direction of the c-axis is about six times smaller than in the direction perpendicular to the c-axis at room temperature. Analysis of infrared transmission measurements at room temperature on cleavage plates perpendicular to the c-axis reveal the energy gap to be 1.07 ± 0.04 ev. The free carrier absorption part of the transmission curve shows a dependence of $\alpha \sim \lambda^2$; analysis of this curve leads to an effective mass $m = 0.4 m_0$ for the holes.

Preparation of CdSb Single Crystals - See 7285

Preparation of ZnSb Single Crystals - See 7286

7274 PREPARATION AND PROPERTIES OF SOME PERITECTIC SEMICONDUCTING COMPOUNDS by D. R. Mason and D. I. O'Kane (U. Michigan); J. Electrochem. Soc., Vol. 107, p. 268C (A), Dec. 1960

Preliminary results on the preparation and properties of ternary semiconducting compounds in the homologous series $I^bInVI_2^b$ and $II^bIn_2VI_4^b$ were presented. These ternary compounds represent a linear combination of two binary constituents, each of which has semiconducting properties. One constituent can be represented by the chemical formula $III_2^bVI_3^b$ and the other constituent either as $I_2^bVI^b$ or as II^bVI^b. Since each of the binary constituents is a pure chemical component, adequate equilibrium relationships can be obtained by investigating only the pseudobinary plane which joins them in the ternary system. A redetermination of the melting points and phase diagrams of some of the binary constituents has been undertaken in order to correct several serious inaccuracies in the literature. The determination of the phase diagrams for the various pseudobinary systems is in progress, using differential thermal analysis, and microscopic and x-ray examinations. It has been found that $HgIn_2Te_4$ is the only compound in either series that is definitely known to be congruently melting; the remaining nine compounds appear to be peritectics. The system $CdTe\text{-}In_2Te_3$ has been characterized quite completely, and homogeneous samples of the peritectic compounds in this system have been prepared using zone refining techniques.

7275 FINE-PARTICLE FERRITES. I. NICKEL FERRITE by W. W. Malinofsky and R. W. Babbitt (USASRDL); Sixth Conf. Magnetism and Magnetic Materials, Nov. 14-17, 1960, New York N.Y.

A process for preparing dense nickel ferrite bodies composed of grains small enough to remain single domain and the magnetic and crystallographic properties of the ferrites were discussed. Two techniques, flame-spraying and hot-pressing, were combined to produce the ferrites and the effect of varying the parameters in each of these was investigated. Powders as fine as 0.02 micron were prepared of single phase ferrites of various Ni/Fe ratios, and these were subsequently densified by hot-pressing while maintaining the crystallite size at 0.06 micron (below the critical size for single-domains). The effect on

μ' and μ" as a ferrite is annealed through the critical size for single-domains was shown. Magnetic measurements performed include μ' and μ" (to 1000 Mc), B_s, B_r, H_c, and incremental μ as well as the temperature dependence of some of these properties. Of practical interest was an improvement in the temperature coefficient of initial permeability over conventionally prepared ferrite. X-ray diffraction determinations of crystalline phases and crystallite sizes and measurements of apparent density were presented. Some theoretical considerations were also discussed.

Preparation of Rare Earth and Transition Metal Compounds - See 7259

Preparation of Samarium Sulfides - See 7258

CRYSTAL SURFACES

7276 SEMICONDUCTOR SURFACES AND FILMS; THE SILICON-SILICON DIOXIDE SYSTEM by M. M. Atalla (Bell Labs.); Properties of Elemental and Compound Semiconductors, (Interscience), pp. 163-182, 1960

An important phase in the study of semiconductor surfaces is one where the semiconductor surface is provided with a chemically bound and well-defined surface film. One such solid-solid interface system has been recently studied; namely, the silicon-silicon dioxide system where the oxide is produced by thermal oxidation. A review of various phases of this work is given.

7277 TECHNIQUE FOR POLISHING SINGLE CRYSTAL YTTRIUM-IRON-GARNET SPHERES by P. D. Gianino, B. R. Capone, and E. Kelly (Air Force Camb. Res. Ctr.) and J. I. Masters (Tech. Operations); IRE Trans., Vol. MTT-8, p. 569 (L), Sept. 1960

A technique for hand-polishing yttrium-iron-garnet spheres in a matter of hours is described. A coarse polished sphere is rolled in a figure eight pattern under light finger pressure in 6μ-grit diamond paste dabbed on a metallurgical polishing cloth. After about an hour the process is repeated with successively finer grits. A table giving the measured line width at each stage of the polishing process is presented. Fractional line width samples are obtained. The process is being mechanized and it is felt that eventually some steps may be eliminated and an optimum polishing time per stage can be determined.

7278 INFLUENCE OF HYDROFLUORIC ACID ON THE MECHANISM OF DISSOLUTION OF GERMANIUM by W. Mehl (RCA); J. Electrochem. Soc., Vol. 107, p. 269C (A), Dec. 1960

The action of hydrofluoric acid in lowering the activation energy for both the electrolytic and the chemical dissolution of germanium was discussed. For the anodic dissolution of p-type germanium, the Tafel slope changes from 130 mv in the absence of HF to a limiting value of 60 mv after the addition of sufficient HF. The anodic limiting current for the dissolution of n-type germanium increases when HF is added to the electrolyte. The implications of these measurements for the theory of the germanium electrode were presented.

Correlation Between Etch Pits and Dislocations in GaAs - See 7244

Flash Etching Technique for Examining Dielectric Breakdown Dendrites on LiF Cleavage Faces - See 7255, 7256

Delineation of Ferroelectric Domains in Triglycine Sulphate by Etching - See 7291

7279 ATOM EJECTION PATTERNS IN SINGLE-CRYSTAL SPUTTERING by G. S. Anderson and G. K. Wehner (Gen'l Mills); J. Appl. Phys., Vol. 31, pp. 2305-2313, Dec. 1960

Experimental studies of the atom ejection patterns in single-crystal sputtering, mostly by Hg^+ ions, are discussed. These patterns give evidence of the anisotropic spread of energy from a collision center, and support the concept of focusing collisions in nearest and next-nearest neighbor directions. In Ge the patterns were found to be strikingly similar to those from a bcc crystal. This could be explained by assuming that under ion bombardment so many interstitials are formed near the surface that the atom arrangement of the Ge crystal resembles that of a bcc lattice.

ENVIRONMENTAL EFFECTS

Formation of Spin Centers in Carbons by Heat Treatment - See 7368

7280 NEUTRON IRRADIATION OF GRAY TIN by A. N. Goland (Brookhaven Nat'l Lab.); J. Phys. Chem. Solids, Vol. 16, pp. 46-52, Nov. 1960

The irradiation of gray tin at 0°C in a reactor in an effort to produce white tin is discussed. The irradiated powder was compared to an un-irradiated specimen by means of x-ray studies at low temperatures. No significant change was found in the amount of white tin present as a result of irradiation. The implications of this result for the thermal-spike concept are discussed and various explanations for the experimental results are offered.

Reactor Irradiation of PbTe, Bi_2Te_3, and ZnSb - See 7402, 7403

SOLID STATE PHYSICS

CRYSTAL PHYSICS
(including Energy Band Structure)

7281 ENERGY-BAND STRUCTURE OF SOLIDS FROM A PERTURBATION ON THE "EMPTY LATTICE" by F. Bassani

(Argonne Natl. Lab.); and V. Celli (U. Illinois); Bull. Am. Phys. Soc., Ser. II, Vol. 5, p. 407 (A), Nov. 25, 1960

A simple perturbation approach to the energy-band structure of solids was described. The unperturbed Hamiltonian consists of the kinetic part and of a uniform potential; the perturbing operator is the crystal potential plus a term which originates from the requirement that valence and conduction states be orthogonal to the inner states. This amounts to an approximation to the O.P.W. method. Reasons for the validity of such a simple scheme were given, and applications to the case of the diamond lattice and of the zinc blend lattice were discussed. It was shown how features of the energy-band structure depend on the symmetry of the lattice, on the lattice parameter, and on the "core states" of the atomic components. Numerical results obtained for diamond, silicon, and BN are in agreement with recent calculations. An energy-band structure consistent with experimental information has been obtained for Ge and GaAs by fixing the values of a few parameters.

7282 BAND STRUCTURE AND ELECTRON TRANSPORT OF GaAs by H. Ehrenreich (GE); Phys. Rev., Vol. 120, pp. 1951-1963, Dec. 15, 1960

Existing experimental data on GaAs are reviewed to determine the band structure in the vicinity of the band edges as well as the parameters characterizing the bands. On the basis of presently existing experimental evidence, chiefly the behavior of the optical band gap in Ga (As, P) alloys and the deduced pressure shift and density of states effective mass, it is thought likely that the subsidiary conduction band minima lie along [100] directions. Analytical expressions including nonparabolic effects are given for the energy and density of states of the [000] conduction band and used to obtain a better value of the effective mass from optical reflectivity data. The experimentally observed structure in the Hall effect in n-type material at elevated temperatures is shown to result from excitation of carriers into the subsidiary conduction band. Changes of resistivity with pressure are explained on the basis of an increase of the [000] effective mass at low pressures and the transfer of carriers to the subsidiary minima at higher pressures. The scattering mechanisms, which are important in connection with transport phenomena, are shown to be polar lattice scattering and charged impurity scattering in the highest mobility samples. The transport calculations leading to the mobility and thermoelectric power as a function of temperature and impurity concentrations are performed using variational techniques, and shown to agree well with experiment. The apparently low mobility in the subsidiary minima is attributed at least in part to the large effective mass and relatively small anisotropy ratio. An estimate shows scattering between the two conduction bands probably to be unimportant.

Reflectance Method of Measuring Energy Band Structure - See 7394

Energy Gap Width of SnS - See 7273

Energy Gap Width in GaAs-GaP Alloys - See 7272

Variation of Energy Gap with Composition in the System Ga_2Te_3-ZnTe - See 7230

Impurity Energy Levels in GaAs and InP - See 7271

Li as a Donor and an Acceptor in ZnO - See 7227

7283 SURFACE PROPERTIES OF SILICON by V. G. Litovchenko and O. V. Snitko (Kiev Phys. Inst.); Soviet Phys.-Solid State, Vol. 2, pp. 554-565, Oct. 1960

The effects of an external electric field on the electrical conductivity, the "field-effect mobility" and its kinetics, the surface recombination, and the capacitor photo-emf in silicon are discussed. Comparison of the results with theory yields information on the densities, the energy positions and the capture cross sections of the surface levels in silicon treated with a standard etch.

Valence Band Structure of Alkali Iodides - See 7320

Energy Band Structure of Bi - See 7372

ELECTRICAL PROPERTIES - GENERAL

7284 ELECTRICAL STRUCTURE OF PbS FILMS by D. P. Snowden and A. M. Portis (U. California); Phys. Rev., Vol. 120, pp. 1983-1995, Dec. 15, 1960

The electrical properties of chemically deposited lead sulfide films as a function of frequency from d-c into the microwave range are discussed. Conductivity and Hall mobility measurements have been made on both the dark and the photo-excited carriers. The dark conductivity is independent of frequency below 100 Mc/sec. It increases by almost an order of magnitude over a decade in frequency and then becomes constant again at higher frequencies. This behavior is typical of a material whose low-frequency conductivity is limited by barriers. Surprisingly the photoconductivity behaves quite differently. The photoconductivity has a hump around 100 Mc/sec but otherwise is relatively independent of frequency. The Hall mobilities of the dark and photocarriers are equal at d-c in agreement with earlier studies. Microwave Hall measurements indicate that the dark carriers have about the same apparent mobility at 10 kMc/sec as at d-c. It is shown that the conventional barrier model with a photoinduced change in carrier concentration cannot account for the behavior of these films. Nor can a model in which the barrier height is modified by illumination. The data suggest that there are connecting channels through the films and that the photoresponse of the films is determined by the behavior of these channels. A simple model is constructed and its parameters are adjusted to fit the conductivity data and the d-c Hall mobility.

Effect of Neutron Radiation on the Electrical Properties of PbTe, Bi_2Te_3, and ZnSb - See 7402, 7403

7285 ANISOTROPY OF ELECTRICAL PROPERTIES OF SINGLE CRYSTALS OF CADMIUM ANTIMONIDE by I. K. Andronik and M. V. Kot (Kishinev State U.); Soviet Phys.-Solid State, Vol. 2, pp. 1022-1026, Dec. 1960

Methods of obtaining single crystals of cadmium antimonide and their electrical properties are described. The electrical properties of single crystals of CdSb are anisotropic.

7286 ANISOTROPY OF CERTAIN ELECTRICAL PROPERTIES OF SINGLE CRYSTALS OF ZINC ANTIMONIDE by M. V. Kot and I. V. Kretsu (Kishinev State U.); Soviet Phys.-Solid State, Vol. 2, pp. 1134-1139, Dec. 1960

Methods of obtaining single crystals of zinc antimonide and their electrical properties are described. Crystals are p-type and their electrical properties are anisotropic.

DIELECTRIC PROPERTIES
(including Ferroelectricity)

Dielectric Breakdown Paths on Cleavage Faces of LiF Crystals - See 7255, 7256

7287 DIELECTRIC CONSTANT AND DIELECTRIC LOSS OF TiO_2 (RUTILE) AT LOW FREQUENCIES by R. A. Parker and J. H. Wasilik (NBS); Phys. Rev., Vol. 120, pp. 1631-1637, Dec. 1, 1960

Measurements of the complex capacitance ($C = C' - iC''$) of undoped, high-resistance, single-crystal TiO_2 (rutile) in vacuum at 78, 195, 273, and 300°K as a function of frequency between 10^1 and 3×10^6 cps with a 0.1-volt a-c signal are reported. With the field in the c direction, one low-frequency loss peak is found at 200 cps. The capacitance C' and loss C'' of a 2-mm cube with the field in the c direction are characterized by $1/2\pi\tau = 200\ \text{sec}^{-1}$, $\tan\delta_{200\,\text{cps}} = 0.7$, and a dielectric constant $(\epsilon')_{1\,\text{Mc/sec}}$ of 170, while $(\epsilon')_{20\,\text{cps}} = 30{,}000$. The loss and low-frequency capacitance of the crystal are directly proportional to the area of the electrodes and depend but slightly on the sample thickness, electrode materials and surface treatment. C' and C'' have been measured at 300°K as a function of the oxygen vacancy concentration in the crystal. C' and C'' have also been measured as a function of d-c bias from 0 to 400 volts; $(C')_{20\,\text{cps}}$, $(C'')_{\max}$ and τ are proportional to v^{-n} where n is between 0.3 and 0.8. The results of the experiments can be explained by an electron-deficient barrier layer whose thickness increases with increasing applied d-c voltage. When the d-c voltage in the c direction is changed, effects with time constants of the order of hours or even days are observed.

Dielectric Properties of Some Semiconducting Oxide Glasses - See 7311

7288 AGING OF BARIUM TITANATE SINGLE CRYSTALS by A. Misarova (Phys. Inst., Czech. Acad. Sciences); Soviet Phys.-Solid State, Vol. 2, pp. 1160-1165, Dec. 1960

Measurements of the time changes of the dielectric permeability, $\tan\delta$, the hysteresis loop, and the conductivity of single crystals of barium titanate during aging in the presence and in the absence of a constant electric field are described. A hypothesis regarding the mechanism of the aging process is proposed as an explanation of the results of these measurements.

7289 THERMAL CONDUCTION IN FERROELECTRIC CERAMICS by I. Yoshida (U. Tokyo and Tokyo Inst. Tech.); J. Phys. Soc., Japan, Vol. 15, pp. 2211-2219, Dec. 1960

Measurements of the thermal conductivity of insulating crystals over the temperature range from -200°C to 600°C are described. For the lower temperature range, an absolute measurement was obtained, while for the higher range, the comparative method was adopted. The thermal conductivities of ferroelectric $PbTiO_3$ and antiferroelectric $PbZrO_3$ showed a rather large step-wise increase, in contrast to the case of $BaTiO_3$, as they passed into the paraelectric state. The relation between the magnitude of thermal conductivity and the crystal structure is discussed. It is pointed out that the anharmonic potential for the smaller ions should be responsible for the scattering of phonons in these substances.

7290 HIGH-TEMPERATURE DISCHARGES IN FERROELECTRIC CERAMICS by J. W. Northrip (Sandia Corp.); J. Appl. Phys., Vol. 31, pp. 2293-2296, Dec. 1960

Ceramic disks of barium titanate and lead zirconate titanate, when heated above 100°C, exhibit current discharges which cannot be attributed to the ferroelectric polarization of the material. These discharges are largest in the temperature interval 300° - 600°C and depend primarily on the electrode material and its method of application. Discharges of several millicoulombs at voltages up to one-half volt have been obtained from a ceramic disk one-half inch in diameter and 30 mils thick having a silver electrode and an indium counter-electrode. Although thermoelectric, pyroelectric, and electret effects are observed in these samples, these phenomena contribute only a very small portion of the total discharge. At constant temperature near 350°C the discharge decays with time as the sum of two exponentials, falling to half-maximum in periods of the order of one-half hour. At higher temperatures the decay rate increases, while temperature cycling produces a voltage cycling superimposed on the decay. These findings support an explanation of the effect in terms of solid state chemical activity between the metallic electrodes and the titanate lattice.

7291 FERROELECTRIC DOMAIN DELINEATION IN TRIGLYCINE SULPHATE AND DOMAIN ARRAYS PRODUCED BY THERMAL SHOCKS by A. G. Chynoweth and W. L. Feldmann (Bell Labs.); J. Phys. Chem. Solids, Vol. 15, pp. 225-233, Oct. 1960

Delineation of the ferroelectric domains in single crystals of triglycine sulphate with high resolution simply by etching the crystal in a water bath for a few seconds at room temperature is described. Both the ends and sides of domains can be revealed where they intersect planes perpendicular and parallel to the ferroelectric axis, respectively. With these techniques many totally internal cigar-shaped domains, with their long axes parallel to the ferroelectric axis, have been discovered. It has also been shown that a very regular array of domains is introduced into the crystal when it is subjected to a thermal shock. A cooling shock gives rise to many small spike-shaped nuclei extending into the crystal from the surfaces. A warming shock results in a regular array of considerably larger domains. It seems that in both cases, the driving force that creates these new domains is the field arising from the polarization discontinuities which, in turn, are caused by the transient thermal gradients set up in the crystal when subjected to the thermal shock. The shapes of the spike-shaped domains introduced by the cooling shock agree with those predicted by a, necessarily, idealized model.

7292 FERROELECTRIC PROPERTIES OF $BaLi_{2x}Al_{2-2x}F_{4x}O_{4-4x}$ by T. G. Dunne and N. R. Stemple (IBM); Phys. Rev., Vol. 120, pp. 1949-1950, Dec. 15, 1960

Single crystals of $BaLi_{2x}Al_{2-2x}F_{4x}O_{4-4x}$, where x = 0.15 to to 0.30, have been found to be ferroelectric with a Curie temperature in the range 127-153°C and a room-temperature spontaneous polarization along the hexagonal c axis of approximately 0.1 μcoul/cm². The structure of these mixed crystals is unrelated to that of any previously known ferroelectric, but appears to be very similar to that of $BaAl_2O_4$.

7293 FERROELECTRIC AND ANTIFERROELECTRIC PROPERTIES OF SOLID SOLUTIONS OF $NaNbO_3$-$PbZrO_3$ by N. N. Krainik (Leningrad Inst. of Semicon.); Soviet Phys.-Solid State, Vol. 2, pp. 633-637, Oct. 1960

A synthesis of the system of solid solutions of the two antiferroelectrics $NaNbO_3$-$PbZrO_3$ and an investigation of the dielectric properties of these materials are reported. A ferroelectric phase has been discovered. The causes of the appearance of ferroelectricity in the given system is discussed.

7294 FERRIELECTRICITY by C. F. Pulvari (Catholic U.); Phys. Rev., Vol. 120, pp. 1670-1673, Dec. 1, 1960

A new group of materials exhibiting ferroelectric behavior is reported. This behavior appears in a mixture of antiferroelectric compounds (sodium vanadate and sodium niobate; also sodium niobate and silver niobate), neither of which exhibits this phenomenon at low field strength in its pure state. Coercivity as well as polarization is composition dependent. The onset of the ferroelectric state is a function of applied field, which in some compositions is considerably higher than the coercive field. Switching transients of a form not previously reported are exhibited by these materials.

CARRIER PROPERTIES

7295 NOTE ON SEMICONDUCTOR STATISTICS by S. Teitler and R. F. Wallis (U.S. Naval Res. Lab.); J. Phys. Chem. Solids, Vol. 16, pp. 71-75, Nov. 1960

The Guggenheim method for treating semiconductor statistics using the grand partition function is applied to multi-level impurities in Ge assuming a model for electron configuration at the impurity based on the present knowledge of the energy band structure of Ge. The results are expressed in terms of effective one-electron energies corresponding to the one-electron levels associated with the impurities. The difference between these effective one-electron energies and actual one-electron energies is emphasized.

7296 STEADY-STATE DISTRIBUTION FUNCTION IN DILUTE ELECTRON GASES by D. C. Mattis (IBM); Phys. Rev., Vol. 120, pp. 52-57, Oct. 1, 1960

It is usually assumed that optically created carriers in a photoconductor rapidly thermalize to a Boltzmann distribution, regardless of the generation and recombination mechanisms. However, it can be shown that this distribution which is characteristic of thermodynamic equilibrium is incompatible with the requirements of steady state. A variational principle is introduced to find the steady-state distribution, which is found to approach the Maxwell-Boltzmann function in the limit of stron thermal scattering. Interband scattering is found to be potentially a strong thermalizing influence, in addition to the intra band scattering usually considered. For a simple model semiconductor, significant deviations from the Boltzmann distribution are found to be possible at temperatures below a few degr Kelvin. This result is then discussed in connection with certai experiments on germanium.

Surface Carrier Density in Diffused Layers - See 7300

7297 RECOMBINATION OF ELECTRONS AND DONORS IN N-TYPE GERMANIUM by G. Ascarelli and S. C. Brown (MI Phys. Rev., Vol. 120, pp. 1615-1626, Dec. 1, 1960

The recombination of electrons and donors in n-type germaniur at helium temperatures is discussed. The excess electron densi is obtained by means of low-temperature breakdown. Experime tal results indicate that the recombination probability varies ap proximately with the inverse of the square of the temperature. Recombination light has been detected. The origin of the disagreement of these measurements with those of S. H. Koenig is discussed, and evidence is given to explain the discrepancies between the two measurements. The magnitude of the recombination cross section appears to depend on the binding energy of the electrons to the donor impurities, but large errors that are present in the determination of N_A are responsible for a large uncertainty in the absolute magnitude of the cross sectio The cross sections vary from 10^{-12} to 10^{-11} cm².

Carrier Trapping by Surface Energy States - See 7267

Trapping Noise in CdS - See 7319

7298 EFFECTIVE MASS IN GRAY TIN FROM KNIGHT SHIFT MEASUREMENTS by W. E. Blumberg and J. Eisinger (Bell Labs.); Phys. Rev., Vol. 120, pp. 1965-1968, Dec. 15, 196

Measurements of the nuclear magnetic resonance of Sn^{119} in gr tin between 200°K and 300°K are reported. The effective g factor was found to increase by about 4 parts in 10^5 over this temperature range. This increase in Knight shift is thought to arise from an increase in the number of conduction electrons. By combining this result with Busch and Mooser's measurements of the magnetic susceptibility over the same temperature range m_l, the single-valley effective mass of the lighter of the charg carriers, is found to be $(0.3 \pm 0.05)m$ if the electron g factor is 2. The experiment also allows one to determine the Knight shift without making a comparison with a diamagnetic substanc The Knight shift of intrinsic gray tin is found to be 6×10^{-5} at 300°K. The fact that the Knight shift is positive shows that th electron g factor is not negative as would be expected if the band structure of gray tin were similar to that of InSb.

Effective Mass in SnS - See 7273

Effective Mass in Ti_2O_3 - See 7309

7299 TRANSPORT IN METALS. II. EFFECT OF THE PHONON SPECTRUM AND UMKLAPP PROCESSES AT HIGH AND LOW TEMPERATURES by M. Bailyn (Northwestern U.); Phys. Rev., Vol. 120, pp. 381-404, Oct. 15, 1960

The nonmagnetic transport coefficients of the alkali metals are

calculated with improvements designed to take into account the effect of the phonon spectrum on both the normal and umklapp regions of scattering. The phonon equations of motion are solved numerically to obtain a spectrum sample, and spectrum averages are then computed in a manner similar to specific heat calculations. No average Debye temperatures are used, but rather the sums are obtained in terms of certain combinations of the elastic constants, which in principle are measurable. Also, improvements on the shielding part and on the ion part of the electronic matrix element are calculated and discussed. The results show that umklapp processes are important down to the lowest measurable temperatures in the ideal component of the electrical and thermal resistivities, being completely dominant in the former. The low-temperature temperature dependence is therefore determined mainly from the umklapp term, which can show a faster variation than T^5 in the electrical resistivity, as is actually observed in sodium. The transverse phonon vibrations dominate the contributions at all temperatures and even the non-umklapp term at low temperatures. General expressions for the transport coefficients are calculated via the Kohler variational principle which are not restricted to the model of spherical energy surfaces. A general expression for the phonon-drag term in the thermo-electric power is given.

Temperature Dependence of the Mobility in Ti_2O_3 - See 7309

Field Dependent Mobility - See 7283, 7304, 7306

Mobility in GaAs-GaP Alloys - See 7272

7300 DETERMINATION OF CARRIER MOBILITY AND DENSITY IN THE SURFACE LAYER OF A SEMICONDUCTOR by V. K. Subashchiev and S. A. Poltinnikov (Semicon. Inst., Acad. Sciences); Soviet Phys.-Solid State, Vol. 2, pp. 1059-1066, Dec. 1960

A method of determining surface density and mobility in a semiconductor layer formed by impurity diffusion in the starting material is described. The method is based on Hall effect and conductivity data and the relationship between the carrier mobility and density. The experimental data relate to diffusion layer measurements in a silicon photocell.

Determination of Surface Mobility - See 7267

Mobilities in GaAs and InP - See 7271

Mobility in Carbon-Doped GaAs - See 7253

Mobility and Scattering in PbS, PbSe, and PbTe - See 7399

7301 SCATTERING OF HOT CARRIERS IN GERMANIUM by E. M. Conwell and A. L. Brown (Gen'l Tel. and Electronics Labs.); J. Phys. Chem. Solids, Vol. 15, pp. 208-217, Oct. 1960

The variation of lattice mobility of hot carriers with their average energy of "temperature" is discussed. An expression is derived for the relaxation time due to single phonon acoustical mode scattering which remains valid to very high carrier temperatures at lattice temperatures of 20°K and above. In the limit where carriers interact mainly with lattice oscillators having only zero point energy it is found that the relaxation time is proportional to the inverse square of the speed rather than to the inverse first power as for thermal carriers. Lattice mobility is plotted as a function of average carrier energy for various values of the ratio of coupling constants for optical and acoustical modes, and various effective masses, for lattice temperatures of 300°, 78° and 20°K. The effect of dropping the assumption of equipartition of energy among the acoustical lattice oscillators is to increase the scattering effect of the acoustical modes, the more so the lower the lattice temperature, the higher the carrier temperature, and the higher the mass of the carriers. Impurity scattering has not been included in the quantitative calculations, but it is shown that the increase in hot-carrier mobility which can be caused by this scattering process will generally be less than has been expected.

7302 SCATTERING ANISOTROPIES IN N-TYPE SILICON by D. Long and J. Myers (Honeywell Res. Ctr.); Phys. Rev., Vol. 120, pp. 39-44, Oct. 1, 1960

Measurements of magnetoresistance effects in several relatively pure samples of n-type silicon undertaken for the purpose of obtaining information on scattering anisotropies are reported. The results indicate that the ratios of relaxation times parallel and perpendicular to a constant-energy-spheroid axis in the six-valley conduction band of silicon are $\tau_{\parallel}/\tau_{\perp} \approx 2/3$ for acoustic mode intravalley lattice scattering and $\tau_{\parallel}/\tau_{\perp} > 1$ for ionized-impurity scattering. Intervalley lattice scattering, important at higher temperatures, is isotropic.

7303 SCATTERING OF CONDUCTION ELECTRONS BY LATTICE VIBRATIONS IN SILICON by D. Long (Honeywell Res. Ctr.); Phys. Rev., Vol. 120, pp. 2024-2032, Dec. 15, 1960

A theoretical model which assumes intervalley lattice scattering by phonons of 630° and 190°K characteristic temperatures in addition to the usual intravalley acoustic lattice scattering is applied to the results of measurements of electrical conductivity, Hall effect, and weak-field magnetoresistance in the 30° to 350°K temperature range in samples of nearly pure n-type silicon. The model gives a good quantitative description of the results when the ratios of the coupling constants for the 630° and 190° phonons to the coupling constant for acoustic scattering perpendicular to an energy-spheroid axis are, respectively, about 2.0 and 0.15. The coupling constant for acoustic scattering parallel to a spheroid axis was found in an earlier study to be about 1.5 times that for the perpendicular direction. The magnitude of the acoustic contribution to the total lattice scattering mobility, as determined empirically here, is in approximate agreement with the predictions of deformation-potential theory.

7304 VARIATIONAL TREATMENT OF WARM ELECTRONS IN NONPOLAR CRYSTALS by I. Adawi (RCA Labs.); Phys. Rev., Vol. 120, pp. 118-127, Oct. 1, 1960

Deviations from Ohm's Law in nonpolar crystals are treated for weak fields by the variational method. A simple band structure is assumed. Scattering by both acoustical and optical phonons, and ionized impurities is included. It is shown that the influence of optical phonons on the field dependent mobility (E^2 term where E is the electrostatic field) is maximum for a temperature which corresponds approximately to the optical phonon energy. The field dependent mobility is highly sensitive to ionized impurity scattering as in the case of acoustical phonons alone. Finally, the convergence of the variational method is established in limiting cases using as a representation a set of polynomials which are orthonormal with respect to the collision operator. Extensive calculations are given for electrons in germanium and comparison with experiment is discussed.

7305 ENERGY LOSS OF WARM ELECTRONS IN n-InSb CAUSED BY PIEZOELECTRIC SCATTERING by R. J. Sladek (Westinghouse Res. Lab.); Bull. Am. Phys. Soc., Ser. II, Vol. 5, p. 408 (A), Nov. 25, 1960

The electron mobility in n-InSb depends on electric field strength F even at quite low fields. To account for the change in mobility at 4.2°K, which is proportional to F^2, a model in which the electrons lose their momentum to ionized impurities but lose their energy to piezoelectrically active acoustic modes was presented. The probabilities of electronic transitions involving such modes have been given by Meijer and Polder. Using these transition probabilities a theoretical expression for energy loss caused by piezoelectric scattering has been derived by the method of Greene. Theoretical predictions for the field dependence of the mobility based on this expression agree well with experimental results on n-InSb samples having between 2.8×10^{14} and 8.7×10^{15} electrons/cc if the piezoelectric constant e_{14} has a value of about 2.6×10^4 (dynes)$^{\frac{1}{2}}$/cm.

7306 QUADRATIC DEVIATIONS FROM OHM'S LAW IN N-TYPE InSb by R. J. Sladek (Westinghouse Res. Lab.); Phys. Rev., Vol. 120, pp. 1589-1599, Dec. 1, 1960

Measurements of the resistivity of n-type InSb of various carrier concentrations as a function of electric field strength at low temperatures are reported. The electric fields were kept small enough so that only a slight heating of the electron distribution occurred and the electron mobility μ satisfied the relation $\mu = \mu_0(1+\beta F^2)$, where μ_0 is the ohmic mobility and F the electric field. Analysis of the experimental values of β yields information about the processes by which electrons lose momentum and energy and about the influence of carrier degeneracy and electron-electron scattering upon these processes. For example, at 4.2°K, piezoelectric scattering is responsible for most of the energy loss, while near 77°K polar optical scattering, enhanced by strong electron-electron scattering, is responsible for energy loss, at least in zero magnetic field. A novel means of changing the sign of the deviation from Ohm's law near 77°K was observed by applying a strong magnetic field.

Electron Transport of GaAs - See 7282

7307 INVESTIGATION OF THE DIFFUSION OF MINORITY CURRENT CARRIERS IN A MAGNETIC FIELD by S. M. Ryvkin, A. A. Grinberg, Yu. L. Ivanov, S. R. Novikov, and N. D. Potekhina (Leningrad Physicotechnical Inst.); Soviet Phys. - Solid State, Vol. 2, pp. 541-553, Oct. 1960

A theoretical and experimental investigation of the minority carrier concentration in a magnetic field during "point" injection is described. It is shown that the study of this distribution, especially convenient during the measurement of the longitudinal magneto-concentration effect, may be used to determine several semiconductor parameters: the "microscopic" carrier drift mobility and the relationships between concentrations of carriers of the same sign but of different effective mass. A value of 2% was obtained for the relationship between the concentrations of light and heavy holes in Ge.

CONDUCTIVITY

Electrical Conductivity of Cd and ZnTe Layers - See 7392

7308 AN ANALYSIS OF THE CIRCUIT OF DAUPHINEE AND MOOSER FOR MEASURING RESISTIVITY AND HALL CONSTANT by L. J. van der Pauw (N. V. Philips); Rev. Sci. Inst. Vol. 31, pp. 1189-1192, Nov. 1960

The Dauphinee and Mooser circuit [Rev. Sci. Instr. 26, 660 (1955)] for the measurement of resistivity and the Hall effect is liable to certain systematic errors due to capacitive effects in the switches. The magnitude of these errors is estimated, and it is shown how they may be eliminated by the use of suitably placed trimming capacitors and by a suitable switching sequence. The sensitivity of the circuit is also calculated.

7309 TEMPERATURE DEPENDENCE OF THE RESISTIVITY, HALL COEFFICIENT, AND THERMAL POWER IN Ti_2O_3 by J. Yahia and H. P. R. Frederikse (NBS); Bull. Am. Phys. Soc., Ser. II, Vol. 5, p. 407 (A), Nov. 25, 1960

Measurements of the resistivity ρ, Hall coefficient R_H, and thermoelectric power Q of nonstoichiometric titanium sesquioxide (1 atomic percent excess oxygen) from 55°K to high temperatures were reported. Ti_2O_3 shows a transition point at 475°K, as evidenced by the sharply dropping resistivity and thermoelectric power. (The Hall coefficient was too small to measure above 400°K.) Above this point there are indications of metallic behavior (i.e., negative Q, positive temperature coefficient for ρ), and below this point the behavior is that of a p-type semiconductor. R_H and ρ increase at a decreasing rate as the temperature is lowered, and in some cases the samples show an approximately constant R_H and ρ below 100°K, suggesting a degenerate hole gas. The temperature dependence of the mobility suggests scattering by polar modes and by impurities at high and at low temperatures, respectively. The mobility is found to be $\sim 3\,cm^2/v\text{-}sec$ at 300°K. The thermoelectric power increases as the temperature decreases and goes through a maximum at about 100°K, decreasing again at lower temperatures. A simple analysis involving R_H, ρ, and Q yields an effective mass $\sim 5m_0$ (where m_0 is the electronic mass), and the same result is obtained from the mobility in the polar scattering range.

7310 PROPERTIES OF THERMALLY INDUCED CONDUCTIVITY IN SINGLE CRYSTALS OF CdS by A. P. Trofimenko, B. A. Fedorus, and A. K. Razmadze (Kiev Inst. Phys.); Soviet Phys. Solid State, Vol. 2, pp. 1033-1038, Dec. 1960

The effect of thermally induced conductivity (TIC) in single crystals of CdS is discussed. It has been observed that the capture cross section for electrons in CdS (S) specimens is dependent on the temperature. The extent to which traps are filled when TIC is maximum has been verified experimentally. The photosensitivity of specimens and the areas under the corresponding TIC curves are compared. A preliminary investigation of the effect of etching and surface treatment with glow discharge on the magnitude of TIC peaks is reported.

Anisotropy of Conductivity in SnS - See 7273

7311 ELECTRICAL PROPERTIES OF CERTAIN SEMICONDUCTING OXIDE GLASSES by V. A. Ioffe, I. B. Patrina, and I. S. Poberovskaya (Leningrad Silicate Chem. Inst.); Soviet Phys. - Solid State, Vol. 2, pp. 609-614, Oct. 1960

The electrical conductivity, thermoelectric power, dielectric losses and permittivity of glasses in the systems V_2O_5-P_2O_5,

V_2O_5-P_2O_5-BaO and WO_3-P_2O_5-K_2O are discussed. All these glasses are n-type semiconductors. The electrical conductivity of the glasses rises with increase of the content of the transition-metal oxides. The mechanism of the electrical conduction in the glasses is similar to the mechanism in crystalline oxides of transition metals. Maxima have been found in the temperature dependence of tan δ of the glasses. The activation energy of relaxation is close in magnitude to the activation energy of conduction.

SUPERCONDUCTIVITY

7312 CRITICAL FIELDS OF SUPERCONDUCTING TIN, INDIUM, AND TANTALUM by R. W. Shaw, D. E. Mapother, and D. C. Hopkins (U. Illinois); Phys. Rev., Vol. 120, pp. 88-91, Oct. 1, 1960

Precise ballistic-induction measurements of the critical field curves of tin, indium, and tantalum are reported. The measurements were made to provide more accurate data on the deviation of the critical field curves from the parabolic law. The resulting deviation functions are generally within the range of uncertainty of earlier measurements. The main experimental error in the observed deviation now arises from uncertainty in the extrapolation of the measurements to $0^\circ K$ from the present lower limit of $1.1^\circ K$. Measurements at lower temperatures which will eliminate some of this uncertainty are to be desired.

7313 ISOTOPE EFFECT IN Nb_3Sn by G. E. Devlin and E. Corenzwit (Bell Labs.); Phys. Rev., Vol. 120, pp. 1964-1965, Dec. 15, 1960

The isotope effect on the superconducting transition of Nb_3Sn is discussed. The measured value of -0.08 for the exponential factor is only 1/5 of that of the elemental superconductors which have been reported.

7314 RF HALL EFFECT IN A SUPERCONDUCTOR by G. Dresselhaus and M. S. Dresselhaus (Lincoln Lab.); Phys. Rev., Vol. 120, pp. 1971-1974, Dec. 15, 1960

The rf Hall field in a superconductor is calculated for the applied d-c magnetic field and the rf electric field both parallel to the metal surface. A two-fluid model and specular reflection boundary conditions are used to solve the transport problem in the limits of the classical and the extreme anomalous skin effects. It is found in both limits that the rf Hall effect is nonzero. The magnitude of the Hall angle in superconducting tin is estimated.

BREAKDOWN

7315 THE PROBLEM OF INTERNAL BREAKDOWN IN NONPOLAR SEMICONDUCTORS by G. V. Gordeev (Leningrad Physicotechnical Inst.); Soviet Phys.-Solid State, Vol. 2, pp. 571-577, Oct. 1960

Internal breakdown in pure nonpolar semiconductors is discussed. It is shown that equality of the energy obtained by electrons from the applied field and the energy transferred by electrons to the lattice may occur at any electron temperature. Consequently, the internal breakdown criterion of Froehlich and Paranjape, who suggested that this equality is not obeyed at finite electron temperatures, loses its physical sense for non-polar semiconductors. A different internal breakdown criterion which allows for ionization and recombination is introduced.

GALVANOMAGNETIC PROPERTIES

7316 HIGH-FIELD TRANSVERSE MAGNETORESISTANCE OF N-TYPE GERMANIUM by T. J. Diesel and W. F. Love (U. Colorado); Bull. Am. Phys. Soc., Ser. II, Vol. 5, p. 408 (A), Nov. 25, 1960

Measurements of the transverse magnetoresistance of high-purity, single-crystal, n-type germanium, in pulsed magnetic fields up to 194 kgauss in the temperature range from $11^\circ K$ to $78^\circ K$ were reported. "Hot electron" effects and nonohmic behavior of the crystal have obscured the results below about $20^\circ K$, but in the quantum limit and above the magnetoresistance was found to increase linearly with magnetic field above 40 kgauss. At $23^\circ K$ and 180 kgauss, the resistance of the crystal was about 19 times its zero field resistance. This resistance ratio has roughly a T^{-1} temperature dependence. The results of these experiments do not agree with theoretical predictions for various scattering mechanisms.

7317 MAGNETORESISTANCE OF HIGH PURITY InSb IN THE QUANTUM LIMIT by R. J. Sladek (Westinghouse Res. Lab.); J. Phys. Chem. Solids, Vol. 16, pp. 1-9, Nov. 1960

Magnetoresistance measurements made on high purity n-type InSb between $111^\circ K$ and $50^\circ K$ using magnetic field strengths up to 28 kG are reported. The results are in qualitative agreement with theory for the quantum limit for the case of piezoelectric scattering and classical statistics. Collision broadening seems to be the mechanism preventing the resistivity in a transverse field from diverging. Limitations on the comparison of the data with theory are discussed.

Measurement of the Hall Effect - See 7308

Anomalous Variation of Hall Coefficient with Temperature in SnS - See 7273

Temperature Dependence of the Hall Coefficient in Ti_2O_3 - See 7309

7318 PROPERTIES OF SEMICONDUCTORS WITH AN EXTREMUM LOOP I. CYCLOTRON AND COMBINATIONAL RESONANCE IN A MAGNETIC FIELD PERPENDICULAR TO THE PLANE OF THE LOOP by E. I. Rashba (Inst. of Physics, Kiev); Soviet Phys.-Solid State, Vol. 2, pp. 1109-1122, Dec. 1960

The absorption of radio waves in semiconductors having a specific band structure where an extremum is reached not at isolated points but over a curve in k-space is discussed. The frequencies and intensities of the transitions are computed. It is shown that as a result of the presence of spin-orbital bonds, transitions involving a change in spin due to the Lorentz force possess significant power.

GALVANOMAGNETIC PROPERTIES (Cont'd)

Magneto-Plasmas in Bi - See 7372

OTHER ELECTRICAL PROPERTIES

7319 TRAPPING NOISE IN CdS by J. J. Brophy (Armour Res. Found.); Bull. Am. Phys. Soc., Ser. II, Vol. 5, p. 408 (A), Nov. 25, 1960

The shape of the high-frequency portion of the current noise spectra observed in lightly doped CdS single crystals under uniform 5200A illumination is characteristic of electron trapping transitions in shallow levels. In many crystals the spectra have a 1/f behavior when the quasi fermi level is not located at a discrete trap. The 1/f trapping noise spectra observed in one sample at three temperatures and for twenty different positions of the electron quasi fermi level between 0.5 and 0.3 ev below the conduction band can be represented by a single expression of the form $(1/\omega)\tan^{-1}\omega\tau$, where τ is determined by the low-frequency turnover of the 1/f noise. From the experimental values of τ in each instance trap depths which are in good agreement with those determined from the discrete trapping spectra have been calculated. Since the low-frequency turnovers of the 1/f spectra are thus related to the discrete traps, rather than to the position of the electron quasi fermi level directly, it appears that the 1/f noise is not associated with a continuous distribution of traps in energy but rather with a dispersion of capture and release times into the discrete traps.

7320 PHOTOEMISSION AND VALENCE BAND STRUCTURE OF ALKALI IODIDES by H. R. Philipp, E. A. Taft and L. Apker (GE); Phys. Rev., Vol. 120, pp. 49-51, Oct. 1, 1960

Energy distributions for external photoelectrons ejected from CsI by photons of energy 11.3ev are described. All but about 5% of the photoelectrons emerge with kinetic energies between 1.5ev and 5.3ev. The conspicuous lack of electrons at lower energies is interpreted in terms of a valence band of width about 3 or 4ev with an upper edge lying about 6ev below the vacuum level. Related results are mentioned for RbI, KI, NaI, CsBr, and CsCl.

7321 INFLUENCE OF RELATIVE HUMIDITY ON SURFACE CONDUCTIVITY OF GERMANIUM by G. Dorda (Inst. Tech. Phys., Prague); Czech. J. Phys., Vol. 10B, No. 11, pp. 820-829, 1960

A study of the influence of relative humidity (from 0.5 - 90%) on the surface conductivity of both p- and n-type germanium having differing resistivity is reported. It was found that the range of changes in the surface potential did not depend on the volume properties of germanium. An analysis of the experimental results shows that the surface potential has values approximately in the range from $\phi_s = -3kT/q$ to $\phi_s = +5kT/q$ for a change in humidity from 0.5 to 90%. Assuming that the Fermi level changes on the outer side of the oxide layer by approximately the same value as on the germanium-germanium oxide boundary as a result of the increase and decrease of slow states, it follows that the levels of the slow centers are considerably distant from the Fermi level during the whole humidity range. It is also shown that on the first monomolecular layer of adsorbed water there is an increment of $(7.5 \pm 0.8) \times 10^{10}$ donor levels per cm^2. This increase in levels either decreases with the number of adsorbed monomolecular layers of water and for 90% humidity has approximately the value $2 \times 10^{10} cm^{-2}$ or remains almost unchanged with the number of layers, if it is assumed that for $\phi_s = 6.0kT/q$ the Fermi level passes through the centers of adsorbed water.

7322 SURFACE SPACE-CHARGE CALCULATIONS FOR SEMICONDUCTORS by D. R. Frankl (Gen'l Tel. and Electronics Labs.); J. Appl. Phys., Vol. 31, pp. 1752-1754, Oct. 1960

Approximation formulas for the surface excesses of carriers at large values of the reduced surface and bulk potentials are derived and computed results are presented.

7323 SOME ELECTRICAL AND OPTICAL PROPERTIES OF InSb-In_2Te_3 ALLOYS by J. C. Woolley, C. M. Gillett, and J. A. Evans (U. Nottingham); J. Phys. Chem. Solids, Vol. 16, pp. 138-143, Nov. 1960

The range of solid solution at the InSb end of the InSb-In_2Te_3 alloy system has been determined by x-ray methods to be about 15 mol per cent In_2Te_3, and the electrical and optical properties of the alloys in this range have been investigated. It is found from the electrical measurements of Hall effect and conductivity that for small percentages of In_2Te_3 (approximately less than 0.05 mol per cent) the added tellurium atoms act as donors in the InSb, giving carrier densities of approximately $10^{19} cm^3$. At higher percentages of In_2Te_3 this number of carriers is still present but the rest of the In_2Te_3 alloys with the InSb, giving vacancies on the indium sublattice. These results are confirmed by the infrared transmission measurements. It is found that in the composition range where the alloying effect predominates the Hall mobility is proportional to $N^{-1/3}$ where N is the fraction of sites vacant on the indium sublattice.

Electrical Properties of Some Peritectic Compounds - See 7274

MAGNETIC PROPERTIES

7324 MAGNETIC SUSCEPTIBILITY OF P-TYPE Ge by R. Bowers and Y. Yafet (Westinghouse Res. Lab.); Phys. Rev., Vol. 120, pp. 62-66, Oct. 1, 1960

Measurements of the magnetic susceptibility of p-type Ge for a range of extrinsic carrier densities extending from $5 \times 10^{17} cm^{-3}$ to $5 \times 10^{20} cm^{-3}$ are reported. The measurements were made in the temperature range 300°K to 1.3°K. The degenerate hole susceptibility was determined from the data. At the lower carrier densities, the data depart appreciably from the Landau-Peierls value; above $10^{20} cm^{-3}$ the data exhibit features due to the population of the split-off band. From the experimental results, it is estimated that the Fermi level touches the minimum of the split-off band at a carrier density of $1.3 \times 10^{20} cm^{-3}$. A qualitative discussion of the factors determining the susceptibility including band degeneracy and spin-orbit coupling is given, but a detailed quantitative analysis is not attempted.

7325 SUSCEPTIBILITY OF DONORS IN GERMANIUM by D. H. Damon and A. N. Gerritsen (Purdue U.); Bull. Am. Phys. Soc., Ser. II, Vol. 5, p. 408 (A), Nov. 25, 1960

Measurements of the magnetic susceptibility of several n-type germanium samples obtained by the Faraday method between

4.2°K and 1.35°K were reported. Sonder and Schweinler have observed that the spin paramagnetism of electrons localized on donors in silicon does not follow the Curie Law at moderate donor concentrations. They have explained this phenomenon in terms of a hydrogen molecule-like interaction between donors, they have predicted that similar behavior would be observed in n-type germanium with donor concentrations below $5 \times 10^{16} cm^{-3}$. The results reported concern germanium samples with donor concentrations between 2 and $6 \times 10^{16} cm^{-3}$. Both antimony and arsenic doped samples have been measured. Within experimental error these results show that the molecule theory predicts the observed temperature dependence of the donor susceptibility at appropriate donor concentrations. The antimony doped samples exhibit a stronger donor interaction and a larger orbital diamagnetism than the arsenic doped samples, consistent with the hydrogen model. The observed orbital diamagnetism of the localized electrons is smaller than that predicted for isolated donors. Again, this might be explained in terms of a hydrogen molecule-like interaction between donors.

7326 ANISOTROPY OF THE MAGNETIC SUSCEPTIBILITY OF GALLIUM by T. Pankey, Jr. (Howard U. and U.S. Geo. Survey); J. Appl. Phys., Vol. 31, pp. 1802-1804, Oct. 1960

Measurements of the bulk magnetic susceptibilities of single gallium crystals and polycrystalline gallium spheres at 25°C are reported. The following anisotropic diamagnetic susceptibilities were found: a axis $(-0.119 \pm 0.001) \times 10^{-6}$ emu/g, b axis $(-0.416 \pm 0.002) \times 10^{-6}$ emu/g, and c axis (-0.229 ± 0.001) emu/g. The susceptibility of the polycrystalline spheres, assumed to be the average value for the bulk susceptibility of gallium, was $(-0.257 \pm 0.003) \times 10^{-6}$ emu/g at 25°C, and $(-0.299 \pm 0.003) \times 10^{-6}$ emu/g at -196°C. The susceptibility of liquid gallium was $(0.0031 \pm 0.001) \times 10^{-6}$ emu/g at 30°C and 100°C. Rotational diagrams of the susceptibilities in the three orthogonal planes of the unit cell were not sinusoidal. The anisotropy in the single crystals was presumably caused by the partial overlap of Brillouin zone boundaries by the Fermi-energy surface. The large change in susceptibility associated with the change in state was attributed to the absence of effective mass influence in the liquid state.

7327 ORIGIN OF MAGNETOELASTIC EFFECTS IN COBALT-IRON FERRITE by J. C. Slonczewski (IBM); J. Phys. Chem. Solids, Vol. 15, pp. 335-353, Oct. 1960

The dependence of magnetostrictive strain and elastic coefficients on temperature and orientation of spontaneous magnetization is calculated for the special case of a cubic crystal containing an orbitally degenerate transition ion in a trigonal crystal field. The functional dependence of strain on orientation has a special form which cannot be expressed by means of standard phenomenological formulas. The strain is an order of magnitude larger than that which Tsuya calculated for certain ferrites not involving orbital degeneracy. The temperature dependence of strain agrees partially with measurements in cobalt-iron ferrite. By fitting theory to experiment a trigonal-field splitting of about $1600 cm^{-1}$ for the ground state of the cobalt ion is inferred. An orbitally degenerate transition ion should have a large electrical polarizability because its first excited state is separated from the ground state by only spin-orbit energy. This polarizability is shown to give rise to elastic energy which depends on orientation of magnetization. This energy should be appreciable in cobalt-iron ferrite.

7328 EQUATION OF STATE AND PHASE TRANSITION OF THE SPHERICAL LATTICE GAS by W. Pressman (USASRDL), and J. B. Keller (New York U.); Phys. Rev., Vol. 120, pp. 22-32, Oct. 1, 1960

The spherical lattice gas is a modification of the ordinary lattice gas in which the occupation number of each cell is permitted to be any real number rather than ±1. However, the sum of squares of the occupation numbers is required to equal the number of cells. This permits one to evaluate the partition function by integrating over the surface of a certain sphere rather than by summing over lattice points on that surface. The partition function and the equation of state of the gas are evaluated in this way. It is found that in three dimensions the gas condenses, but not in one or two dimensions. Graphs of the phase transition curve and of the isotherms in three, two, and one dimension are presented. The analytical work is simplified by taking advantage of the relationship between the properties of the lattice gas and of the Ising model of a ferromagnet. This relationship, demonstrated by C. N. Yang and T. D. Lee for the ordinary lattice gas and Ising model, also applies to the spherical lattice gas and the spherical model of a ferromagnet. The properties of the latter have been evaluated by T. H. Berlin and M. Kac. Graphs of the isotherms of the spherical model of the magnet are also presented.

7329 METHOD FOR DETERMINING GROUND-STATE SPIN CONFIGURATIONS by D. H. Lyons and T. A. Kaplan (Lincoln Lab.); Phys. Rev., Vol. 120, pp. 1580-1585, Dec. 1, 1960

The method of Luttinger and Tisza for finding the rigorous minimum of a quadratic form subject to certain strong constraints is generalized. In the extended method, one still minimizes the quadratic form with respect to a single weak constraint, which however now contains adjustable parameters. In determining the ground state for the classical Heisenberg exchange energy, some cases involving crystallographically nonequivalent spins can now be handled. The following applications are made. The ground state for a linear chain with two different types of spins is obtained. It is then proved that in the cubic spinel the Néel configuration is the ground state if it is locally stable - that is, it is never metastable. This result was assumed in a recent perturbation theory of spin configurations. Finally, a similar result concerning the Yafet-Kittel triangular configurations in noncubic spinels is discussed. In the course of the analysis it is shown that the ground state is always a spiral for any lattice in which the spins are equivalent.

7330 CONSIDERATIONS ON THE PROPAGATION AND GENERATION OF MAGNETOSTATIC WAVES AND SPIN WAVES by P. C. Fletcher and C. Kittel (Hughes Res.); Phys. Rev., Vol. 120, pp. 2004-2006, Dec. 15, 1960

The dispersion relation, magnetization distribution, and group velocity of magnetostatic waves in an infinite circular cylinder with the static magnetic field parallel to the cylinder axis are discussed. The dispersion relation of the modes with $e^{i\phi}$ angular dependence is, for $kR \gg 1$, $\omega \cong \gamma H_0 + \gamma 2\pi M_s (x_i/kR)^2 + (D/\hbar)k^2$, where x_i is a root of $J_0(x) = 0$; R is the cylinder radius; and D is the exchange constant. The group velocity of magnetostatic pulses at low wave vectors is shown to be considerably higher than magnon velocities.

7331 GENERAL SPIN-WAVE DISPERSION RELATIONS by R. F. Soohoo (Lincoln Lab.); Phys. Rev., Vol. 120, pp. 1978-

1982, Dec. 15, 1960

The general spin-wave dispersion relation obtained by a simultaneous solution of the equation of motion of the magnetization and Maxwell's equations is given. In contrast to previous calculations, the effects of conductivity, relaxation, exchange, and propagation are all properly taken into account. The resulting algebraic equation, being biquadratic in the square of the wave number, k^2, has four possible pairs of solutions. Some of these solutions correspond to growing plane waves while others represent attenuated ones in the direction of propagation. Whereas an analytical solution for k could be easily obtained for the special case where the wave vector k is in the direction of the static magnetic field ($\theta_k = 0$), the solution for the cases where $\theta_k \neq 0$ could be conveniently obtained only by numerical solution. The solutions for the latter cases have been obtained by using an IBM 709 computer and some of the representative results are given in graphical form. When relaxation and eddy current damping are neglected, the result reduces to that of Herring and Kittel in the static limit ($\omega \to 0$). Furthermore, it was found that the uniform precessional mode ($k = 0$) can truly exist only under very special conditions, namely, under the condition of zero permeability for one of the two normal modes in a gyromagnetic medium.

7332 DISPERSION RELATION FOR SPIN WAVES IN A FCC COBALT ALLOY by R. N. Sinclair and B. N. Brockhouse (Atomic Energy of Canada); Phys. Rev., Vol. 120, pp. 1638-1640, Dec. 1, 1960

Use of the technique of neutron spectrometry to measure the dispersion curve of the spin waves in a metal is discussed. The momentum distributions of inelastically scattered neutrons from a single crystal of fcc cobalt containing 8% of iron have been observed under constant energy transfer conditions. The observed neutron groups (which satisfied momentum and energy conservation between the neutrons and the spin-wave quanta) enabled the dispersion relation to be established. The response of the intensity of the neutron groups to an applied magnetic field was used to identify those of spin-wave origin. The dispersion relation is in agreement with the form predicted by the Bloch-Heisenberg spin-wave theory. Over the range of measurements, which was limited by the available spectrum of neutron energies, approximate isotropy was observed to hold. The value of the product of the exchange integral and the atomic spin is found to be $JS = (1.47 \pm 0.15) \times 10^{-2}$ ev. Assuming $S = 0.92$ the value for J is in poor agreement with a value obtained from the spin-wave interpretation of low-temperature magnetization data. Study of the widths of the neutron groups leads to the conclusion that the mean lifetimes of some of the spin waves are greater than 3×10^{-13} sec.

7333 SPIN-WAVE SPECTRUM OF YTTRIUM IRON GARNET by R. L. Douglass (U. California); Phys. Rev., Vol. 120, pp. 1612-1614, Dec. 1, 1960

The spin-wave spectrum of yttrium iron garnet is treated using a Hamiltonian involving nearest-neighbor a-a, d-d, and a-d isotropic exchange interactions. Values of the exchange constants are estimated from the molecular field constants of Pauthenet. Anisotropy and magnetic dipole-dipole interactions are neglected. Twenty spin-wave modes are found and their energies are calculated at points of cubic symmetry in k space. The dispersion relation of the single "acoustical" spin-wave mode is found to agree with the value previously reported by Meyer and Harris.

7334 THE CHANGE OF THE CURIE TEMPERATURE OF IRON-NICKEL ALLOYS DUE TO HYDROSTATIC PRESSURE by T. Kaneko (Tohoku U.); J. Phys. Soc. Japan, Vol. 15, pp. 2247-2251, Dec. 1960

Measurements of the change of the Curie temperature due to hydrostatic pressure for two iron-nickel alloys with a nickel concentration of 30 and 32 atomic percent respectively are reported. Hydrostatic pressure was produced with an apparatus of the Bridgman type and the measurements of magnetization were performed by the ballistic method. The change of the Curie temperature due to pressure was estimated to be -3×10^{-3} and -2.7×10^{-3} deg. $kg^{-2}cm^2$ for specimens with a nickel concentration of 30 and 32% respectively. Based on Smoluchowski's formula, the volume dependence of saturation magnetization at absolute zero $1/I_0 \cdot \partial I_0/\partial\omega$ and that of the molecular field coefficient $1/N \cdot \partial N/\partial\omega$ for a 30% nickel alloy were found to be 27 and -16 from the experimental results. Taking into consideration the volume dependence of the saturation magnetization at absolute zero, the relations among the volume dependence of the Curie temperature, molecular field coefficient and exchange integral are discussed.

7335 DIRECT EXCHANGE IN FERROMAGNETS by R. Stuart (Lawrence Radiation Lab.) and W. Marshall (Atomic Energy Res. Estab.); Phys. Rev., Vol. 120, pp. 353-357, Oct. 15, 1960

The direct exchange integral which occurs in the Heisenberg theory of ferromagnetism is evaluated for all internuclear spacings. It is found to be always positive, whereas Bethe originally suggested it would be positive only at large spacing and more recently it has been suggested that the integral should always be negative. However, at the observed internuclear separation the calculated magnitude is of the order of 70 times too small to explain the experimentally determined exchange constant in ferromagnetic metals, and it is therefore concluded that direct exchange is not responsible for ferromagnetism in these metals.

7336 MODEL OF EXCHANGE-INVERSION MAGNETIZATION by C. Kittel (U. California); Phys. Rev., Vol. 120, pp. 335-342, Oct. 15, 1960

A thermodynamic theory of a class of magnetic crystals which transform from ferromagnetic to antiferromagnetic states with a change in temperature is presented. Applications to $Mn_{2-x}Cr_xSb$ and to crystals having the nickel arsenide type structure are suggested. It is shown that the exchange magnetoelastic energy is often important in such transformations and leads to an additional interaction energy of the form $(S_A \cdot S_B)^2$ in the effective spin Hamiltonian. It is suggested that one of the exchange constants goes linearly through zero near a critical value of some lattice coordinate characterizing the transition. There are important differences in the behavior of compact and non-compact antiferromagnetic lattices, under the assumption of nearest-neighbor interactions between sublattices. A triangular array, such as might arise in crystal structures of the NiAs type, is treated.

7337 NEUTRON DIFFRACTION STUDIES OF CHROMIUM-MODIFIED Mn_2Sb by W. H. Cloud, H. S. Jarrett (du Pont), A. E. Austin and E. Adelson (Battelle Mem. Inst.); Phys. Rev., Vol. 120, pp. 1969-1970, Dec. 15, 1960

Existence of a ferrimagnetic to antiferromagnetic phase transition with decreasing temperature in Mn_2Sb modified with 2.3 weight percent chromium is confirmed by neutron diffraction.

7338 EXCHANGE ANISOTROPY IN COBALT-MANGANESE ALLOYS by J. S. Kouvel (GE); J. Phys. Chem. Solids, Vol. 16, pp. 107-114, Nov. 1960

Magnetization measurements between 4.2° and 750°K on Co-Mn alloys of about 25, 30 and 35 atomic per cent Mn indicate that no simple disappearance of ferromagnetism takes place with increasing Mn concentration, although the magnetic properties of these alloys are very sensitively dependent on composition. When cooled to 4.2°K in a magnetic field, all these alloys exhibit hysteresis loops that are asymmetrical with respect to the origin. This behavior, similar to that recently reported for Ni-Mn alloys, is believed to arise in this case also from exchange anisotropy interactions between regions of ferromagnetic and antiferromagnetic spin alignment. From the high temperature paramagnetic susceptibilities of these Co-Mn compositions and of disordered Ni-Mn alloys of 20 to 35 atomic per cent Mn, it is concluded that an increasing number of atomic moments are antiferromagnetically aligned with increasing Mn concentration in both alloy systems. It is shown that this result combined with the statistical composition fluctuations inherent to a disordered alloy provides a plausible model for the exchange anisotropy in these materials.

7339 EXCHANGE ANISOTROPY IN ALLOYS OF COMPOSITION (Ni, Fe)$_3$Mn by J. S. Kouvel (GE); J. Phys. Chem. Solids, Vol. 16, pp. 152-157, Nov. 1960

Disordered face-centered cubic alloys in which the nickel in the composition Ni_3Mn is partially replaced by iron have been studied magnetically over a wide temperature range (4.2-750°K). When cooled to 4.2°K in a magnetic field the alloys of less than about 50 atomic per cent iron exhibit hysteresis loops that are displaced from their symmetrical positions about the origin, as previously reported for the Ni_3Mn. At higher iron concentrations this exchange anisotropy behavior disappears, and the temperature and field dependences of magnetization become those characteristic of a simple antiferromagnet. This information together with paramagnetic susceptibility data suggest that while the Fe-Ni exchange coupling is strongly ferromagnetic both the Fe-Mn and Fe-Fe interactions are antiferromagnetic in this alloy system.

7340 THE STATISTICS OF SUPEREXCHANGE INTERACTION AND IONIC DISTRIBUTION IN SUBSTITUTED FERRIMAGNETIC RARE EARTH IRON GARNETS by S. Geller (Bell Labs.); J. Phys. Chem. Solids, Vol. 16, pp. 21-29, Nov. 1960

Ideas on the statistics of superexchange interaction developed and applied to substituted yttrium-iron garnets by Gilleo are extended and applied to substituted rare earth iron garnets. It is shown by means of structural considerations that only four interactions per c site ion with d site ions are important in determining the contribution of the c site ions to the 0°K saturation magnetization. The statistical theory accounts especially well for the behavior of n_B (0°K) vs x (=y+ z) of the system $\{Gd_3\}\,[Al_yFe_{2-y}]\,(Al_zFe_{3-z})\,O_{12}$ and for $\{Gd_{2.4}Ca_{0.6}\}\,[Al_yFe_{2-y}]\,(Al_{z-0.6}Si_{0.6}Fe_{3-z})\,O_{12}$ corrects the previously obtained ionic distribution which had been considered anomalous. Other systems are also considered. Crystal chemical aspects of some of the results, compensation points and some minor limitations of the treatment are discussed.

7341 ANISOTROPIC SUPEREXCHANGE INTERACTION AND WEAK FERROMAGNETISM by T. Moriya (Bell Labs.); Phys. Rev., Vol. 120, pp. 91-98, Oct. 1, 1960

A theory of anisotropic superexchange interaction is developed by extending the Anderson theory of superexchange to include spin-orbit coupling. The antisymmetric spin coupling suggested by Dzialoshinski from purely symmetry grounds and the symmetric pseudodipolar interaction are derived. Their orders of magnitudes are estimated to be $(\Delta g/g)$ and $(\Delta g/g)^2$ times the isotropic superexchange energy, respectively. Higher order spin couplings are also discussed. As an example of antisymmetric spin coupling the case of $CuCl_2 \cdot 2H_2O$ is illustrated. In $CuCl_2 \cdot 2H_2O$, a spin arrangement which is different from one accepted so far is proposed. This antisymmetric interaction is shown to be responsible for weak ferromagnetism in α-Fe_2O_3, $MnCO_3$, and CrF_3. The paramagnetic susceptibility perpendicular to the trigonal axis is expected to increase very sharply near the Néel temperature as the temperature is lowered, as was actually observed in CrF_3.

7342 LINEAR DECREASE IN THE MAGNETOCRYSTALLINE ANISOTROPY by C. Abraham and A. Aharoni (Weizmann Inst. Sci.); Phys. Rev., Vol. 120, pp. 1576-1579, Dec. 1, 1960

A previous attempt to reduce the theoretical coercive force by assuming that the magnetocrystalline anisotropy constant vanishes in a certain region is modified. The magnetocrystalline anisotropy is now taken as zero in a part of the "imperfection" region and assumed to increase linearly to its constant value in the remaining part. The coercive force is calculated as a function of two parameters: the dimensions of the zero and linear parts of the imperfection region. A further reduction in the coercive force has been obtained with respect to the previous case, but there is still a large discrepancy between the calculated and experimental values, for reasonable defect size.

7343 VALUE OF G' FOR SUPERMALLOY by G. G. Scott (GM); Phys. Rev., Vol. 120, pp. 331-332, Oct. 15, 1960

The gyromagnetic ratio of supermalloy determined by measurements of the Einstein-deHaas effect is reported. The value of 1.905 ± 0.002 obtained for g' is equivalent to a spectroscopic splitting factor g of 2.105. This is in good agreement with values obtained by ferromagnetic resonance experiments.

7344 KINETICS OF MAGNETIC ANNEALING IN COBALT-SUBSTITUTED MAGNETITE by W. Palmer (IBM); Phys. Rev., Vol. 120, pp. 342-352, Oct. 15, 1960

Measurements of the time dependence of the magnetic annealing effect in single crystals of magnetite containing various amounts of substituted cobalt by a technique which permits observation of the effect at the annealing temperature are reported. The annealing kinetics in a particular crystallographic direction are determined by measuring the decay of the torque in the (001) plane following a preparatory anneal in a direction 45° removed. The directions chosen for study are the [100] and [110] directions, which are nodes of the cubic torque curve. The absence of a cubic torque in the directions of measurement allows precise observation of the anneal-induced uniaxial torque. The annealing kinetics observed in the two directions are different, and the nature of the torque decay in both directions depends upon the cobalt concentration of the sample. The torque decay in the [100] direction is attributed to the redistribution of single cobalt ions and certain pairs of adjacent cobalt ions over the octahedral cation sites, whereas the decay in the [110] direction is attributed to the redistribution of cobalt ion pairs only. The results of a theoretical analysis of the

annealing kinetics that would result from such ionic redistribution are in good agreement with the experimental observations. Comparison of the annealing behavior of samples in different states of oxidation indicates that ionic redistribution occurs by a vacancy diffusion mechanism, and the activation energy observed for this process is 1.05 ± 0.03 ev. In addition to the measurements performed at the annealing temperature, the torque in the [110] direction was determined as a function of temperature in a sample which had been quenched at the end of its preparatory anneal. These two measurements are used to show that there exists a repulsive interaction energy of 0.093 ± 0.04 ev between two adjacent cobalt ions.

Magnetic Properties of Fine-Particle Nickel Ferrites - See 7275

7345 DOMAINS IN THIN MAGNETIC FILMS OBSERVED BY ELECTRON MICROSCOPY by H. W. Fuller and M. E. Hale (Lab. for Electronics); J. Appl. Phys., Vol. 31, pp. 1699-1705, Oct. 1960

A new method for observing full domains in thin magnetic films by electron microscopy is described. Observations are made with standard transmission instruments utilizing an off-centered objective aperture diaphragm as a knife edge. The method has the high-resolution advantage that the microscope is focused on the specimen during domain observations. Limitations of the method and comparisons with the previously reported defocusing technique are presented. Applications to the interpretation of complex domain patterns and cross-tie walls are demonstrated. The observations were made with electrostatic-focusing microscopes, the AEG-Zeiss and Trueb-Taeuber instruments, which allow the use of full objective power without influencing the magnetization distribution of low coercive force films. A second method using a knife edge that would potentially permit a simple measurement of the detailed magnetization distribution of a domain wall in a thin film is proposed.

7346 FERRIMAGNETIC RESONANCE IN EUROPIUM-IRON GARNET by T. Miyadai (Nippon Tel. and Tel.); J. Phys. Soc. Japan, Vol. 15, pp. 2205-2210, Dec. 1960

A ferrimagnetic resonance experiment in a single crystal and polycrystalline samples carried out by a microwave technique is described. It has been found, for the single crystal, that the temperature variations of the g-factor and the line width are similar to those of erbium-iron garnet (ErIG) except for the existence of a broad maximum in line width at about 200°K. These behaviors agree well with Kittel's theory proposed recently. At room temperature, $g_{eff} = 1.32$, $\Delta H = 600$ oe (anisotropy in line width having been hardly observed) and $K_1/M_s = -400$ oe (which is an order of magnitude larger than that of YIG). For polycrystalline samples, g_{eff} is essentially the same as for the single crystal sample. In the absorption curve, a secondary peak appears, below 200°K, in the lower magnetic field side of the main absorption peak. The electronic state of Eu^{3+} in the garnet crystal is briefly discussed.

7347 FERRIMAGNETIC RESONANCE IN RARE-EARTH DOPED YTTRIUM IRON GARNET by J. F. Dillon, Jr., and J. W. Nielsen (Bell Labs.); Phys. Rev., Vol. 120, pp. 105-113, Oct. 1, 1960

Resonance experiments on YIG crystals doped with each of the rare earth ions except Lu, Gd, and Pm are reported. Except for Ce these are thought to replace Y as trivalent ions. Measurements of the field for resonance in the (110) plane at 1.5°K for each of these samples are presented. In several cases there are also data up to about 25°K. Except for Ce, Eu, and Tm the curve H_{res} in (110) at 1.5°K shows characteristic structure. For Pr, Ho, and Tb this structure is dominated by very narrow peaks in H_{res}. For Nd, Sm, Dy, and Er it is relatively broad in angle. For Yb most of the structure is relatively broad in angle, but there is a very sharp but small spike in H_{res}. Or in the case of Tb and Yb do sharp spikes appear at other than symmetry directions. In some cases the height of the peaks falls off rapidly with increasing temperature starting at the lowest temperatures, but in other cases it does not change at first, then falls off.

7348 SUBSIDIARY RESONANCE IN THE COINCIDENCE REGION IN YTTRIUM IRON GARNET by F. C. Rossol (Bell Labs.); J. Appl. Phys., Vol. 31, pp. 2273-2275, Dec. 1960

The measurement of h_{crit}, the threshold rf field for subsidiary resonance, as a function of frequency throughout the coincidence region, and the behavior of μ''_{max} at rf fields exceeding h_{crit} are presented for a single-crystal yttrium iron garnet sphere at room temperature. The sphere has a linewidth of 480 moe measured at 3000 Mc. The h_{crit} curve obtained was quite flat at approximately 0.3 moe from 2000 Mc to 3300 Mc and increased by more than a factor of 6 within 150 Mc of either end; a much more sudden increase than was the case for previously measured spheres of wider linewidth. The measured curve is compared to a curve computed from Suhl's theory of subsidiary resonance at high power levels, and the effects of the linewidths ΔH and ΔH_k on the shape of the curve are considered. The variation of μ''_{max} with rf power above the threshold followed Suhl's $P^{-1/2}$ law rather closely for frequencies above 2700 Mc but exhibited fine structure and a slower fall-off for frequencies below.

Line Widths of Polished Single Crystal YIG Spheres - See 72[illegible]

7349 INTERMETALLIC COMPOUNDS BETWEEN LANTHANONS AND TRANSITION METALS OF THE FIRST LONG PERIOD II. FERRIMAGNETISM OF AB_5 COBALT COMPOUN[illegible] by K. Nassau, L. V. Cherry, and W. E. Wallace (U. Pittsburg[illegible] J. Phys. Chem. Solids, Vol. 16, pp. 131-137, Nov. 1960

Magnetizations determined at various temperatures for a series of substances represented by the type formula ACo_5, in which A is either Ce, Sm, Gd, Dy, Ho, Y or a mixture of Gd and Y were reported. The purpose of the study was to ascertain whether the atomic moments are aligned, at sufficiently low temperatures, and if so to elucidate as far as possible the nature of the alignment. The magnetization-temperature curves for YCo_5 and $SmCo_5$ indicate that they are normal ferromagnetic compounds at least down to 80°K, with Curie points at 975 and 1015°K, respectively. Their saturation magnetic moments indicate that the cobalt moments are aligned ferromagnetically. The curves for the other compounds show well defined Curie temperatures ranging from 685 to 1125°K but are unusual in that below a certain temperature, ranging up to 575°K, magnetization shows an anomalous fall with diminishing temperature. Analysis of these results and the observed saturation magnetizations show that the moments are aligned, but not ferromagnetically. The compounds appear to be ferrimagnetic. A discussion of the possible modes of alignment is presented. Thermomagnetic analysis shows that in most instances the compounds decompose when heated to the point at which the alignment of the atomic moments is destroyed.

7350 NUCLEAR RESONANCE STUDY OF ELECTRONIC MAGNETISM IN COPPER-NICKEL by D. L. Weinberg and N. Bloembergen (Harvard U.); J. Phys. Chem. Solids, Vol. 15, pp. 240-248, Oct. 1960

Alloying with 27, 38 or 43 per cent nickel is found to produce extreme broadening and asymmetry of the NMR of copper. Almost every observable copper nucleus appears to undergo a decrease in magnetic field. The width between derivative peaks is increased by as much as twelve times. It is satisfactorily proportional to or independent of applied field, according as electronic paramagnetism (in the 27 per cent alloy) or weak ferromagnetism is expected to be involved, but the central portion of the line expands in proportion to the field. The concentration dependences are much slower than that of the macroscopic magnetization. Isotropic indirect exchange coupling between the copper nuclei and the time average magnetic moments of the nickel atoms, and inhomogeneity of the Knight shift account for the measurements approximately. It is necessary to include large contributions from copper nuclei in non-cubic environments. The field and concentration dependences are interpreted in terms of inhomogeneous electronic magnetism in the ferromagnetic alloys. The nickel paramagnetism cannot be identified in alloys of up to 15 per cent nickel because of quadrupole effects.

7351 NUCLEAR MAGNETIC RESONANCE INTENSITIES IN ALLOYS by D. L. Weinberg (Harvard U.); J. Phys. Chem. Solids, Vol. 15, pp. 249-260, Oct. 1960

The steady state magnetic resonances of ^{63}Cu, ^{27}Al and ^{7}Li have been studied in the majority constituents of the Cu-Ni, Cu-Au, Al-Zn and Li-Mg alloy systems, over wide ranges of composition, magnetic field and temperature. Nuclear electric quadrupole effects are most prominent. The line widths, shapes and frequencies can be qualitatively understood in simple cases, but the predictions of the general statistical problem have not been obtained. Initial intensity reductions in copper alloys are consistent with screening of excess charge by conduction electrons and enhancement by antishielding factors. The field gradients seem to be primarily of charge origin when there is a valence difference, but those arising from size differences can be comparable. The intensity falls markedly less rapidly above about 20 per cent solute in Cu-Ni and Cu-Au, and increases very strongly at about 40 per cent Ni. The anomalous intensity is believed to arise from non-cubic configurations of solute atoms which give rise to small field gradients at the central nucleus. The influence of order in Cu-Au on the intensity is described better by the conventional long range order than short range order, because the former distinguishes between the Cu and Au sublattices. The predictions are compared with effects of heat treatment.

7352 NUCLEAR MAGNETIC RESONANCE IN TANTALUM METAL by J. I. Budnick (IBM) and L. H. Bennett (NBS); J. Phys. Chem. Solids, Vol. 16, pp. 37-38, Nov. 1960

Observations of the nuclear magnetic resonance of Ta^{181} in tantalum metal are discussed. The sample was a stack of high purity foil which was degassed and annealed. No resonance was observed in tantalum metal powder.

7353 NUCLEAR RESONANCE ABSORPTION IN Dy^{161} SITUATED IN Dy_2O_3 AND DYSPROSIUM IRON GARNET by S. Ofer, P. Avivi, R. Bauminger, A. Marinov, and S. G. Cohen (Hebrew U.); Phys. Rev., Vol. 120, pp. 406-408, Oct. 15, 1960

The recoil-free resonant absorption of the 26-kev γ ray ($T_{\frac{1}{2}} \sim 3\times10^{-8}$ sec) emitted in the decay of Tb^{161} by absorbers containing Dy^{161} is discussed. High Mössbauer efficiencies at room temperatures have been observed for sources and absorbers in the form of oxide and rare earth iron garnet. The line shapes obtained were very broad, of the order of 100 times the natural widths, and showed no resolved lines. The broad lines are interpreted as due to a wide complicated hyperfine spectrum whose details have been smoothed out by transitions between magnetic sublevels induced by paramagnetic relaxation. In the rare earth iron garnet, the exchange field acting on the rare earth ion should decouple the nuclear and electron spins. The effective magnetic field at the nucleus in the rare earth garnet is about 2×10^{6} oe.

7354 SELECTIVE SPIN EXCITATION AND RELAXATION IN NUCLEAR QUADRUPOLE RESONANCE by M. J. Weber and E. L. Hahn (U. California); Phys. Rev., Vol. 120, pp. 365-375, Oct. 15, 1960

An investigation of nuclear relaxation in a quadrupole spin system by selectively exciting nuclei into particular magnetic levels and observing the transient recovery of the spin system toward an equilibrium population distribution is reported. Selective excitation is achieved by correlating the frequency and processional behavior of nuclei in certain states with applied elliptically and linearly polarized, pulsed radio-frequency fields. A quantum-mechanical analysis is presented to describe the excitation of a quadrupolar spin system produced by a pulsed, elliptically polarized rf field. Using selective excitation techniques, several new modes of longitudinal relaxation are observed. Experiments using the chlorine quadrupole resonance in a single crystal of $KClO_3$ demonstrate how these new relaxation modes are used (1) to study dynamic spin-spin interactions and cross relaxation between overlapping resonance lines, and (2) to determine the individual $\Delta m = \pm 1$ and ± 2 quadrupolar spin-lattice relaxation transition probabilities. A method is introduced by which the magnetic dipole-dipole contribution to the resonance linewidth can be determined independently of static quadrupole broadening, by observing the decay of the beat modulation of certain free-induction signals caused by precession in a small magnetic field. The measured magnetic line-width of Cl^{35} in $KClO_3$ is in good agreement with the value obtained from a second-moment calculation.

7355 CROSSOVER TRANSITIONS by M. W. P. Strandberg (MIT); J. Phys. Chem. Solids, Vol. 16, pp. 39-43, Nov. 1960

Finite-rotation operators are used to simplify the calculation of second-order, crossover transitions for a spin 3/2 system with trigonal symmetry. The resonant frequency and transition probabilities for the + 3/2, - 1/2 crossover transition with negative D (or + 1/2, - 3/2 with positive D) are calculated.

7356 PARAMAGNETIC SUSCEPTIBILITY OF AN ELECTRON GAS IN ALKALI METALS by M. Shimizu (Tokyo Metropolitan U.); J. Phys. Soc. Japan, Vol. 15, pp. 2220-2235, Dec. 1960

The paramagnetic susceptibility of an electron gas is calculated by making use of the Bohm-Pines description of electron interactions. The contribution from the long-range correlation to the susceptibility calculated by Pines is modified by using the larger cutoff wave vector of plasma oscillations and including the new contribution from the zero-point energy of plasma

oscillations. The contribution from the second-order perturbation-theoretic calculation of the screened Coulomb interactions is obtained by a proper approximation. The contribution from the third-order perturbation-theoretic calculation of the interactions is obtained by a rather crude approximation. The comparisons of paramagnetic susceptibility with experimental values for alkali metals are made and the agreements for Li and Na are satisfactory. The volume dependences of paramagnetic susceptibility for alkali metals are examined by comparing the experimental results on the pressure dependence of the Knight shift with the Brooks calculations of the Fermi interaction.

7357 EFFECT OF CONFIGURATION MIXING AND COVALENCY ON THE ENERGY SPECTRUM OF RUBY by S. Sugano and M. Peter (Bell Labs.); Bull. Am. Phys. Soc., Ser. II, Vol. 5, p. 415 (A), Nov. 25, 1960

For the purpose of improving a previous analysis of the optical and microwave spectrum of ruby, a calculation has been performed in the strong cubic field scheme, taking into account the effect of configuration mixing of the higher excited t_2^2e states into the t_2^3 states. In the calculation, covalency of the t_2 and e electrons is also introduced in a simplified fashion besides the spin-orbit interaction, trigonal field, and Zeeman energy. The result shows that the configuration mixing and the covalency play very important roles in giving zero-field splittings and g-values of the t_2^3 states. It is also found that there is not much difference in the degrees of covalency for the t_2 and e electrons, although they are fairly large for both electrons. The best zero-field splitting of the ground quartet thus obtained is $0.24\,cm^{-1}$ with the correct sign.

7358 CRYSTAL FIELD SPLITTING IN $KNiF_3$ by K. Knox, R. G. Shulman, and S. Sugano (Bell Labs.); Bull. Am. Phys. Soc., Ser. II, Vol. 5, p. 415 (A), Nov. 25, 1960

The cubic perovskite crystal $KNiF_3$ in which the Ni^{++} ion is surrounded by a regular octahedron of fluoride ions allows a direct comparison between crystal field theory and the optical absorption spectrum. Measurements of the optical spectrum of a single crystal from $4000\,cm^{-1}$ to $45,000\,cm^{-1}$ in a Cary double-beam spectrometer from $300^{\circ}K$ to $4.2^{\circ}K$ were reported. Seven bands and two lines have been identified and shown to agree with the spectrum predicted by assuming the crystal field splitting to be $10\,Dq = 7250\,cm^{-1}$. At low temperatures the $^1\Gamma_3$ line splits into two lines at $15,800\,cm^{-1}$ and $16,190\,cm^{-1}$. In $KNiF_3$ the bands shift to higher frequencies by several hundred wave numbers, going from $300^{\circ}K$ to $77^{\circ}K$ through T_N, whereas for paramagnetic $KMgF_3$:5% Ni the shift is much smaller. With the ligand field functions determined by nuclear magnetic resonance experiments it is possible to calculate values of 10 Dq and the other observed parameters. A comparison between theory and experiment was presented.

Crystalline Field for Ni^{2+} and Co^{2+} in Single Crystals of MgO, ZnO, ZnS, $MgAl_2O_4$ and YGaG - See 7379

7359 PULSED FIELD MEASUREMENTS OF LARGE ZERO-FIELD SPLITTINGS: V^{3+} in Al_2O_3 by S. Foner and W. Low (Lincoln Lab.); Phys. Rev., Vol. 120, pp. 1585-1588, Dec. 1, 1960

Use of pulsed magnetic fields for determining large zero-field splittings of paramagnetic ions is considered. Measurements of zero-field splittings of over $50\,cm^{-1}$ are feasible; a numerical example for S=1 is discussed in order to indicate the present range and limitations of the method. The method is applied to measurements of the zero-field splitting of V^{3+} in Al_2O_3 a $4.2^{\circ}K$ and $1.5^{\circ}K$. Assuming $g_{\parallel} = 1.92$, $D = 7.85\,cm^{-1}$ was determined from experiments with 4mm and 8mm wavelength radiation and pulsed magnetic fields of the order of 100 kilogauss. The magnitude and sign of D are in good agreement wi earlier estimates from optical and microwave measurements.

7360 ZEEMAN EFFECT OF THE PURELY CUBIC FIELD FLUC ESCENCE LINE OF MgO:Cr^{3+} CRYSTALS by S. Sugano, A L. Schawlow and F. Varsanyi (Bell Labs.); Phys. Rev., Vol. 120, pp. 2045-2053, Dec. 15, 1960

Both transverse and longitudinal Zeeman effects of the most conspicuous red emission line ($14\,319\,cm^{-1}$) of a MgO:Cr^{3+} single crystal are discussed. The Zeeman patterns are exam ined experimentally, with a magnetic field parallel to the [001], [110] and [111] axes, with linear polarizations paralle and perpendicular to each direction of the magnetic field anc with circular polarizations around the magnetic field. Compa ing these patterns with those theoretically calculated under t reasonable assumptions, it is found that the line is a magnetic dipole radiation due to the $t_2^3\,{}^2E \rightarrow t_2^3\,{}^4A_2$ transition of chrom ium ions with purely cubic environments. It is also found tha the Jahn-Teller coupling of chromophoric electrons and lattic in the excited state may be ignored in explaining the Zeemar effect.

7361 ROTATIONAL PROPERTIES OF PARAMAGNETIC RESC NANCE SPECTRA OF NON-CUBIC CRYSTALS by M. Sachs (Lockheed); J. Phys. Chem. Solids, Vol. 15, pp. 291-305, Oct. 1960

The complete symmetry group for each of the twenty-seven nc cubic point groups is exploited in a derivation of the rotation properties of paramagnetic resonance spectra of non-cubic cr tals. The energy eigenvalues for the magnetic substates of th ground state energy level of the paramagnetic crystal (in a un iform magnetic field) are derived as a function of the polar ar azimuthal angles which locate the direction of the applied mc netic field with respect to the crystal coordinate system. The theory, which gives the line positions to second order in $|\langle e\phi_c\rangle|/|\langle \mu \cdot H\rangle|$, is applicable to an analysis of micro wave spectra in which the non-cubic part of the electrostatic potential energy of the crystal ($e\phi_c$) is small compared with th magnetic energy term ($-\mu \cdot H$). The results of the general formulation are applied explicitly to the case in which the local electrostatic crystalline potential field at the magnetic ion site is any of the trigonal or hexagonal symmetry types.

7362 RADIATION INDUCED PARAMAGNETIC DEFECTS IN POTASSIUM AZIDE by D. Mergerian and S. A. Marshall (Armour Res. Found.); Bull. Am. Phys. Soc., Ser. II, Vol. 5, p. 419 (A), Nov. 25, 1960

Electron paramagnetic resonance absorption observed in single crystals of potassium azide irradiated by a 50-kv x-ray source at room temperature was discussed. These crystals take on a deep brown coloration and exhibit a magnetic resonance absorption in the neighborhood of g=2 which consists of from 12 to 14 lines. Of these, 6 lines are from 5 to 10 times more intense than the remainder and appear to form two distinct group of 3 lines each which saturate at different rates. One of the groups of 3 lines further shows a hyperfine structure consisting of at least 7 lines with line widths of approximately 1 œ. Each group of 3 lines is attributed to a separate defect center; this hypothesis is further supported on the basis of the two optical absorption bands observed in similarly colored crystals by Tom kins and Young. Orientation studies and saturation effects

observed at 77°K on each of the 3 line groups were also presented.

7363 PARAMAGNETIC RESONANCE OF NO IN KCl by C. Jaccard (Argonne Natl.Lab.); Bull. Am. Phys. Soc., Ser. II, Vol. 5, p. 418 (A), Nov. 25, 1960

Crystals of KCl doped in the melt with KNO_2 or KNO_3 and irradiated with x-rays at room temperature show in EPR many different paramagnetic centers. One of these, a triplet, is strongly anisotropic up to room temperature, where it decays in half an hour. The principal axis (z) of the g and HFS tensors is in the [100] direction, and the x- and y-axes in [011] and [0$\bar{1}$1]. The g values are $g_z = 2.0038 \pm 0.0002$, $g_x = 2.0070 \pm 0.0004$, $g_y = 2.0097 \pm 0.0004$, and the HFS parameters at -50°C are $A = 30.9 \pm 0.2$, $B + 7.0 \pm 0.3$, and $C = 5.0 \pm 0.3$ gauss. The relative concentration of this center is enhanced in a pure crystal heated at 700°C for two days in a flow of NO gas, and the bleaching of F centers increases markedly the ERP signal intensity. One of the models considered is an NO^+ (in a positive ion vacancy) which has trapped an electron during irradiation to become an NO molecule. Although the vacancy volume would allow the center to rotate, it must be bound with a neighboring chlorine ion to give the anisotropy.

7364 ELECTRON PARAMAGNETIC RESONANCE OF MANGANESE IN TiO_2 by H. G. Andresen (USASRDA); Phys. Rev., Vol. 120, pp. 1606-1611, Dec. 1, 1960

Measurements of the paramagnetic resonance spectrum of a manganese-doped single crystal of TiO_2 in its rutile structure at a frequency of 9.505 kMc/sec at room temperature are reported. The following results were obtained: The manganese atoms replace the Ti^{4+} ions in the rutile and exist as tetravalent ions having a spin value of $S = 3/2$ and strong admixtures of covalent bonds to their six oxygen neighbors. The parameters of the spin Hamiltonian were determined to be $g = 1.990$, $|D| = 12.1$ kMc/sec, and $|E| = 0.388$ kMc/sec. Within the accuracy of this experiment the magnetic hyperfine structure was isotropic and could be described by $|A| = 215$ Mc/sec.

7365 PARAMAGNETIC RESONANCE SPECTRUM OF Mn^{2+} IN $ZnSiF_6{:}6H_2O$, $\Delta m = \pm 1$ TRANSITION by E. Friedman and W. Low (Hebrew U.); Phys. Rev., Vol. 120, pp. 408-410, Oct. 15, 1960

In the spectrum of Mn^{2+} in $ZnSiF_6{:}6H_2O$ a number of weaker lines are observed at intermediate angles of the magnetic field H with respect to the crystal axis, in addition to the 30 allowed transitions $\Delta M = \pm 1$, $\Delta m = 0$. These lines have been measured and assigned to $\Delta M = \pm 1$, $\Delta m \pm 1$ transitions. The relatively strong intensity is explained and the intensity of the lines is shown to be proportional to $(D/A)^2 \cos^2\theta \sin^2\theta$. These forbidden transitions can be utilized for dynamic polarization of manganese nuclei.

7366 CROSS RELAXATION IN DILUTE PARAMAGNETIC SYSTEMS by A. Kiel (Johns Hopkins U.); Phys. Rev., Vol. 120, pp. 137-140, Oct. 1, 1960

The theory of cross relaxation developed by Bloembergen, Shapiro, Pershan, and Artman is applied to the case of highly diluted paramagnetic salts. It is found that the second moment for cross relaxation between two diluted paramagnetic species may be far greater than the sum of the second moments of individual lines which would be obtained from ordinary line width measurements. The dominance of cross relaxation in cases where the separation between the interacting resonances is up to twenty times the sum of the diluted linewidths can thus be explained.

7367 TRAPPED RADICALS IN ORGANIC DEPOSITS by R. Mangiaracina and S. Mrozowski (U. Buffalo); Bull. Am. Phys. Soc., Ser. II, Vol. 5, p. 419 (A), Nov. 25, 1960

The preparation of polymeric deposits showing a paramagnetic absorption by passing an electrical discharge through vapors of relatively simple organic compounds was described. Very high-spin concentrations (10^{20} per gram) were obtained in films formed using naphthelene vapor ($C_{10}H_8$), the absorption having a line width of 9 gauss. The nature of the deposited films varies with the distance from the electrodes, the color changing from dark brown to yellow and the spin absorption decreasing as the distance increases. To check whether these spin centers are related to the centers formed when organic substances are charred, such films were heat treated to various temperatures. It was found that above 200°C, as the heat-treatment temperature increases, the spin concentration rapidly diminishes, reaching a minimum at around 400°C. Above 400°C a strong absorption develops (maximum at around 650°C) which shows all the features of the absorption observed in chars. Thus there seems to be no relation between the molecular type radicals present in such polymers and the spin centers in chars, as suspected. Further work on these polymers including studies of infrared and ultraviolet absorption is in progress.

7368 FORMATION OF SPIN CENTERS IN CARBONS BY CHEMICAL ATTACK by K. Antonowicz (U. Buffalo); Bull. Am. Phys. Soc., Ser. II, Vol. 5, p. 419 (A), Nov. 25, 1960

It was reported that high concentrations of electron spin centers can be obtained in carbon originally heat treated at temperatures 1000-2400°C by reheating them to around 1000°C in an oxidizing (oxygen, sulfur) or reducing (hydrogen) atmosphere. The free spins were detected at room temperature using a paramagnetic spin resonance spectrometer. The intensity, width, and shape of the absorption line depend on the pressure of the gas, duration and temperature of the reheat, as well as the whole previous history of the carbon sample. Observed width varied from 25 to 0.9 gauss, with the shape varying from Lorenzian for narrow to Gaussian-like for broad lines. Unsymmetrical lines were obtained under special conditions, becoming symmetrical upon further treatment. All spin centers are destroyed by heating the sample to above 1000°C in vacuum. In some cases a strong reversible broadening by oxygen atmosphere was found, the oxygen sensitivity depending on the conditions of preparation. The observed data indicate that the spin centers are created by chemical attack at the boundaries of carbon crystallites and are essentially similar to those observed in chars.

OPTICAL PROPERTIES

7369 THE PIEZO-OPTIC AND ELECTRO-OPTIC CONSTANTS OF ZINCBLENDE by R. Bechmann (USASRDL); J. Phys. Chem. Solids, Vol. 16, pp. 100-101, Nov. 1960

The piezo-optic constant, Π_{44}, the elasto-optic constant, p_{44}, and the electro-optic constant, r_{41}, of zincblende are

considered. The values for the piezo-optic constants Π_{44} and p_{44} given in the literature are corrected.

7370 EXCITON AND MAGNETO-OPTICAL EFFECT IN STRAINED AND UNSTRAINED GERMANIUM by D. F. Edwards and V. J. Lazazzera (U. Michigan); Phys. Rev., Vol. 120, pp 420-426, Oct. 15, 1960

Measurements of the direct transition magneto-optical effect in strained and unstrained germanium at 77°K are reported. The results indicate that the absorption peaks correspond to transitions to exciton levels associated with each Landau level, in qualitative agreement with the calculations of Loudon, and Howard and Hasegawa. A definitive experiment is suggested to test this theory.

7371 THE EFFECT OF ELASTIC STRAIN ON THE ANOMALOUS TRANSMISSION OF X-RAYS IN GERMANIUM by G. E. Brock (IBM); Properties of Elemental and Compound Semiconductors, (Interscience), pp. 211-224, 1960

The intensity of anomalously transmitted x-rays through a nearly perfect single crystal may be changed by elastically straining it. Using CuK Radiation, the integrated intensity for the 220 Laue reflection has been determined as a function of elastic bending strain for various germanium crystals. The results indicate that simple models previously proposed to explain intensity changes are not satisfactory. It is found that dislocation-free germanium crystals show a high anomalous transmission which decreases quite rapidly with applied bend whereas crystals containing 100 dislocations/cm^2 or more transmit less but show little intensity variation with bend. Annealing experiments suggest that transmission may be related to strain centers associated with point defects.

7372 FAR INFRARED STUDIES OF BISMUTH by W. S. Boyle and A. D. Brailsford (Bell Labs.); Phys. Rev., Vol. 120, pp. 1943-1949, Dec. 15, 1960

Zero-field and magneto-optic studies of bismuth covering a range of frequencies where the plasma effects are large and rapidly changing are reported. It is found that the data lend themselves to an interpretation in terms of classical magneto-plasma theory when anisotropy is taken into account. The contribution of the free carriers to the optical properties can be isolated from the interband transitions and hence the static value of the dielectric constant, ϵ_0, the number of free electrons per cc, n, and the effective-mass parameters for the electron band can be determined when used in conjunction with the results of cyclotron resonance studies.

7373 THEORY OF INFRARED ABSORPTION IN CRYSTALS by L. E. Gurevich and Z. I. Uritskii (Leningrad Inst. Phys. and Tech.); Soviet Phys.-Solid State, Vol. 2, pp. 1123-1133, Dec. 1960

Absorption of long-wave radiation by crystals at frequencies $\omega<\omega_0$ (ω_0 is the photoelectric threshold) and also in the fundamental absorption region is discussed. In the first case phonon absorption was investigated by inducing with light in crystals virtual excitations which decayed with the production of phonons. It was shown that in the continuous and discrete absorption regions the most important is absorption accompanied by the production of two phonons. Absorption by free carriers in a magnetic field was also investigated. The absorption coefficient was found to oscillate when degeneracy was present and also in the case when there was no degeneracy, but in a strong magnetic field $\hbar\Omega \gg T$ (Ω is the Larmor frequency and T is temperature expressed in energy units). For the fundamental absorption in a magnetic field, oscillations of the absorption coefficient were a function of $\frac{\omega-\omega_0}{\Omega}$ with a period equal to one. In the case of degeneracy the absorption edge was displaced, and oscillated owing to the oscillations of the Fermi level.

7374 ABSORPTION OF INFRARED RADIATION BY A SEMICONDUCTOR IN AN ELECTRIC FIELD by N. V. Fomin (Leningrad Polytechnic Inst.); Soviet Phys.-Solid State, Vol. 2, pp. 566-568, Oct. 1960

The dependence of the absorption of infrared radiation by current carriers in nondegenerate semiconductors on the angle between the directions of polarization of light and the electric field is considered. It is shown that when $eEl \ll kT$ (where E is the field, l the carrier mean free path) the effect becomes squared with respect to the field.

7375 EFFECT OF ISOTOPIC COMPOSITION ON INFRARED ABSORPTION OF SOLID LITHIUM HYDRIDE by W. B. Zimmerman and D. J. Montgomery (Michigan State U.); Bull. Am. Phys. Soc., Ser. II, Vol. 5, p. 415 (A), Nov. 25, 1960

Measurements of infrared absorption spectra from 12.5 μ to 25 μ at room temperature for thin films of lithium hydride made from varying proportions of Li^6 and Li^7, H^1 and H^2 were reported. With suitable film thicknesses (0.03 μ - 2 μ), distinct and reproducible absorption maxima were observed. For the isotopically pure compounds, a single absorption maximum was observed, the position shifting as the square root of the reduced mass. This behavior, in conformity with the predictions of the simple Born theory, has been observed in Li^6F and Li^7F, and in Li^7H and Li^7H^2. For isotopically impure compounds in which the departure from purity is slight, or in which the isotopes differ only slightly in mass, the behavior cannot be differentiated from that expected for a single isotopic species of the average isotopic mass. But otherwise the behavior is complicated, the shape of the patterns changing and the shifts following no obvious rule.

7376 FREE CARRIER ABSORPTION ARISING FROM IMPURITIES IN SEMICONDUCTORS by S. Visvanathan (Philco); Phys. Rev., Vol. 120, pp. 379-380, Oct. 15, 1960

The free carrier absorption due to ionized impurities in semiconductors is essentially the inverse process of bremsstrahlung. The cross section for bremsstrahlung is readily available in the literature and one can calculate the spectral distribution of bremsstrahlung for the carriers in a semiconductor; furthermore, by using Kirchhoff's law of radiation, relating the emission and absorption in the semiconductor, one arrives quite easily at the absorption coefficient. The results so obtained agree with those of previous authors who have used a different method of calculation. The inadequacy of the Born approximation in the calculation of the ionized impurity effects on free carrier absorption is brought out clearly in this treatment.

7377 OPTICAL ABSORPTION AND RECOMBINATION RADIATION IN SEMICONDUCTORS DUE TO TRANSITIONS BETWEEN HYDROGEN-LIKE ACCEPTOR IMPURITY LEVELS AND THE CONDUCTION BAND by D. M. Eagles (SERL); J. Phys. Chem. Solids, Vol. 16, pp. 76-83, Nov. 1960

A simplified theory of the expected form of the optical absorption and recombination radiation spectra due to direct

transitions between hydrogen-like acceptor levels and the conduction band in a semiconductor with simple bands is given. Some necessary modifications to the simple theory are discussed, and it is shown that transitions from acceptor levels could be the cause of an observed shift of the absorption edge to longer wavelengths on passing from n- to p-type GaAs. For recombination radiation, some experimental curves on the III-V compounds which probably involve transitions to impurity levels are rather broader than those predicted by the simple theory.

7378 EVIDENCE FOR INTERNAL ROTATION IN THE FINE STRUCTURE OF THE INFRARED ABSORPTION OF OXYGEN IN SILICON by H. J. Hrostowski and B. J. Alder (Bell Labs.); J. Chem. Phys., Vol. 33, pp. 980-990, Oct. 1960

Interpretation of the spectra of silicon saturated with oxygen highly enriched with O^{18} confirms that oxygen is located in an interstitial site. The over-all features of the absorption indicate that the oxygen is in a nonlinear Si_2O configuration. The fine structure in the asymmetric Si-O stretching vibration and its temperature dependence can be largely explained by motion of the oxygen in a potential barrier with six-fold symmetry. A symmetry analysis of this process predicts additional structure some of which has now been observed under higher resolution. The spectra of oxygen contaminated silicon containing 2% germanium corroborate this explanation of the fine structure. The potential barrier hindering rotation of the oxygen about the axis joining its two bonded silicons has been ascribed to the surrounding silicon lattice. Calculation of the potential shows that as the oxygen rotates it can also wobble. Since the fine structure indicates that the ground-state splitting due to rotation is near $2\,cm^{-1}$, the barrier hindering rotation is about 200 cal/mole. Calculation of this barrier then indicates that the maximum wobble angle is 0.2° and the Si-O-Si angle near 150°.

7379 OPTICAL ABSORPTION OF Ni^{2+} AND Co^{2+} IN CUBIC SYMMETRY by R. Pappalardo, D. L. Wood, and R. C. Linares, Jr. (Bell Labs.); Bull. Am. Phys. Soc., Ser. II, Vol. 5, p. 416 (A), Nov. 25, 1960

Measurements of the optical absorption of Ni^{2+} and Co^{2+} in single crystals of MgO, ZnO, ZnS, Mg Al_2O_4, and yttrium gallium garnet at room temperature, $78^\circ K$ and $4.2^\circ K$ in the $2.5\,\mu$ to $0.2\,\mu$ region were reported. In all these systems the crystal field acting on the impurity ion has predominantly cubic symmetry, while the coordination number can be four, six, or eight. In MgO crystals with low impurity level the usual intense intra-system bands have been resolved into individual components, some of which are narrow lines, with half-width $\sim 5\,cm^{-1}$ at $4.2^\circ K$. Considerable fine structure was also found in the spectrum of the ZnO crystals, and its connection to spin-orbit coupling effects was discussed. Finally, the spectra of Ni^{2+} and Co^{2+} in MgO and ZnO were used to infer the site symmetry of these ions in Mg Al_2O_4 and yttrium gallium garnet.

7380 FREE CARRIER ABSORPTION DUE TO POLAR MODES IN THE III-V COMPOUND SEMICONDUCTORS by S. Visvanathan (Philco); Phys. Rev., Vol. 120, pp. 376-378, Oct. 15, 1960

The longitudinal polar modes of vibration in the III-V compound semiconductors play an important part in determining their transport properties, such as mobility. One would therefore expect them to be important for free carrier absorption, as well, in these semiconductors. A quantum mechanical calculation of the free carrier absorption arising from these modes which gives an absorption varying as $\lambda^{2.5}$ is presented. Such behavior has been reported experimentally in InP and GaP. The calculated value of the absorption coefficient in InP is in good agreement with experiment.

7381 PHOTON ABSORPTION BY VALENCE ELECTRONS IN MAGNESIUM by H. Kroger and D. H. Tomboulian (Cornell U.); Bull. Am. Phys. Soc., Ser. II, Vol. 5, p. 415 (A), Nov. 25, 1960

Use of a normal incidence vacuum spectrograph having a dispersion of 4.26 A/mm to measure the photon absorption by magnesium in the spectral region extending from 230 A to 650 A was reported. This region corresponds to photon energies in the 55-ev to 20-ev range. The resolution at the high-energy end is better than 0.1 ev. Measurements made on evaporated films (thickness 500 A to 4000 A) indicate that fine structure exists on the low-energy side of the L absorption edge. Such structure must be ascribed to photon absorption by valence electrons since the threshold energy corresponding to the $L_{2,3}$ edge is located at 49.5 ev. For magnesium, absorption maxima are found at the following photon energies expressed in ev: 21.7, 28.0, 31.7, 35.0, 38.7, 40.7, 44.5, and 46.7. These results were compared with x-ray fine structure data and with recently published results on eigen loss measurements.

Color Centers - See 7234, 7235, 7236, 7237, 7238, 7239

7382 PROPOSED MECHANISM FOR FAR INFRARED ABSORPTION IN IONIC CRYSTALS by K. Dransfeld and H. E. Bömmel (Bell Labs.); Bull. Am. Phys. Soc., Ser. II, Vol. 5, p. 416 (A), Nov. 25, 1960

For low frequencies and high temperatures the far infrared absorption in ionic crystals may be considered as a relaxation process. The low-frequency electric field of the incident radiation leads to a shift of the vibrational energy states of the crystal, predominantly for phonons of very short wavelengths, thereby disturbing the thermodynamic equilibrium. In order to re-establish equilibrium the occupation numbers will rearrange themselves in a relaxation time τ, determined by phonon-phonon collisions. The absorption per cm of electromagnetic waves of frequency ω due to this relaxation process should vary as ω^2 at high temperatures ($\omega\tau<1$) as observed for NaCl and KCl, and it should disappear at low temperatures ($\omega\tau>1$) consistent with absorption measurements for the same salts down to liquid air temperature.

7383 OPTICAL ABSORPTION SPECTRA OF THE FIRST TRANSITION SERIES IONS IN CdS by R. E. Dietz and R. Pappalardo (Bell Labs.); Bull. Am. Phys. Soc., Ser. II, Vol. 5, p. 416 (A), Nov. 25, 1960

Doping of single crystals of CdS by diffusion with ions of the first transition series and measurements of the corresponding optical absorption in the $2.5\,\mu$ to $0.5\,\mu$ region at $300^\circ K$, $78^\circ K$, and $4.2^\circ K$ were discussed. Absorptions showing considerable fine structure have been found for CdS:Ni and CdS:Co, while broad bands were found in crystals doped with Cu, V, Mn, and Cr. The absorptions of the crystals doped with N, Co, and Cu are consistent with the predictions of the crystal field theory for the corresponding divalent ions in tetrahedral coordination. The absorptions found experimentally for CdS:V, CdS:Cr, and CdS:Mn were compared with predictions of the crystal field theory

for the corresponding divalent and trivalent ions in tetrahedral coordination.

7384 THEORY OF THE ABSORPTION EDGE IN SEMICONDUCTORS IN A HIGH MAGNETIC FIELD by R. J. Elliott and R. Loudon (Clarendon Lab.); J. Phys. Chem. Solids, Vol. 15, pp. 196-207, Oct. 1960

A theory based on the effective mass approximation is given for hole-electron pairs in a semiconductor in a magnetic field. The intensity of the absorption edge is determined by the wave function of relative motion of the pair, so that essentially it becomes necessary to solve the Schroedinger equation for a hydrogen atom in a magnetic field. This is done in an approximation valid in high fields which assumes that the Coulomb term affects only the motion along the field, and uses a potential form which allows the solutions to be written in terms of confluent hypergeometric functions. The results show that the main absorption in the continuum is reduced to an insignificant shoulder. The peaks observed in the so-called magneto-optic effect will all be exciton peaks.

Absorption Properties of SnS - See 7273

Absorption Properties of GaAs - GaP Alloys - See 7272

7385 ENERGY MODEL FOR EDGE EMISSION IN CADMIUM SULFIDE by L. S. Pedrotti and D. C. Reynolds (Wright-Patterson AFB); Phys. Rev., Vol. 120, pp. 1664-1669, Dec. 1, 1960

Measurements of the blue and green fluorescence emitted by CdS single crystals subjected to ultraviolet radiation at low temperatures in the temperature interval from 4.2°K to 77°K are reported. The spectral position and relative intensity of certain lines found in this fluorescence have been measured as a function of temperature between 4.2°K and 77°K. The degree of polarization of the fluorescence has been investigated at 4.2°K. From this data an energy model is proposed which accounts for the transitions leading to the blue and green fluorescence at 4.2°K, the change in these transitions as the temperature increases from 4.2°K to 77°K, and the transitions leading to the blue and green fluorescence at 77°K.

7386 STRAIN-INDUCED SPLITTING OF A CHROMIUM FLUORESCENCE LINE by A. Piksis, S. Sugano, and A. L. Schawlow (Bell Labs.); Bull. Am. Phys. Soc., Ser. II, Vol. 5, p. 415 (A), Nov. 25, 1960

In a purely cubic crystal field (as at a cubic site in MgO) the ^2E state of the Cr^{3+} ion has a two-fold orbital degeneracy and emits a single sharp fluorescence line. If the surrounding octahedron of oxygen ions is distorted, as in ruby, the degeneracy is removed, and two fluorescence lines are seen. The line splittings which result from the application of pressure along [100], [110], and [111] directions in MgO crystals were discussed. From the polarization, the sign of the field is obtained, and the trigonal field resulting from compression is found to be positive. The nature of the splitting depends on the stress direction and, for a [111] stress, involves spin-orbit coupling. Theoretical estimates agree well with the observations. Although the fluorescence lines are quite sharp ($\sim 0.25\ cm^{-1}$), the line width is shown to be primarily caused by strain, and more perfect crystals could be expected to give considerably narrower lines.

7387 PRESSURE EFFECTS IN LUMINESCENCE: CLASSICAL ESTIMATES by L. Reiffel (Armour Res. Found.); Bull. Am. Phys. Soc., Ser. II, Vol. 5, p. 416 (A), Nov. 25, 1960

The magnitudes of pressure effects on various characteristics of phosphors with temperature-dependent decay time were estimated using a classical, one-dimensional configurational coordinate approach. Effects considered include the already experimentally established pressure-induced changes in trap depth and absorption peak position as well as changes in band width, fluorescence efficiency, and energy storage efficiency along with associated changes in decay time and light intensity. Large spectral shifts in either prompt or phosphorescent spectra which could arise from various band overlap effects or alterations in the populations of two communicating states were also considered. A classical approach to estimating pressure-induced effects is justified by the technical difficulty of low-temperature, high-pressure experiments. Preliminary results also were given concerning the activation volumes associated with trap escape in mixed halide crystals such as NaBrI (Tl) as compared to single halide crystals such as NaI (Tl) and NaBr(Tl). Interpretation in terms of possible disruption of the synchronous breathing-mode motion of the anions surrounding substitutional Tl^+ was suggested. This interpretation rests critically on the pressure dependence of cross-over probability between states which has been treated semiclassically.

7388 EFFECTS OF ILLUMINATION UPON SODIUM CHLORIDE THERMOLUMINESCENCE by A. E. Stoddard (Calif. Research); Phys. Rev., Vol. 120, pp. 114-117, Oct. 1, 1960

Illumination of a sodium chloride crystal at liquid nitrogen temperature after x-ray irradiation at a higher temperature or higher temperature annealing has two effects upon its thermoluminescence. Glow peaks stable at the temperature of x-ray irradiation or annealing are diminished in intensity. Missing glow peaks, unstable at the temperature of x-ray irradiation annealing, reappear in the glow curve. Both effects are greatest for illumination in the F band. The results are not consistent with existing models of the thermoluminescence process.

7389 THERMOLUMINESCENCE OF POTASSIUM AZIDE by H. J. Mueller and H. D. Tiller (USASRDL); Bull. Am. Phys. Soc., Ser. II, Vol. 5, p. 415 (A), Nov. 25, 1960

Studies of the thermoluminescence of potassium azide by means of an UV-sensitive photomultiplier were reported. Glow curves were taken in the temperature range from -190°C to + 400°C. Both untreated and UV-irradiated samples emitted light when thermolytically decomposed. The glow curves of UV-irradiated samples displayed additional peaks between -150°C and -50°C which are ascribed to the extinction of color centers. The spectral characteristics of the emitted radiation were investigated. The results obtained were related to previous work on color centers and exo-electron emission of potassium azide. Measuring techniques were described.

7390 OPTICAL PROPERTIES OF KCl:Tl IN THE EXTREME ULTRAVIOLET REGION by K. Aoyagi and G. Kuwabara (U. Tokyo); J. Phys. Soc. Japan, Vol. 15, pp. 2334-2342, Dec. 1960

The optical properties of KCl:Tl in the vacuum ultraviolet range between room and liquid nitrogen temperatures are discussed. A new band has been observed in both the absorption and excitation spectra on the long wave length tail of the exciton band, i.e. 7.19 ev at -180°C. From the measurements of the temperature dependence and the emission spectrum the

band is supposed to be associated with a transition in Cl ions in the neighborhood of a Tl ion. Excitation and emission spectra of fluorescence by the light in the fundamental band region, as well as thermal glow and optical stimulation curves of phosphorescence were also measured. The process of this luminescence is discussed.

7391 INVESTIGATION OF THE KINETICS OF INFRARED IMPURITY PHOTOCONDUCTIVITY IN CdS INDUCED BY PRELIMINARY ILLUMINATION by E. N. Arkad'eva, L. G. Paritskii, and S. M. Ryvkin (Physicotech. Inst., Acad. Sciences); Soviet Phys.-Solid State, Vol. 2, pp. 1051-1058, Dec. 1960

Measurements of the photoconductivity of CdS single crystals in the infrared region from 2 to 4μ arising from pre-excitation due to illumination at a wavelength corresponding to intrinsic absorption are reported. The measurements were made at a temperature of 77°K. It is suggested that the infrared photoconductivity is connected with the transition of electrons to the conduction band from trapping levels which are filled with electrons as the result of the preliminary illumination. An appropriate model has been constructed and compared with experimental data concerning the kinetics of infrared conductivity. This comparison served as the basis for determining the cross section for capture of a photon by a charged center, the coefficient of light absorption in the infrared, and the filling of the trapping levels. In addition estimates were made of the density of the levels, their location in the forbidden zone, and the cross section for capture by these levels of an electron from the conduction band.

7392 ELECTRICAL CONDUCTIVITY AND PHOTOELECTRIC PROPERTIES OF CADMIUM AND ZINC TELLURIDE LAYERS by P. P. Konorov and I. B. Shevchenko (Leningrad State U.); Soviet Phys.-Solid State, Vol. 2, pp. 1027-1032, Dec. 1960

Measurements of the electrical conductivity and photoelectric properties of cadmium and zinc telluride layers obtained by vacuum deposition are reported. Layers of cadmium telluride of about 1 μ thickness displayed a high photosensitivity in the visible and near infrared parts of the spectrum and could be used as photoresistors, sensitive over this spectral region. Hypotheses concerning the mechanism of sensitization of these layers are presented. Layers of zinc telluride did not show any large photosensitivity after both deposition and subsequent heat treatment.

7393 EFFECT OF OXYGEN UPON SINTERED CADMIUM SULPHIDE PHOTOCONDUCTING FILMS by S. Kitamura (Matsushita Elec. Ind.); J. Phys. Soc. Japan, Vol. 15, pp. 2343-2350, Dec. 1960

The dark conductivity and decay time of sintered CdS films prepared by firing in nitrogen gas were higher than those of sintered CdS films prepared by firing in the mixture of nitrogen gas and hydrogen sulphide. Accordingly it was thought that the sintered CdS films prepared by firing in nitrogen gas have many sulphur vacancies acting as donors. As a result of heat-treatment in oxygen of the sintered CdS films prepared by firing in nitrogen gas, the dark conductivity and decay time decreased. A new peak appeared at 680 mμ in spectral response of the photo-current. The activation energy obtained by measuring the slope of the curve of logarithm of dark conductivity plotted against $1/T$ (°K) increased, while the trap concentration obtained by measuring the thermally stimulated current decreased with the increase in temperature of heat-treatment in oxygen. The results of experiments supported the interpretation that sulphur vacancies acting as donors had been occupied by oxygen atoms, and then vanished. At the same time there were produced new exciting centers at about 1.8 ev below the bottom of the conduction band. By electron-microscopic observations it was found that by heat treatment above 400°C in oxygen, CdO grains were produced on the surface or near the grain boundary of the sintered CdS film, and when the whole surface of the CdS film was coated by CdO layers, photoconductivity was not observed.

Photoconductivity of PbS Films - See 7284

7394 OPTICAL CONSTANTS OF SILICON IN THE REGION 1 TO 10 EV by H. R. Philipp and E. A. Taft (GE); Phys. Rev., Vol. 120, pp. 37-38, Oct. 1, 1960

Measurements of the reflectance, $|r(\lambda)|^2$, of single crystal silicon in the range 1 to 11.3 ev are reported. The phase, $\theta(\lambda)$, has been computed from these data using the Kramers-Kronig relation between the real and imaginary parts of the complex function $\ln r = \ln |r| + i\theta$. The optical constants, n and k, have been determined from the Fresnel reflectivity equation. The real part of the refractive index, n, shows a sharp maximum of magnitude 6.9 at 3.3 ev. The extinction coefficient, k, shows maxima of magnitude 3.1 at 3.5 ev and 5.1 at 4.3 ev; optical absorption above 3 ev is associated with the onset of strong direct transitions. The results indicate that much useful information, applicable to band structure calculations for both silicon and germanium, could be obtained from limited reflectance studies (2 to 5 ev) on Ge-Si alloys.

7395 MICROWAVE FARADAY EFFECT IN SILICON AND GERMANIUM by J. K. Furdyna (Northwestern U.) and S. Broersma (U. Oklahoma); Phys. Rev., Vol. 120, pp. 1995-2003, Dec. 15, 1960

The Faraday rotation and ellipticity in a system of quasifree carriers is discussed and applied to microwave measurements on semiconductors. The theoretical expressions for these effects are analyzed with a digital computer for various ranges of the magnetic field B, the mobility μ, the conductivity σ, the frequency ω, the collision time τ and the dielectric constant of the host material. It is possible to simplify these expressions in certain limiting cases. For μB smaller than unity, the rotation and ellipticity are proportional to B. For μB larger than both unity and ωτ, they decrease as B^{-1} and B^{-3}, respectively. A maximum occurs near $\mu B = 1$ when ωτ is small. Rotation measurements on n- and p-type single crystals of silicon at room temperature, with resistivities from 0.5 to 40 ohm-cm, utilizing 9.6- and 35-kMc/sec radiation, are compared with the theory. Results for n-type germanium at 78°K, with μB varied up to about 6, agree with the calculated low- and high-field behavior. Faraday ellipticity measurements on n-type germanium crystals at 78°K are in qualitative agreement with the theory. In the case of small losses, the sign of the ellipticity is determined by the sign of the quantity $(4\omega\tau - \sigma/\omega\epsilon_{st}')$.

7396 SOME OPTICAL PROPERTIES OF CdSe SINGLE CRYSTALS by S. P. Keller and G. D. Pettit (IBM); Phys. Rev., Vol. 120, pp. 1974-1977, Dec. 15, 1960

Optical transmission and reflection measurements made on a single crystal of CdSe (crystal class C_{6v}) with light polarized parallel and perpendicular to the c axis are reported. The absorption coefficients, $\mu_\perp$ and $\mu_\parallel$, are presented as functions of

incident photon energy, at room temperature. The selection rule, $\mu_{\perp} > \mu_{\parallel}$, expected for all solids in the crystal classes C_{nv} and C_n, where n = 3, 4, or 6, is very well obeyed in CdSe. The absorption coefficients are not simple functions of the photon energy, but are nearly exponential and almost follow Urbach's rule. The fluorescence of the single crystal has been measured at 77°K. It is peaked at 920 mμ and it is slightly polarized perpendicular to the c axis. The results are similar to what has been obtained for hexagonal ZnS.

7397 THE OPTICAL AND PHOTOELECTRIC PROPERTIES OF ZINC SELENIDE AND TELLURIDE by G. A. Zholkevich (Vologodskii State Pedagogic Inst.); Soviet Phys.-Solid State, Vol. 2, pp. 1009-1011, Dec. 1960

The optical properties of ZnSe and ZnTe are reviewed. On the basis of these properties, the compounds of zinc with selenium and tellurium border directly on the group of semiconductors of the CdS type. In the series ZnS, ZnSe, and ZnTe, zinc sulfide, which has desirable luminescent properties, has been studied most intensively. Zinc selenide is widely used in cathodoluminescence. Its high photosensitivity was first reported by Miller and Strang. The photoconductivity of zinc telluride has recently become known.

Optical Properties of $InSb-In_2Te_3$ Alloys - See 7323

THERMAL PROPERTIES

Specific Heat of β Tin - See 7405

Thermal Conduction in Ferroelectric Ceramics - See 7289

7398 IMPURITY SPECIES EFFECT (As, Sb) ON THE THERMAL CONDUCTIVITY AND THERMOELECTRIC POWER OF GERMANIUM AT LOW TEMPERATURES by J. F. Goff and N. Pearlman (Purdue U.); Bull Am. Phys. Soc., Ser. II, Vol. 5, pp. 407-408 (A), Nov. 25, 1960

At temperatures below that of the thermal conductivity k maximum T_m, Ge single crystals containing between 6×10^{16} and $2 \times 10^{18} cm^{-3}$ nominally noncompensated Sb impurities show a thermal resistivity w which increases with impurity concentration and exhibits a T^{-n} dependence where n is approximately 4. Sb doped samples, heavily compensated (80% or more) in the melt with Ga, exhibit a decreased w; and it is possible to correlate w (T) with n_{ex} the exhaustion carrier concentration. Thus w apparently arises from an electron-phonon interaction that is independent of the electron transition probabilities in the impurity band (as indicated by the differing electrical resistivities of the noncompensated and compensated samples at these temperatures). Further, similar Ge samples containing 2×10^{16} to 1×10^{17} nominally noncompensated As impurities per cm^3 show less w per carrier than do the Sb doped ones and exhibit a T^{-3} dependence approximately, while a degenerate As doped sample yields results like the degenerate Sb doped ones. These results were discussed with respect to the Keyes model of thermal resistance. The thermoelectric power Q of the noncompensated, nondegenerate Sb and As doped samples differ markedly in that Q (Sb) decreases at these low temperatures ($T < T_m$) while Q (As) increases (the degenerate As doped sampl behaves similarly to the degenerate Sb ones).

7399 THERMOELECTRICITY AND THERMAL CONDUCTIVITY IN THE LEAD SULFIDE GROUP OF SEMICONDUCTORS by D. Greig (Natl. Res. Council); Phys. Rev., Vol. 120, pp. 358-365, Oct. 15, 1960

Measurements of the thermal conductivity and thermoelectric power of six specimens of PbS and one each of PbSe and PbTe at temperatures ranging from 4°K to 100°K are reported. In the same temperature region the charge carrier mobility in thes samples has been determined from measurements of electrical resistivity and Hall coefficient. Four of the PbS samples were natural and n type, while the other specimens were synthetic and p type. The synthetic samples contained only a few single crystals but two of the natural specimens were highly polycrystalline. At low temperatures the charge carrier mobilities tend to high constant values similar to those reported elsewhere in single crystals of the same materials. An estimate of the scattering cross section of the point defects provides evidence for explaining this behavior in terms of metallic rather than semiconducting properties. Maxima attributed to phonon drag have been observed below 20°K in the thermoelectric power of the specimens of highest thermal conductivity. The thermal conductivity was similar in all samples at 100°K but varied by as much as two orders of magnitude at 10°K. In order to explain these results it is necessary to consider scattering of phonons by point imperfections, free electrons, and dislocations.

7400 MATERIALS FOR THERMOELECTRIC APPLICATIONS by R. W. Ure, Jr., R. Bowers and R. C. Miller (Westinghouse Res Lab.); Properties of Elemental and Compound Semiconductors (Interscience), pp. 245-259, 1960

The relation between the thermoelectric figure of merit and the basic properties of a semiconducting material such as mobility, effective mass, lattice thermal conductivity, and energy gap is reviewed. The principles are illustrated with data on the figure of merit of $Bi_{2(1-x)}Sb_{2x}Te_{3(1-y)}Se_{3y}$, InSb, $InAs_{1-x}P_x$, and GeTe.

Temperature Dependence of the Thermal Power in Ti_2O_3 - See 7309

7401 THERMOELECTRIC PROPERTIES OF ALLOYS OF THE PSEUDOBINARY SYSTEM Sb_2Te_3-Bi_2Te_3 by G. V. Kokosh and S. S. Sinani (Leningrad Inst. Semicon.); Soviet Phys.-Solid State, Vol. 2, pp. 1012-1018, Dec. 1960

The effect of impurities on the properties of alloys of the syster Sb_2Te_3-Bi_2Te_3 is considered. A general description of the effect of additions on solid solutions of semiconductors with disturbed stoichiometry is presented. The effect of firing on the electrical conductivity and thermal EMF of pressed specimens is described. The properties of alloys made of materials of different purity are compared. The part of the system exhibiting maximum values of the thermal EMF is examined.

7402 REACTOR IRRADIATION OF PbTe, Bi_2Te_3, AND ZnSb by R. T. Frost, J. C. Correlli, and M. Balicki (Knolls Atomic Power Lab.); Bull. Am. Phys. Soc., Ser. II, Vol. 5, p. 420 (A), Nov. 25, 1960

Instrumented samples of polycrystalline n-type PbTe and Bi_2Te_3 and p-type ZnSb have been irradiated in the Engineering Test Reactor (ETR) to a total integrated flux-time of $1.2 \cdot 10^{20} cm^{-2}$

of neutrons having energies greater than 1 Mev. The corresponding thermal flux time was $6.1 \cdot 10^{20} cm^{-2}$. Electrical resistivity and Seebeck coefficient were monitored by means of seven leads attached to each of the three samples, which were located within a cylindrical region in the reactor 1/2 in long and 3/4 in in diameter. Thermal and resonance neutron reactions on tellurium produced iodine approaching the amount used in the initial doping of the n-type materials. Gamma-ray spectroscopy on uninstrumented sampled irradiated to comparable flux-times failed to disclose lines due to long-lived daughters of fast neutron-induced reactions. The changes in electrical properties of uninstrumented PbTe and Bi_2Te_3 samples induced by a fast (>1-Mev) neutron flux time of $1.5 \cdot 10^{19} cm^{-2}$ are essentially completely annealed in the range of temperature from 170° to 190°C, respectively.

7403 CHANGES IN THE THERMOELECTRIC PROPERTIES OF PbTe, Bi_2Te_3 AND ZnSb DURING IRRADIATION by J. C. Corelli and R. T. Frost (Knolls Atomic Power Lab.); Bull. Am. Phys. Soc., Ser. II, Vol. 5, p. 420 (A), Nov. 25, 1960

An instrumented in-pile experiment previously described [see 7402] has yielded the following changes. The Seebeck coefficient of the n-type Bi_2Te_3 sample increased by ≈10% during the irradiation while the resistivity was increased by a factor of ~2.8 with no significant changes for fast (>1-Mev) flux times greater than $5 \times 10^{19} n/cm^2$. In the case of p-type ZnSb the resistivity increased by a factor of ~12 with no large changes resulting beyond a fast flux time of $6 \times 10^{19} n/cm^2$. The p-type ZnSb converted to n-type after an accumulated fast flux time of $\sim 1.6 \times 10^{17} n/cm^2$, and thereafter its Seebeck coefficient exhibited a gradual increase of ≈15% with increased in-pile time. The resistivity of n-type PbTe increased by a factor of ~25 after a total accumulated fast flux-time of $1.2 \times 10^{20} n/cm^2$ with no large changes observed for fast flux-times greater than $\sim 6 \times 10^{19} n/cm^2$. Auxiliary experiments suggest that a significant part of resistivity increases for all samples because of stress-induced damage during reactor power transients. In some cases temperatures during irradiation were near the annealing threshold for PbTe and Bi_2Te_3.

Thermoelectric Power of Some Semiconducting Oxide Glasses - See 7311

7404 THEORY OF THE ETTINGSHAUSEN EFFECT IN SEMICONDUCTORS by B. V. Paranjape and J. S. Levinger (Louisiana State U.); Phys. Rev., Vol. 120, pp. 437-441, Oct. 15, 1960

The Ettingshausen effect in semiconductors is mainly due to the generation of electron-hole pairs at one side of the sample and their recombination at the other side. The Ettingshausen coefficient is calculated, in agreement with Putley, as $P = (E_g/kec) z(1+z)^{-2} (\mu_e + \mu_h)$ where $z = (n_h \mu_h / n_e \mu_e)$ - ratio of hole conductivity to electron conductivity. E_g is the gap energy, and k the thermal conductivity. This formula is discussed for intrinsic, p-type and n-type semiconductors. P goes through a maximum for p-type semiconductors near the temperature at which the Hall voltage goes through zero. These results agree reasonably well with the measurements of Mette, Gaertner, and Loscoe of P as a function of temperature for different samples of germanium and silicon.

MECHANICAL PROPERTIES

7405 ELASTIC CONSTANTS OF β TIN FROM 4.2°K TO 300°K by J. A. Rayne and B. S. Chandrasekhar (Westinghouse Res. Lab.); Phys. Rev., Vol. 120, pp. 1658-1663, Dec. 1, 1960

Measurements of the adiabatic elastic constants of β tin in the temperature range 4.2 to 300°K using the ultrasonic pulse technique are reported. An unusually large variation with temperature of the shear constant $\frac{1}{2}(c_{11}-c_{12})$ has been observed. From the elastic constants extrapolated to 0°K, the limiting value of the Debye temperature of tin has been calculated. Using this value, the low-temperature specific heat data on both normal and superconducting tin have been re-evaluated.

7406 ELASTIC CONSTANTS OF ORDERED AND DISORDERED Cu_3Au FROM 4.2 to 300°K by P. A. Flinn, G. M. McManus, and J. A. Rayne (Westinghouse Res. Lab.); J. Phys. Chem. Solids, Vol. 15, pp.189-195, Oct. 1960

Measurements of the elastic constants of ordered and disordered Cu_3Au in the temperature range from 4.2 to 300°K are reported. The room temperature data are in good agreement with previous work. At liquid helium temperatures the ordered material, with S = 0.95, gives $c_{11} = 1.893 \pm 0.015 \times 10^{12} dyn\,cm^{-2}$, $c_{12} = 1.319 \pm 0.015 \times 10^{12} dyn\,cm^{-2}$, $c_{44} = 0.736 \pm 0.002 \times 10^{12} dyn\,cm^{-2}$. The corresponding value of Debye temperature is $\theta_{ordered} = 283.8 \pm 3.5°K$, which compares very well with the calorimetric figure of 285 ± 2°K. For the disordered alloy, the elastic data give a Debye temperature of $\theta_{disordered} = 281.6 \pm 3.5°K$, which is within experimental error of the calorimetric value of 278±2°K. The elastic constants for the disordered alloy indicate that the Fermi surface is less distorted than that in pure copper.

SOLID STATE DEVICES

JUNCTION DIODES

7407 NEW RESULTS IN THE FIELD OF POWER SEMICONDUCTOR RECTIFIERS IN CZECHOSLOVAKIA [in Czech.] by A. Kloss and M. Kubat (CKD); Elektrotech. Obzor, Vol. 49, pp. 554-557, Nov. 1960

A brief technical description of silicon rectifiers newly developed by the engineering works CKD Prague for heavy electrolysis, for mine haulage and for an electric locomotive in an a-c traction system of 50 cps is presented.

7408 STATIC CHARACTERISTICS OF COMBINATIONS OF NEGATIVE RESISTANCE DEVICES by R. A. Johnson and C. O. Harbourt (Syracuse U.); Proc. 1960 Natl. Electronics Conf., pp. 427-437

The composite static volt-ampere characteristics of the simplest combinations of two-terminal negative resistance devices are discussed. Primary consideration is given to the series connection of two voltage controlled (S-type) devices. Simple graphical constructions based on the individual device characteristics reveal a composite characteristic which may differ remarkably from that of either component device. Experimental curves obtained using tunnel diodes in series are presented and shown

to be entirely consistent with predicted performance. The great complexity of some of the constructed composite characteristics leads to the question of whether these characteristics are real in the sense that they are actually observable in practice. The advisability of distinguishing between the stability and the accessibility of various portions of the composite characteristic is considered. Stability may be determined by conventional linear (small-signal) analysis in the neighborhood of any point on the constructed characteristic. It is shown that a point may be stable in this sense and yet inaccessible for some combinations of external circuit elements.

7409 THEORY AND APPLICATIONS OF AVALANCHE DIODES by R. W. Lade (Marquette U.); Proc. 1960 Natl. Electronics Conf., pp. 779-784

The theory and applications of the avalanche diode are discussed. Proof of the existence of negative resistance is given, a result which follows the development of an expression for the ionization rate for charge carriers in terms of the well known multiplication factor M and an empirical constant, n. Several useful applications are cited where the collector base junction of a linear gradient transistor, alloyed junctions and point contact junctions are exploited in oscillator and amplifier circuitry. The one port amplifier has been employed successfully as a repeater in a simulated telephone transmission line operating at audio frequencies.

Reference Diodes - See 7535

7410 EXCESS AND HUMP CURRENT IN ESAKI DIODES by R. S. Claassen (Sandia); Bull. Am. Phys. Soc., Ser. II, Vol. 5, p. 406 (A), Nov. 25, 1960

An energy dissipating tunnel transition from a localized defect level in the transition region was proposed to explain the excess current I_x in Esaki diodes and the relation of I_x to bias voltage V_F was shown. The hump current may be explained in terms of equi-energy defect-to-band tunneling analogous to the band-to-band tunneling. Electron irradiation (2 Mev) has produced large humps in germanium diodes and two distinct humps in silicon and gallium arsenide diodes, indicating defect levels in fair agreement with those observed by other techniques. The appearance of the humps is accompanied by two straight-line portions of the $\ln I_x$ vs V_F curve. This model differs from that of Logan and Chynoweth in that discrete defect levels account for I_x.

7411 TUNNELING FROM TRAP STATES IN ESAKI DIODES by P. J. Price (IBM Watson Lab.); Bull. Am. Phys. Soc., Ser. II, Vol. 5, pp. 406-407 (A), Nov. 25, 1960

It has been suggested that excess current in Esaki diodes entails a tunneling transition between a localized trap state and the conduction (or valence) band. The probability per unit of tunneling from a trap has been calculated. It is approximately $\pi^2 m^*/h^3 d\ |W|^2 e^{-2\theta}$, where W is the matrix element, between the band-edge Bloch state (normalized in unit volume) and the trap state, of the local trap potential in excess of the crystal potential; d is the length of the "forbidden path" terminating at the trap; and θ is the usual integral appropriate to this path. The expected dependence of excess current on voltage is different for this mechanism, for tunneling with radiation, and for the Shockley-Read process with the transitions to and from the "forbidden tails" of band states.

7412 EFFECTS OF MAGNETIC FIELDS ON ESAKI TUNNELING by R. R. Haering and E. N. Adams (IBM); Bull. Am. Phys Soc., Ser. II, Vol. 5, p. 407 (A), Nov. 25, 1960

It has been observed by Esaki and by Calawa, Rediker, Lax, and McWhorter that the tunneling current of an Esaki diode m be considerably reduced by a sufficiently strong magnetic fiel in either transverse or longitudinal orientation. Calawa and Price have given an expression for the current reduction in the longitudinal orientation. A brief qualitative account of the physical mechanism of current reduction in strong fields was given and the result of a calculation of the current reduction for the transverse orientation was reported. The situations in the two orientations are somewhat different. In the longitudinal case, the tunneling must be predominately from the states of zero point motion about the field, since these have the maximum amount of energy available for tunneling. In the transverse case, the quantized motion about the field must provide the kinetic energy for tunneling, and hence tunneling is predominately from states of the largest possible quantum number; but because of the circling motion of the carrier only a part o the transverse energy is available for tunneling. The critical energy is not the zero point energy but a quantity which depe on the width of the junction and on the reduced carrier mass. Expressions for the magnitude of the current reduction for eith orientation were given, in the approximation in which the shi of the Fermi level is ignored.

Gallium Arsenide Tunnel Diodes - See 7431

7413 VOLTAGES AND ELECTRIC FIELDS OF DIFFUSED SEM CONDUCTOR JUNCTIONS by C. D. Root (Raytheon); IRE Tr Vol. ED-7, pp. 279-282, Oct. 1960

Equations and graphs which show a functional relationship between electric field and space-charge widening and also bet reverse bias voltage and space-charge widening for diffused di odes are presented. Planar geometry, with the diffusion mace from a constant surface concentration (C_0) into material of cor stant impurity density, is assumed. The voltage vs space-char width relation is presented graphically for the case of silicon. Graphs for other materials are not included, since they would differ from the silicon graphs only by a constant in the voltage axis. These graphs illustrate that for small reverse voltages th junction may be considered as being essentially linear, while for large reverse voltages it may be considered as an abrupt ju tion. A graph which may be used to gain a qualitative indica tion of the electric field distribution within the space-charge region is provided. This graph also gives an indication of the transition of junction behavior from nearly linear to nearly abrupt as the reverse voltage is increased.

7414 AN ANALYSIS OF INERTIAL INDUCTANCE IN A JUN TION DIODE by I. Ladany (U.S. Naval Res. Lab.); IRE Tran Vol. ED-7, pp. 303-310, Oct. 1960

When the injected carrier concentration is not small compared the equilibrium concentration, drift and diffusion processes interact and an inductance is developed in the base region. Thi phenomenon is analyzed by calculation of the small-signal impedance of a PIR diode. Simple expressions are obtained for t case $\Omega \ll 1$ as well as $\Omega \gg 1$, where Ω^2 is the product of the radian frequency and the diffusion transit time. For intermedi ate values of Ω, the impedance contains an integral which ha been expressed in terms of a tabulated function. Curves showi the diode impedance as a function of frequency and forward bi are presented. For low bias the reactance is capacitive, but

with increasing bias, provided the frequency is not too high, the reactance becomes inductive. The resistive component also shows a frequency dependence. The maximum inductive reactance occurs when $\Omega = 1$ and the Q does not exceed 1.

7415 NONLINEAR OPERATIONS ON PULSES BY MEANS OF P-N JUNCTIONS by G. Giannelli and L. Stanchi (Centro Studi Nucleari); Nuc. Instr. Methods, Vol. 8, pp. 79-91, July 1960

An investigation of the voltage-current characteristics of p-n junctions is described. It has been found that a transistor can be connected in such a way that its emitter-base junction shows a characteristic that approximates the theoretical one much better than diodes do. In particular, some types of transistors have been found whose i_E, V_{EB} characteristic is strictly logarithmic over more than five decades of current while selected samples attain six decades. The use of such junctions for multiplying or dividing between them two or more pulses is described and the various problems arising in such applications and in more general ones, like exponentials, are analyzed.

7416 VOLTAGE BREAKDOWN OF SILICON RECTIFIERS AS INFLUENCED BY SURFACE ANGLE by O. M. Clark (Motorola); J. Electrochem. Soc., Vol. 107, p. 269C (A), Dec. 1960

In high-voltage silicon rectifiers, the angle at which the space charge region of a reverse biased junction intersects the die edge can influence surface breakdown. Reverse biased junctions having shallow angles at the die edge have been observed to have higher surface breakdown voltages. Since the breakdown voltage of a given junction can be increased by spreading the space charge at the die surface over a greater area, a new method of producing single junction multikilovolt rectifiers is feasible. Single junction devices have been produced which can be reverse biased as high as 3500 v with less than 10 μa of leakage current.

7417 AVALANCHE BREAKDOWN VOLTAGES OF DIFFUSED SILICON AND GERMANIUM DIODES by C. D. Root, D. P. Lieb, and B. Jackson (Raytheon); IRE Trans., Vol. ED-7, pp. 257-262, Oct. 1960

Avalanche breakdown is defined in terms of the diode's electrical characteristics as well as the internal physical processes. Using the latter definition, and the basic diffusion equation, breakdown voltage is rigorously computed for various diffused junctions. The calculation process is described and similarities to both linear and abrupt junctions are pointed out. Graphs showing breakdown voltage as a function of diffusion parameters for both germanium and silicon are presented. Intermediate charts used in the calculations are also shown. These give maximum electric field in junction and normalized breakdown voltage for families of diffusions.

7418 CALCULATION OF THE TRANSIENT PROCESS IN A P-N JUNCTION AT ARBITRARY INJECTION LEVELS by M. I. Iglitsynz, Iu. A. Kontsevoi, and K. V. Temko; Radio Engrg. Electronics, Vol. 5, No. 3, pp. 215-223, 1960

The results of a theoretical analysis of the transient characteristic in a plane p-n junction at arbitrary injection levels are presented. Calculations were carried out numerically on an electronic computer. Graphs of the transient processes and a formula for calculating the carrier lifetime at arbitrary injection levels are obtained.

7419 PREPARATION OF P-N JUNCTIONS BY THE DECOMPOSITION OF COMPOUNDS by M. Genser and W. P. Allred (Battelle Mem. Inst.); U.S. Pat. 2,950,220, Issued Aug. 23, 1960

The preparation of p-n junctions in compound semiconductors by heating the semiconductor in a vacuum to cause one of the constituents to vaporize from the surface is described, particularly for n-type aluminum antimonide. Here the vaporization of antimony produces a p-type layer on the surface. The vaporized material is condensed at some distance from the semiconductor. The depth of the layer can be varied by varying the temperature and heating time. P-type layers can also be produced in n-type GaAs and InP and n-type layers can be produced on p-type ZnO by this technique.

7420 NEW FINDINGS IN THE TECHNOLOGICAL DEVELOPMENT OF THE MANUFACTURE OF GERMANIUM AND SILICON RECTIFIER ELEMENTS [in Czech.] by G. Pisa, P. Spiess, S. Sebek, V. Vendlerova, and J. Vinopal (CKD); Elektrotech. Obzor., Vol. 49, pp. 579-583, Nov. 1960

Some problems treated in the development laboratories for semiconductors of the engineering works CKD-Prague are described. The first part, on germanium diodes, deals with the dependence of the magnitude of the inverse voltage upon the density and distribution of dislocations, with new methods of etching large-area semiconductor elements, and with the stabilization of their surfaces. The second part, on silicon rectifiers, discusses some problems encountered in the manufacture of p-n junctions on silicon, in the surface protection of these junctions, and in their packaging.

Parameters of Si Single Crystals for Power Rectifiers - See 7263

7421 COOLING OF POWER SEMICONDUCTOR RECTIFIERS [in Czech.] by L. Sofar (CKD); Elektrotech. Obzor., Vol. 49, pp. 570-574, Nov. 1960

The problems of cooling power semiconductor rectifiers are considered and methods of cooling rectifier valves, the design of cooling bodies by means of electrothermal analogy, and special technological procedures in the manufacture of cooling bodies are described. Methods and results of some temperature and airflow measurements on rectifier valves are presented and the problems of the cooling of complete rectifying units are discussed.

JUNCTION TRANSISTORS

30-Ampere Silicon Power Transistors - See 7536

7422 A SILICON MEDIUM-POWER TRANSISTOR FOR HIGH-CURRENT HIGH-SPEED SWITCHING APPLICATIONS by J. F. Aschner, C. A. Bittmann, W. F. J. Hare, and J. J. Kleimack (Bell Labs.); IRE Trans., Vol. ED-7, pp. 251-256, Oct. 1960

A diffused base, diffused emitter, n-p-n silicon switching transistor developed for high-current applications such as switching magnetic memories is described. The transistor is designed to operate as a switch at the 0.75-ampere level. For a collector current of 0.75 ampere, the large signal current gain is 20 and the saturation voltage drop 4 volts. The break-

down voltages are 75 volts collector-to-base, and 6 volts emitter-to-base. The unit shows fast switching characteristics. The rise, storage, and fall times are each of the order of 0.1 μsec. It has a common emitter unity gain frequency greater than 50 Mc. The transistor employs a localized emitter produced by photoresist techniques and oxide masked diffusion. Lead attachment is accomplished by compression bonding. The silicon wafer is bonded through a molybdenum intermediary to a massive copper stud. The design theory of the device, and the variation of device characteristics with temperature are given. The applicability of this device to RF amplifier service is also discussed.

7423 BASE-LAYER DESIGN FOR HIGH-FREQUENCY TRANSISTORS by H. S. Veloric, D. Rauscher and C. R. Fuselier (RCA); J. Electrochem. Soc., Vol. 107, p. 269C (A), Dec. 1960

Total base impurity concentrations were presented for the complementary error function (erfc) distribution, an out-diffused impurity distribution, and the Gaussian distribution. Base-width control and "reach-through" voltage have been considered for the three cases. The "reach-through" voltage has been calculated from the solution of Poisson's equation for each type of distribution. For the distributions considered, control of base width in the range of 0.02-0.03 mil was shown to be difficult. Experimental results were presented for the "box method" of boron deposition and for diffusion.

7424 A FOUR-TERMINAL P-N-P-N SWITCHING DEVICE by M. Klein (IBM); IRE Trans., Vol. ED-7, pp. 214-217, Oct. 1960

A four-terminal germanium p-n-p-n switching transistor is described. In an appropriate circuit the device has useful switching gain for both the turn-on and turn-off operations. A pulse of one polarity turns the switch on, and a pulse of the opposite polarity turns it off. In the absence of triggers, the state is maintained. Equivalence to a pair of complementary conventional transistors in a direct-connected, common-base emitter-follower regenerative circuit is shown. The collector junction is common to both transistor sections so that saturation is simultaneous. Saturation current is kept small in one section, and the switch is turned off by withdrawing the small saturation current. Expressions are derived for switching gain, and requirements on device parameters are obtained. Common-emitter gain for one transistor section must exceed the ratio of load current to off-trigger current. Device structure is described. A combination of alloy, diffusion, and post-alloy diffusion techniques is used for fabrication. One transistor section with a thin base has high common-emitter gain, and the other has moderate gain. Switching performance data are given. A load current of 20 ma at 20 volts is switched with 2-ma pulses. Trigger pulse durations of the order of the switching time are required. Switching times of about 100 nsec are obtained.

Silicon P-N-P-N Controlled Switch - See 7537

7425 CURRENT BUILD-UP IN AVALANCHE TRANSISTORS WITH RESISTANCE LOADS by D. J. Hamilton (U. Arizona); IRE Trans., Vol. EC-9, pp. 456-460, Dec. 1960

A transient analysis for the avalanche transistor is carried out through the use of a diffusion model described in terms of charge variables. Basically, the current is calculated as a function of time by taking the gradient of the minority carrier charge stored in the base region. Two methods of approximating the distribution of stored charge are described. Good agreement has been obtained between calculated and experimental results; it is found that the rise time for the resistance-load case is about four times that for a capacitance-load case which produces the same peak current. A practical pulse generator circuit is described in which the resistance load takes the form of a delay-line. The performance of this circuit is compared with that of a capacitance-load relaxation oscillator; while the rise time of the former is longer, the pulse shape is more easily controlled.

7426 THE EFFECT OF EMITTER CURRENT ON CRITICAL FREQUENCY AND OUTPUT ADMITTANCE OF ALLOY TRANSISTORS by M. A. Abdiukhanov (M. V. Lomonosov Moscow State U.); Radio Engrg. Electronics, Vol. 5, No. 3, pp. 173-189, 1960

The critical frequency of the current gain and the output admittance of alloy transistors in the common-base circuit are experimentally studied as functions of the emitter current. The cause of reduction of critical frequency at very small and very large emitter currents is explained. Calculations and quantitative estimates which agree well with experiment are presented.

7427 SWITCHING TRANSISTORS by J. N. Barry (GE Ltd.); Electronic Tech., Vol. 37, pp. 442-449, Dec. 1960

The various methods for predicting the performance of switching transistors are described and their validity under conditions of large collector current is discussed. Departures from the behavior predicted by simple theory have been found, and these are described in some detail. A modified equivalent circuit to represent this behavior is suggested and its validity is briefly considered. Various transistor types fabricated by different techniques are considered. It is concluded that at high-current levels evaluation of switching times in terms of the charge control parameters is to be recommended, provided values of these parameters which correspond to the currents required in practice are known.

7428 LARGE-SIGNAL STATIC CHARACTERISTICS AND TRANSIENT PROCESSES IN TRANSISTORS by G. N. Berestovskii (M. V. Lomonosov Moscow State U.); Radio Engrg. Electronics, Vol. 5, No. 3, pp. 147-162, 1960

A theoretical and experimental study of non-stationary processes in junction transistors is carried out, taking into account the non-linear dependence of the electron component of emitter current on collector current. It is shown that for a transistor in the common-emitter circuit this non-linear dependence has a substantial effect on the character and duration of the transient processes in the transistor. With increase of amplitude of the input rectangular base current pulses, the risetimes of the collector current pulses rapidly decrease, and the current gain also decreases. Experimental verification has shown that this relatively simple and clear method gives good results.

7429 CORRELATION BETWEEN INPUT AND OUTPUT TRANSIENT TIMES FOR JUNCTION TRANSISTORS by R. P. Nanavati (Syracuse U.); Proc. 1960 Natl. Electronics Conf., pp. 729-734

A theory which shows that certain correlations exist between input and output transient times for junction transistors is developed. The problem is attacked by solving the time dependent diffusion equation for minority carriers in the base region of the transistor subject to appropriate boundary conditions.

JUNCTION TRANSISTORS (Cont'd)

The analysis takes into account both the cases where the collector junction recovers before the emitter junction and where the emitter junction recovers before the collector junction. The analysis shows that the input rise time always correlates with the output delay time. It also shows that for a wide range of drives the input storage time correlates with the total output turn-off time under the condition that the collector junction recovers before the emitter junction. When the collector junction recovers after the emitter junction, the input total turn-off time correlates with the output storage time. The conditions under which the above correlations exist are discussed in detail. Experimental results on a number of junction transistors confirm the results of the theory. An important implication of the theory is that the measurements made on transistor transients at the low impedance junction (and hence easy to make) give information regarding transients at the high impedance junction.

7430 THE TRANSIENT CHARACTERISTICS OF A TRANSISTOR IN GROUNDED EMITTER AND COLLECTOR CIRCUIT CONFIGURATIONS by A. A. Grinberg; Radio Engrg., Vol. 15, No. 3, pp. 63-74, 1960

The transient characteristics of a transistor operating in the grounded collector and grounded emitter configurations are calculated. The calculation is carried out taking into account the collector capacitance. The transistor is controlled by an e.m.f. generator with a finite internal resistance. The effect of the emitter efficiency on the transient characteristic $^{(G)}g_c$ is established subject to the form of control.

Epitaxial Films of Ge and Si for Mesa Transistors - See 7268

7431 RESEARCH ON HIGH-TEMPERATURE SWITCHING DEVICES by E. Zimmerman (Philco); U.S. Gov. Res. Rep., Vol. 34, p. 721 (A), Dec. 16, 1960 PB 149 832

A theoretical and experimental investigation of semiconductor switching devices capable of high-temperature (150°C or more) performance, and comparable or superior at low and medium temperatures to existing devices is reported. The wide-gap material GaAs was used initially in analog type, subsequently in bipolar transistor structures, and finally in tunnel diodes. Single-crystal GaAs was grown by horizontal zone-melt techniques. Two main purification methods were investigated: reaction conditions were held constant while element purification procedures were varied; a standard purification procedure was used to study probable contamination from boat materials. Two diffusion methods — box diffusion and sealed-tube diffusion — were studied as techniques for forming junctions and for converting crystals to the desired type and resistivity. Three bipolar transistor structures were evaluated: the homogeneous base n-p-n and p-n-p transistors, and mesa n-p-n transistor. Techniques were developed that yielded high-frequency GaAs tunnel diodes with an f_{max} of 3.5 Gc and a potential f_{max} of 10 Gc.

Identification of Phases Formed During Attachment of Leads to Silicon Transistors - See 7228

7432 NEW AUTOPSY TECHNIQUES FOR TRANSISTORS AND RELAYS by C. B. Clark and E. F. Duffek (Stanford Res. Inst.); IRE Trans., Vol. RQC-9, pp. 20-22, Dec. 1960

A new method for opening hermetically-sealed metal cans is described. Instead of mechanically sawing or cutting the metal, an electrochemical process is used. The static electrolysis (anodic dissolution) and the jet electrolysis methods are described. The method is illustrated by the "autopsy" of failed transistors with 6-mil Kovar shells and relays with 15-mil brass shells.

UNIPOLAR TRANSISTORS

7433 SILICON CARBIDE TRANSISTORS by L. F. Wallace and H. C. Chang (Westinghouse); J. Electrochem. Soc., Vol. 107, p. 269C (A), Dec. 1960

High-temperature unipolar transistors exhibiting power gain which use n-type α-SiC for the channel material were described. The p-type gates were formed by the aluminum-diffusion process. The high-purity material was prepared in a Lely-type furnace and has a minimum resistivity of about 500 ohm-cm at room temperature. Control of the channel geometry was achieved by diffusion and electrolytic etching techniques. The design principles and electrical characteristics were presented.

INTEGRATED CIRCUITS

7434 SILICON INTEGRATED CIRCUITS by W. B. Glendinning (USASRDL); IRE Trans., Vol. MIL-4, pp. 459-468, Oct. 1960

The use of semiconductor integrated circuitry to reduce size and weight of military electronic systems is discussed. The pure semiconductor integrated circuit approach used to obtain microminiaturization levels is reviewed and characterized. The design and construction of a silicon integrated AM demodulator are described and experimental measurements of the electrical performance and the thermal behavior of the microcircuit are presented. The silicon structure is analyzed in terms of internal and external geometry, material properties, and electrical performance.

OTHER SEMICONDUCTOR DEVICES

Magnetoresistive Multipliers - See 7514

Varistor Squaring Unit - See 7513

Injection-Controlled Variable Resistance - See 7485

PHOTODEVICES

7435 SILICON PHOTO-VOLTAIC CELLS FOR INSTRUMENTATION AND CONTROL APPLICATIONS by V. Magee and A. A. Shepherd (Ferranti); J. Brit. IRE, Vol. 20, pp. 803-819, Nov. 1960

The operation of silicon p-n junction photovoltaic cells as detectors of visible and near infrared illumination is discussed.

The detection mechanism and the processes utilized to fabricate the cell are described. Several applications of these devices are given including a photocell-transistor relay system, a moiré fringe system for machine tool control, a fast photoelectric binary counter, and a punched card reading system.

7436 PHOTOEFFECT ON DIFFUSED P-N JUNCTIONS WITH INTEGRAL FIELD GRADIENTS by A. G. Jordan and A. G. Milnes (Carnegie Inst. Tech.); IRE Trans., Vol. ED-7, pp. 242-251, Oct. 1960

A detailed analysis of a diffused junction photodiode in which the illumination, monochromatic or broadband, is applied to the diffused face is presented. The electric field produced by the impurity distribution, assumed exponential, assists the transport and collection of minority carriers created by photons absorbed in the graded region. The theoretical study covers both the steady-state and the transient response, and takes into account the effect of surface recombination velocity. The presence of the built-in field increases the photocurrent and reduces the dark current compared with homogeneous base diodes. For p-n silicon photodiodes with 5-micron base widths and acceptor concentrations of, say, 2×10^{18} atoms/cm^3 at the surface, photosensitivities approaching 0.01 ampere per lumen may be achieved. The transient-response analysis considers the extrinsic delay imposed by the time constant of the junction capacitance and the load resistance, and also the inherent delay caused by the transit time of the minority carriers. With moderate or high load resistances, the extrinsic delay is much larger than the transit-time delay. However, for comparable graded- and homogeneous-base photodiodes, the capacitances of graded junctions are lower, and therefore the transient response is improved on this account. The graded junctions also are shown to have greatly reduced transit-time delays because of the built-in field effect.

7437 THERMAL AND OPTICAL BEHAVIOUR OF PHOTOTRANSISTORS by D. Shaw and B. Crump (United Steel); Electronic Engrg., Vol. 32, pp. 753-757, Dec. 1960

The thermal and optical characteristics of two phototransistors have been investigated in order to facilitate the design of photoheads for use under heavy industrial conditions. Circuits have been devised for one phototransistor which allow relay operation in ambient temperatures up to 55°C. For precise position measurements, the optical-mechanical characteristics are not stable to better than ±0.06 in so that individual calibration is necessary to achieve a higher degree of accuracy. This condition is made worse if bi-directional movement employing relay indication is used, the errors typically amounting to ±0.1 in. The second phototransistor allows operation up to at least 90°C ambient temperature but is about 1000 times less sensitive than the first in its present form.

7438 SPECTRAL RESPONSE OF SOLAR CELL STRUCTURES by L. M. Terman (Stanford U.); U.S. Gov. Res. Rep., Vol. 34, p. 500(A), Oct. 14, 1960 PB 148 597

Measurements of the spectral response of silicon solar cell structures and observations of the way in which the response varied with the depth of the p-n junction are reported. Spectral response is defined as the relative short-circuit current as a function of the wavelength of incident light for equal energy incident upon the cell at all wavelengths. Cells have been made with the junction depths varying from 0.6 to 5.0 μ, and having smooth (etched) surfaces and rough (lapped) surfaces. Response curves indicate that in order to increase the relati short-wavelength response ($\lambda < 0.75\,\mu$) the junction should be made closer to the surface, while in order to increase the rel tive long-wavelength response ($\lambda > 0.75\,\mu$) the junction must l made comparatively far below the surface. The effect of hav ing a lapped surface on the cell is to reduce the lifetime nea the surface, thus reducing the response to short wavelengths c incident light. A simple theoretical model which appears to adequately describe the mechanism involved in determining th shape of the response curves is then presented.

7439 CURRENT APPLICATIONS OF ELECTROLUMINESCEN by P. W. Ranby and P. J. Clemer (Thorn Electrical Ind.); Tra Illum. Eng. Soc., Vol. 25, No. 4, pp. 267-280, 1960

The construction of electroluminescent lamps using ceramic enamelling techniques is described and their properties are compared with the electroluminescent lamp which employs organic dielectric materials. These "ceramic" lamps lend ther selves to applications where a low brightness source of robus construction is required together with long life, for example, instrument lighting as in automobile dashboards, electric clocks, and telephone dials. The 'organic' lamp is already used for aircraft signs, but digital indicators and other indicator panels can be constructed. The 'organic' type can als be combined with photoconductance materials to provide a number of interesting devices such as 'optrons' and image intensifiers and converters, and the X-ray image converter i a particularly promising application. Some new phosphors which show a marked d-c electroluminescence when used in ceramic constructions are described.

Thermoluminescent Dosimeter - See 7502

THERMAL DEVICES

7440 STATIC ANALYSIS OF RADIATION-POWERED THERM ELECTRIC GENERATORS by P. E. Gray (MIT); Proc. 1960 N Electronics Conf., pp. 123-133

The static performance characteristics of a thermoelectric gen erator subject to the thermal boundary conditions of a fixe temperature at the cold junctions and a fixed power input a the hot junctions is treated theoretically. These differ from t boundary conditions established for the usual analysis in whic it is assumed that both junction temperatures are fixed, and correspond physically to the situation in which the generator powered thermally by a radiation absorber, as in the case of a solar-powered generator. It is shown that the generator is no longer electrically linear when operated in this manner. The temperature drop and terminal voltage are quadratic functions of the current. Consequently, the load condition for maximu efficiency, which in this case is identical to the load conditi for maximum power output, is different from that produced by the usual boundary conditions. The analysis presented permit the calculation of the optimum load condition and allows dire comparison of the results with the results based upon the usual boundary conditions. It is shown that the differences are significant for those cases in which the figure of merit of the thermoelements, and the open circuit temperature drop across the generator, are large.

MAGNETIC DEVICES

Ferromagnetic Parametric Amplifier - See 7476

7441 REVERSAL OF A LOADED FERROMAGNETIC CORE by N. Cushman (Sprague Electric) and D. Park (Williams Coll.); IRE Trans., Vol. CP-7, pp. 117-124, Dec. 1960

The performance of a toroidal square-loop ferromagnetic core as a circuit element is discussed. The analysis takes account of two different physical processes in the core. These are a reversible one which contributes to the fast initial rise of the output signal, and an irreversible one, tentatively described as domain rotation, which is mainly responsible for switching the core. A differential equation which governs the entire physical system, including the external circuit, is set up. This leads to a calculation of the output signal and its dependence on the secondary loading. Core parameters determined experimentally for an open-circuited core are used to predict the output signal when the core is loaded, and close agreement is found with measured values.

7442 MAGNETIZATION IN TAPE-WOUND CORES by R. C. Barker (Yale U.); Commun. and Electronics, pp. 482-501, Nov. 1960

A non-mathematical review of the state of knowledge of soft magnetic materials, specifically as used in commercially available tape-wound cores, is presented. The first section, which is basic enough to be applicable to all magnetic materials, deals with the ferromagnetism of magnetically soft materials, beginning with a qualitative description of ferromagnetic domains. The second section is directed toward tape-wound toroidal cores and gives a qualitative description of the physical and electrical properties of magnetic tapes in terms of simple experiments.

Coaxial Ferrite Isolator - See 7538

Mechanical Filters with Ferrite Transducers - See 7539

7443 THE OPTIMUM LINE WIDTH FOR A REFLECTION CAVITY MASER by G. J. Troup (Weapons Res. Est.); Aust. J. Phys., Vol. 13, pp. 615-616 (L), Sept. 1960

It is shown that the optimum line width for the transition in a reflection cavity maser gives the maximum value of $(\text{gain})^{\frac{1}{2}} \times$ bandwidth product for a given cavity maser system. The simplest way to adjust the transition line width in a paramagnetic maser is to utilize an inhomogeneous magnetic field. Experimental work of others which shows that there is an optimum line width for a given maser system and that an inhomogeneous magnetic field is a practical means for adjusting the line width is cited.

7444 RECOVERY TECHNIQUE FOR SATURATED MASERS by G. K. Wessel (GE); IRE Trans., Vol. ED-7, pp. 297-302, Oct. 1960

The practical application of masers is often hindered by saturation effects of the maser material. Any strong signal frequency (e.g., the transmitter pulse of a radar system leaking into the maser) will cause saturation. This paralyzes the maser for a period of time, too long for most intended applications. In this report, a method which has been used in desaturating a four-level ruby maser is described. The saturation is caused by equalizing the populations of levels one, two, and three of the maser crystal by the leakage of the transmitter pulse, in addition to the action of the maser pump. The application of a desaturation pulse between levels one and four will then desaturate the maser, restoring the excess population density between levels two and one. In a cavity maser, full recovery of the amplification capabilities has been achieved within less than 1 msec after the maser has been saturated. Repetition rates up to 120 cps are tolerable.

Optical Masers - See 7540

FERROELECTRIC DEVICES

7445 BISTABLE AND LOW-VOLTAGE FERROELECTRIC-CONTROL CONFIGURATIONS FOR ELECTROLUMINESCENT DISPLAY DEVICES by W. P. Caywood, Jr. (Westinghouse Res. Labs.); Proc. 1960 Natl. Electronics Conf., pp. 693-700

Ferroelectric ceramic devices have proven advantageous over competing methods for control of electroluminescent display screens. They have mechanical and electrical properties that are commensurate with electroluminescent cells, and they are economical. The major disadvantage of the present usage of ferroelectric control for electroluminescent display devices lies in the need for large control potentials (100 volts or more) and in the difficulty of obtaining memory of control potential over large periods of time. The technical and economic problems as they exist are discussed in the literature. Recent developments of ferroelectric control configurations allow an extension of the obtainable properties. New regenerative circuits reduce the required control potentials by a factor of ten or more. Bistable circuits allow control signal storage for unlimited periods. Also achievable is an inherent discrimination against control potential changes outside the critical ones, facilitating signal distribution through matrices and facilitating translations such as to alphanumerical digits. In some cases the new circuits reduce considerably the requirements on certain circuit components, compounding their advantages by competition in cost with previous methods.

SUPERCONDUCTIVE DEVICES

7446 PROBLEMS AND LIMITATIONS IN CRYOTRONICS by M. L. Cohen (Arthur D. Little); Solid State Journal, Vol. 1, pp. 25-30, Sept.-Oct. 1960

The problems and limitations in cryotronics are reviewed and some methods for maximizing the usefulness of cryotrons are presented. Speed limitations are discussed and suggestions on how to maximize the speed, usefulness, and efficiency are given.

Characteristics of Cryotrons - See 7511

7447 A REVIEW OF THE THIN FILM CRYOTRON by W. B. Ittner III (IBM); Solid State Journal, Vol. 1, pp. 44-47, July-Aug. 1960

A review of the thin film cryotron when used as a gate circuit is presented. The cryotron consists essentially of a wide film of material whose superconductivity can be destroyed by a small magnetic field. This field can be produced by currents through the material or by currents through a wire near the

material. When two of these are in parallel, the current can be made to go down either leg by destroying the superconductivity in the other leg. Switching speed is discussed in relation to both electromagnetic and thermal time constants and with considerations of cryotron gain. Size, power dissipation, and heat control in computer circuits are discussed.

7448 PHYSICS AND CHARACTERISTICS OF THE CROSSED-FILM CRYOTRON — A REVIEW by V. L. Newhouse, J. W. Bremer and H. H. Edwards (GE); Solid-State Electronics, Vol. 1, pp. 261-272, Sept. 1960

A discussion of thermal nucleation and propagation phenomena of superconducting films and an analysis of the static and dynamic characteristics of crossed-film cryotrons which depend on joule heating are presented. The analysis is based on standard electromagnetic theory and the results are found to agree with experiment. An analog storage circuit used to measure the time constant of one CFC driving another is described. The time constant of the CFC has been found to be independent of the area if gain and temperature are held constant. With present materials, τ lies between 0.1 and 0.4 μsec for $T_c - T \sim 0.08^\circ K$.

7449 OPERATION AND ANALYSIS OF PLANAR CRYOTRONS AND SIMPLE CRYOTRON CIRCUITS by G. B. Rosenberger (IBM); Solid-State Electronics, Vol. 1, pp. 388-398, Sept. 1960

Simple cryogenic loops containing two drive cryotrons and a number of sensing cryotrons are described. It is possible with such loops to study both the operating characteristics of the individual cryotrons as well as the static and dynamic switching characteristics of the loop. Some of the characteristics of the individual cryotrons and the reproducibility of cryotrons with these characteristics are discussed. The speed with which current can be transferred from one branch of the loop to another has been both measured experimentally and calculated theoretically from the dimensions and various measured parameters of the loop and its cryotrons. There is found to be good agreement between theory and experiment. The loops have been run dynamically in an effort to detect thermal effects associated with heat dissipation in the resistive cryotron elements. The upper limit to the dynamic operation is currently set by the viewing equipment and, to date, no adverse heating effects have been observed.

Cryotron Memory Plane - See 7543

7450 BRITISH RESEARCH ON THE CROWE CELL by D. H. Parkinson (RRE); Solid-State Electronics, Vol. 1, pp. 306-311, Sept. 1960

Construction techniques and computer applications of Crowe cells are reviewed. The switching time of faster Crowe cells has been found to be compatible with pulse lengths of about 100 mμsec. Current has been satisfactorily stored for intervals of 10 minutes and has been unaffected by many half read or write pulses, hence the cells can be used in coincidental current work. Experimental Crowe cell stores with write-in selection and pick-up circuits are described.

MAGNETOSTRICTIVE DEVICES

7451 DESIGNING MAGNETOSTRICTION FILTERS by E. J. Neville, Jr. (Raytheon); Electronics, Vol. 33, pp. 88-89, Dec. 16, 1960

Bandpass filters, using magnetostrictive resonance units, with a frequency range from 45 - 300 kc and 12 db attenuation per bandwidth octave are described. A high-Q nickel-iron alloy rod is driven in the longitudinal mode. Applying ac to the drive coil generates a magnetic field causing strain waves to propagate along the rod and reflect from the ends. The filter resonates when the driving frequency causes the applied waves to reinforce the reflected waves. Since the lengthening of the rod is independent of the direction of the magnetic field, the resonant frequency is twice the applied field frequency. Barium-ferrite bias magnets are used to compensate for this and to improve filter stability. Frequency is adjusted by removing metal from the rod, which changes the mass distribution along the rod. The filters are useful in test equipment, command receivers and telemetry applications.

BASIC SOLID STATE DEVICE CIRCUITS

GENERAL (Network Theory, etc.)

7452 ABOUT THE TRANSFER GRAPHS OF A LINEAR SYSTEM [in French] by Y. Chow and E. Cassignol; Comptes Rendus, Vol. 251, pp. 1365-1367, Oct. 3, 1960

A new method for the construction of transfer graphs of a linear system based on the "no node" concept is proposed. This representation permits the diagrams of Coates and Mason to be combined. The method is also used for the study of the transistor amplifier.

7453 A FREQUENCY-DOMAIN THEORY FOR PARAMETRIC NETWORKS by B. J. Leon (Hughes Res. Labs.); IRE Trans., Vol. CT-7, pp. 321-329, Sept. 1960

A frequency-domain method for analyzing the transient and steady-state behavior of a class of linear, variable parameter networks is presented. This class is defined as follows: A "lumped, linear, parametric network" (LLPN) consisting of a finite number of lumped circuit elements, R's, L's, and C's, whose values vary periodically with time, imbedded in a network of fixed R's, L's, and C's, and sources. In any particular LLPN, the frequencies of all the time-variant elements are commensurable. The method of analysis, based upon the theory of linear difference equations, is exact. There are no approximations which restrict the analysis to networks containing sharply tuned filters. For a single sinusoidally varying element a precise numerical method that is readily performed by a digital computer is presented. In addition, some interesting properties of single-element linear parametric amplifier networks are presented.

7454 NECESSARY AND SUFFICIENT CONDITIONS FOR THE EXISTENCE OF ±R, C NETWORKS by B. K. Kinariwala (Bell

Labs.); IRE Trans., Vol. CT-7, pp. 330-335, Sept. 1960

Necessary and sufficient conditions for the existence of networks containing positive resistors (+R), negative resistors (-R), and positive capacitors (C) are presented. It is shown that the elements of the open-circuit impedance matrices of ±R, C n-ports can have poles only on the real axis of the complex frequency plane and these poles must be simple. The matrices of residues in all the finite poles must be positive semidefinite, and if there are any poles at infinity the matrices of residues in them must be negative semidefinite. These conditions are sufficient as well as necessary. Further, any matrix satisfying the above conditions can be characterized by a passive RC n-port, in a modified frequency variable, with a negative resistor added in series at each of the ports. As a consequence of these conditions, driving-point impedance functions of ±R, C networks can have only simple zeros and poles alternating on the real axis and the residues in all the finite poles must be positive.

Static Characteristics of Negative Resistance Devices - See 7408

7455 EXTENSION OF BRUNE'S ENERGY FUNCTION APPROACH TO THE STUDY OF LLF NETWORKS by P. Bello (Sylvania); IRE Trans., Vol. CT-7, pp. 270-280, Sept. 1960

An effective analytic approach to the study of the fundamental properties of driving point and transfer functions of RLC networks (also designated LLFPB networks) is based upon expressing the network functions in terms of energy functions associated with the network. Using this approach, Brune deduced the well-known necessary conditions on driving point and transfer functions of LLFPB networks. It is the aim of this paper to extend this approach to a class of active non-bilateral RLC networks (designated as LLF networks) generated by augmenting RLC networks through the addition of resistive, capacitive, and inductive multiterminal-pair devices which are not required to be passive or bilateral. In order to derive effectively the properties of LLF networks using the energy function approach, it is desirable to be able to analyze networks whose elements are multiterminal-pair devices. Such a method of analysis is suggested as a generalization of a method due to Guillemin. Using the energy function approach, necessary conditions are derived for driving point and transfer functions of several classes of LLF networks. In addition, some of these conditions are shown to be sufficient. Networks which consist of resistors, inductors and capacitors, both positive and negative, in addition to gyrators and generalized versions of gyrators (to an inductive and capacitive nature) are considered.

7456 ON THE SOLUTION OF NETWORKS BY MEANS OF THE EQUICOFACTOR MATRIX by G. E. Sharpe and B. Spain (Brit. Telecommun. Res.); IRE Trans., Vol. CT-7, pp. 230-239, Sept. 1960

In the solution of electrical networks, there arise matrices with the property that the sum of the elements of every row and of every column equals zero. On the node basis this is a direct consequence of Kirchhoff's current law coupled with the fact that the currents are invariant to a change of all node potentials by the same amount. As a consequence, all the first cofactors associated with determinants of such matrices are equal. These matrices are designated equicofactor matrices and a general discussion of the solution of networks based on these matrices is presented. A new sign notation is introduced and problems of admittance-impedance conversion are treated. A proof of a theorem called Jeans' theorem which relates to the second cofactor matrix is given. This theorem is a consequence of the fact that, in the solution of networks, it is immaterial which node (mesh) is taken as reference and which equation is considered superfluous and suppressed from the given set, since the final answer must be the same. The theorem also shows that only $(n-1)^2$ coefficients associated with an n-node (n-mesh) network are independent, regardless of whether the network is described on an admittance or impedance basis. It is therefore concluded that there is perfect duality between the admittance and impedance description of networks, whatever their complexity.

7457 MODES IN LINEAR CIRCUITS by C. A. Desoer (U. California); IRE Trans., Vol. CT-7, pp. 211-223, Sept. 1960

It is shown that the concept of modes applies to any linear time invariant circuit. This is accomplished by reducing the network equations to the standard vector form $y = Ay + f$. In particular, it is shown that 1) any free oscillation of a linear circuit can be thought of as a superposition of non-interacting modes, 2) in the case of free oscillations, the amount of excitation of each mode can easily be expressed in terms of the initial conditions, 3) any forcing function excites each mode independently, and finally, 4) the resonance phenomenon is easily interpreted and the importance of the proper type of excitation is made obvious. Vector notation is used throughout. Examples of RC, RLC and active circuits are included.

7458 EQUIVALENT CIRCUIT OF A PARAMETRIC DIODE by A. K. Kamal, K. E. Lytal, and H. W. Pass (Purdue U.); Proc. 1960 Natl. Electronics Conf., p. 801 (A)

An attempt to synthesize an equivalent circuit for a silicon mesa diode is described. From theoretical considerations, the diode is regarded as a three-port network: two waveguide ports and a third port at which the semiconductor appears. Coaxial-type diodes have been mounted in X-band waveguide so that the electric field of the TE_{10} mode was parallel to the axis of the diode cartridge. The guide beyond the cartridge was terminated by a matched termination. By making impedance measurements on the cartridge alone, the characteristics of the cartridge as a network has been determined. A similar set of measurements has been made on several diodes. An LGP-30 digital computer has been used to reduce the data in the equivalent circuit synthesis. It was noted that the diode impedance was inductive in X-band. This is due to the cartridge, which resembles an inductive post in this configuration. A detectable change of impedance with power level at relatively low power levels was also noted. V-I characteristics of the diode with RF applied indicate the appearance of a negative resistance region with the application of RF.

7459 NOISE IN TUNNEL DIODE CIRCUITS by E. G. Nielsen (GE); Proc. 1960 Natl. Electronics Conf., pp. 785-790

Noise figures in the order of 3 db are obtainable with present tunnel diodes at moderate frequencies. As the frequency approaches the diode's cutoff frequency this figure increases rapidly. When a tunnel diode is used as a preamplifier, the noise figure is a function of the tunnel diode noise as well as the noise of the other elements of the system. However, it is shown that within certain limitations the overall noise figure can approach as a minimum a quantity which is a characteristic of the tunnel diode by itself. This quantity is readily calculated.

The minimum system noise figure is approached by suitable scaling of the diode and the circuit immittances. It is approached most efficiently when an optimum relation exists between the signal source immittance and the diode negative immittance.

7460 THEORY OF LIMITING FUSES [in Czech.] by B. Novotny (CKD); Elektrotech. Obzor., Vol. 49, pp. 600-604, Nov. 1960

One of the principal problems of the melting of a fusible conductor as a quick-acting limiting fuse for semiconductor rectifiers is discussed. A detailed mathematical analysis of the time dependence of the temperature over the length of the conductor shows that the melting of an arbitrary conductor with electron conductivity in an arbitrary short time requires no higher voltage than that increased by 6.6 to 13.6% — the so-called welding voltage — recalculated to 0°C. This theory of limiting fuses affords a reliable means of protecting semiconductor rectifiers.

7461 DESIGN OF SYSTEMS TO TOLERATE VARIABLE PARAMETERS by P. E. Merritt (Stanford U.); Diss. Abstr., Vol. 21, pp. 831-832 (A), Oct. 1960

System design methods which allow for component variations such as those exhibited by transistors are presented. By employing the parameter statistics, the statistical variance of a selected performance function is used to measure the spread of the circuit performance. The parameter correlation matrix of the production units is found to be the essential measure of variations of transistors. Through the use of a small-motions approximation the variance of performance is related to the average transistor parameters, the correlation matrix of the transistor parameters and the circuit parameters to be selected. An illustrative design in which the Q and turns ratio of transformers of an IF amplifier are chosen to minimize the spread from a prescribed gain is discussed. The solution provides design curves from which one can make various compromises between percentage of amplifiers rejected, width of allowed spread, transformer quality, and prescribed gain. The statistical problem of designing for parameter variations is also related to techniques of signal theory. By interpreting the variations of parameters as being equivalent to internally generated noise signals the statistical problem is formulated by means of a signal-flow graph. Parameter variations are accounted for by combining additional inputs into the original system flow graph. The design becomes one of reducing the equivalent noise power at the output when the system has a prescribed average response from input to output. The procedure is extended to include variations in the time response of a dynamic system. The mean square error and integral square error averaged over the ensemble population is minimized in order to give reproducibility of response from system to system within a production population.

7462 THE CHARACTERIZATION OF TRANSISTORS by A. R. T. Turnbull (U. Melbourne); Proc. IRE, Aust., Vol. 21, pp. 530-539, Aug. 1960

The small signal characterization of transistors in terms of device parameters is discussed. The equivalent circuit representation employed gives sufficient accuracy over the normal range of operating conditions and frequency. The performance of transistors with drift fields in the base region deviates from the simple theory of diffusion type devices, but it is shown that the drift transistor can also be characterized with very little modification of the simple equivalent circuit. Theoretical relationships between the various semiconductor properties and transistor parameters allow the prediction of the variation of transistor parameters with operating point and temperature. The problem of deducing device parameters from terminal measurements is also considered and circuits for performing these measurements are described.

7463 TRANSISTOR EQUIVALENT CIRCUIT CRITERIA by T. L. Martin, Jr. and D. J. Sakrison (Arizona U.); U.S. Gov. Res. Rep., Vol. 34, p. 709 (A), Dec. 16, 1960 PB 147 539

A hybrid parameter equivalent circuit for the common emitter connection is developed. The basic circuit is modified for high frequency use in such a way that the parameters of the equivalent circuit are independent of frequency. Methods of measuring these various parameters are discussed in detail and circuit diagrams are provided for each such measurement. The proposed transistor equivalent circuit is then used in the analytical development of circuit design equations and criteria for low pass, high pass, and band pass amplifiers.

7464 HYBRID π-SHAPED EQUIVALENT CIRCUIT FOR A SEMICONDUCTOR TRIODE AND THE DEPENDENCE ON FREQUENCY OF THE Y-PARAMETERS by V. K. Labutin; Radio Engrg., Vol. 15, No. 5, pp. 47-55, 1960

The frequency relationship of the y-parameters of a transistor are derived from a hybrid π-shaped equivalent circuit and a set of generalized relationships which facilitates the design of transistorized high-frequency systems is given.

7465 BIASING TRANSISTORS FOR UNIFORM GAIN by K. Redmond (Amperex); Electronics, Vol. 33, pp. 74-75, Dec. 9, 1960

A method of obtaining uniform gain, despite beta variation, by analysis of Thevenin equivalent circuits is described. The transistor bias network is reduced to a single resistor between the base and collector supply by application of Thevenin's theorem. The resulting circuit is analyzed and the equations are developed. Experimental results show a 10 percent change in emitter current for a 400 percent change in beta.

7466 DETERMINING TRANSISTOR POWER DISSIPATION by J. G. Naborowski (Pacific Semicon.); Electronics Ind., Vol. 19, pp. 110-111, Aug. 1960

A method for determining the minimum load resistance for a given supply voltage and transistor power rating is described. Maximum power is delivered to a load when the voltage across the load is one half the supply voltage. Using this fact along with the formulation of the safe power level, the minimum resistance can be found in terms of the supply voltage or the maximum current. A method for determining power dissipation and change in power dissipation in transistors is also formulated in terms of the supply voltage and load resistance.

AMPLIFIERS

7467 AMPLIFICATION — MODERN TRENDS, TECHNIQUES AND PROBLEMS by L. S. Nergaard (RCA Labs.); RCA Rev., Vol. 21, pp. 485-507, Dec. 1960

The characteristics of various types of small-signal amplifiers,

Including traveling-wave tubes, tunnel diodes, cooled and uncooled parametric amplifiers, and masers are reviewed. The type of amplifier best suited for a particular application is determined by a number of factors, among which noise considerations and frequency are the most important. Areas of usefulness for each type of amplifier are described. In addition, there is a brief discussion of existing high-power transmitting tubes and their fundamental power limitations. It is suggested that a major breakthrough may be necessary before an order-of-magnitude improvement can be expected.

Study of Transistor Amplifiers by Transfer Graphs - See 7452

Design of Low Pass, High Pass, and Band Pass Amplifiers - See 7463

7468 THE LOWER CUT-OFF FREQUENCY OF A STABILIZED AMPLIFIER STAGE WITH A TRANSISTOR OR A PENTODE [in German] by W. Steimle (Tech. Hochschule, Stuttgart); Nachrichtentech. Z., Vol. 13, pp. 473-474, Oct. 1960

The loci curve of the mutual conductance in a transistor amplifier stage in a grounded emitter circuit with an RC network in the emitter line is explained and the lower cutoff frequency is calculated. It has been found that this cutoff frequency is approximately equal to the 45° frequency of the emitter capacitor in conjunction with the inner impedance r_e of the emitter. By means of a perturbation method the results obtained are applied to a pentode circuit with a cathode impedance.

7469 THE THERMAL STABILITY EQUATION FOR DIFFERENT TYPES OF TRANSISTOR VOLTAGE AMPLIFIERS by Iu. R. Nosov and B. I. Khazanov; Radio Engrg., Vol. 15, No. 3, pp. 53-62, 1960

The thermal stability equation for a voltage amplifier which takes into account a variation of the parameters of the transistors is derived. The solutions of this equation for commercial types of germanium and silicon transistors are examined.

7470 LOW-IMPEDANCE SHUNT-FEEDBACK VIDEO AMPLIFIER DESIGN by W. E. Owen (Louisiana State U.); Solid State Journal, Vol. 1, pp. 48-54, July-Aug. 1960, pp. 39-44, Sept.-Oct. 1960, pp. 35-44, Nov.-Dec. 1960

A method for designing transistorized video amplifiers suitable for use with low-impedance input and output circuits is presented. Three cascaded common-emitter stages with negative feedback around each stage are used. The design example has a flat current and voltage amplification from 3.2 kc to 32 Mc, a voltage amplification of 20 db and an input and output impedance of 50 ohms. Comparisons between the calculations and measurements are made.

Properties of Linear Parametric Amplifier Networks - See 7453

7471 PARAMETRIC AMPLIFICATION BY JUNCTION DIODES by E. L. Steele (Hughes Semicon.); Electronic Ind., Vol. 19, pp. 81-83, Oct. 1960

The basic theory of parametric amplification using junction diodes is outlined.

7472 ESAKI DIODE AMPLIFIERS AT 7, 11, AND 26 KMC by R. F. Trambarulo (Bell Labs.); Proc. IRE, Vol. 48, pp. 2022-2023 (L) Dec. 1960

Gallium arsenide Esaki diode amplifiers consisting of a reflection cavity containing the diode with input and output separated by means of a circulator or directional coupler are described. The cavity is coupled into by means of a large loop and can be adjusted to give gains from 5 to 38 db. When the gain is high, it is particularly sensitive to small changes in the bias. The gain and frequency response were found to be dependent on reflections from the circulator. Stable gains were measured up to 38 db at 6.8 kMc and 10.8 kMc and 36 db at 25.8 kMc. Measured noise figures were 7.5 db at 6.8 kMc, 10.7 db at 9.7 kMc and 11.5 db at 10.8 kMc.

7473 NOISE FIGURE MEASUREMENTS RELATING THE STATIC AND DYNAMIC CUTOFF FREQUENCIES OF PARAMETRIC DIODES by C. R. Boyd (GE); Proc. IRE, Vol. 48, pp. 2019-2020 (L), Dec. 1960

An attempt to confirm predicted noise behavior and to establish an experimental correlation between the static cutoff frequency and the dynamic cutoff frequency of parametric diodes by means of parametric amplifier noise figure measurements at the lower edge of the X-band is described. Degenerate-mode amplification was obtained at about 8,200 Mc with a number of diffused-junction mesa-type silicon and germanium diodes. A qualitative correspondence between experimental and analytical behavior was evident, and an f_c/f_d ratio of about 10 was obtained.

7474 GAIN OF A TRAVELING-WAVE PARAMETRIC AMPLIFIER USING NONLINEAR LOSSY CAPACITORS by W. Jasinski (Philco); Proc. IRE, Vol. 48, pp. 2018-2019 (L), Dec. 1960

A traveling-wave paramagnetic amplifier using nonlinear lossy capacitors is analyzed. Reversed biased diodes are considered to be the lossy capacitors, the resistive element being provided by the diode spreading resistance only. By assuming the dependence of the capacitance of the traveling-wave circuit on the pumping frequency and the fractional modulation of the diode capacitance, relations are found between the fractional modulation of the diode capacitance, the pumping frequency, the Q of the diode and the signal frequency for which amplification can be a maximum. Curves showing the dependence between parameters are also presented.

7475 THE DEGENERATE AND QUASI-DEGENERATE MODE OF PARAMETRIC AMPLIFICATION by P. Bura (ITT Labs.); IRE Trans., Vol. CT-7, pp. 200-210, Sept. 1960

An analysis of the degenerate mode of parametric amplification based on the theory of linear differential equations with periodically varying coefficients is presented. A steady-state (particular integral) solution of Mathieu's equation is obtained and expressions for gain, bandwidth and noise figure are derived for varying signal, pump and resonance frequencies. Similar expressions are derived for the lower-sideband or idler response. The gain and bandwidth of the idler response approaches that of the signal as the variation of capacitance is increased. When the fractional capacitance variation becomes equal to 2/Q, oscillations at half the pump frequency are excited. Due to the frequency inversion of the idler response, the practical application of the degenerate mode is very limited. In quasi-degenerate mode, when idler and signal responses are sufficiently removed to prevent the intermixing of the sidebands, both the gain and the noise figure deteriorate by approximately 3 db.

7476 THEORETICAL AND EXPERIMENTAL CHARACTERISTICS OF A FERROMAGNETIC AMPLIFIER USING LONGITUDINAL PUMPING by R. T. Denton (Bell Labs.); Sixth Conf. Magnetism

and Magnetic Materials

A ferromagnetic parametric amplifier requiring fractional watt of pump power was described. The amplifier employs magnetostatic modes as resonances which are parametrically pumped by a longitudinal RF magnetic field. A theoretical discussion of the characteristics of longitudinal parametric pumping on the magnetostatic modes was presented including selection rules for determining which pairs of modes can be pumped and an expression for the threshold pump field required for pumping the modes to oscillation. A model of the amplifier which utilizes X-band pump power and amplifies at C-band frequencies has been built. The signal circuit is a coaxial line with a loop connected from the center conductor around a sphere of yttrium iron garnet providing coupling to the magnetostatic mode at the signal frequency. Results of measurements on the amplifier at room and liquid nitrogen temperatures were presented and compared with the results of a theoretical analysis. In addition speculation on the sources of noise in this amplifier was included.

Avalanche Diode Amplifiers - See 7409

7477 THE DESIGN OF DIRECT COUPLED PRE-AMPLIFIERS by L. Dally, B. M. Johnstone and I. D. Pugsley (U. Melbourne); Proc. IRE, Aust., Vol. 21, pp. 465-467, July 1960

Two hybrid (electrometer) triode-transistor amplifiers are discussed. Positive feedback effectively reduces the input capacity of one amplifier. The analysis of this feedback is given.

OSCILLATORS

7478 MINIATURE TRANSISTORIZED CRYSTAL-CONTROLLED PRECISION OSCILLATORS by W. L. Smith (Bell Labs.); IRE Trans., Vol. I-9, pp. 141-148, Sept. 1960

Crystal-controlled transistor oscillator circuits employing precision AT-cut quartz resonators which provide frequency stability comparable to vacuum-tube frequency-standard oscillators are described. These transistor oscillators are considerably reduced in size and in power drain, and possess excellent short-time stability. Oscillators suitable for fixed-station applications, capable of operating in widely varying ambient conditions and oscillators designed for very low power drain and capable of withstanding the extreme mechanical environments of satellite and missile-borne applications are discussed. Performance test results for operation during quiet conditions and during vibration, shock, and static acceleration are given.

7479 NONLINEAR ANALYSIS OF A TRANSISTOR HARMONIC OSCILLATOR by D. O. Pederson and R. S. Pepper (U. California); U.S. Gov. Res. Rep., Vol. 34, p. 713(A), Dec. 16, 1960 PB 149 497

An analysis of a tuned-collector transistor oscillator using both graphical and piece-wise linear techniques for obtaining the composite negative resistance characteristic presented to the tank circuit is given. With the negative resistance characteristic, conventional phase plane and limit cycle analysis can be used to predict the oscillator output. Higher order effects are inspected, and it is found that the simplifying assumptions made are quite valid. Thus, the second order differential equation provides a good approximation of the system. Experimental results that show predicted and observed values to be within a few percent for amplitude of oscillation, period of oscillation, and wave shape, i.e., harmonic content, are given.

Transistorized Blocking Oscillator Discriminator - See 7532

SWITCHING CIRCUITS

7480 BACK-TO-BACK ZENER DIODE BRIDGE GATING CIRCUIT by L. Finkel (Am. Bosch Arma); U.S. Pat. 2,965,771, Issued Dec. 20, 1960

A coupling circuit which provides extremely low impedance during a conducting interval initiated by a gating signal and very high impedance between gating signals is described. A double anode Zener diode or a pair of back-to-back Zener diodes connected across diagonal terminals of a bridge network is utilized. The circuit, which has application in sampling or commutating circuits, minimizes feedback or leakage between the source of the signal to be sampled and the output or storage circuit during intervals between gating pulses.

7481 COINCIDENCE SENSING DEVICE by A. W. Vance (U.S.A.); U.S. Pat. 2,964,649, Issued Dec. 13, 1960

A device designed to sense coincidence in amplitude of two or more voltages, such as might be required in a summing circuit, monitoring circuit, or other voltage comparing circuit, is described. The device makes use of the small non-linear portion of a diode or rectifier characteristic found about zero applied voltage, employing it as a generator of a second or higher harmonic null signal. A prototype employing a germanium diode has achieved an average accuracy of 0.1%. The system is simpler, less expensive in cost and operation, and more compact than previous systems.

7482 SWITCHING LEVELS IN TRANSISTOR SCHMITT CIRCUITS by T. J. Galvin (Space Tech. Labs.), R. A. Greiner and W. B. Swift (U. Wisconsin); IRE Trans., Vol. I-9, pp. 309-314, Dec. 1960

The operation of a Schmitt trigger circuit using transistors is briefly reviewed. A graphical method of calculating switching levels which converges rapidly is presented. Sensitivity of switching levels to changes in element values is analyzed by an approximate analytical method and by experiment.

7483 TRANSISTOR SWITCH by N. W. Bell (Consolidated Electrodynamics); U.S. Pat. 2,965,769, Issued Dec. 20, 1960

A technique for producing a very high open circuit impedance of a transistor switch without affecting its closed circuit impedance is described. A resistor is connected in parallel with the transistor and a control signal generator is connected between the base and collector electrodes of the transistor. When the signal generator applies a reverse bias voltage between the base and collector, the parallel impedance also applies a reverse bias between the emitter and the base. With both junctions reverse biased, a high impedance results. The parallel resistance does not affect the circuit when the transistor is forward biased. The circuit permits the switch to be used at higher temperatures than would otherwise be possible.

7484 HIGH-SPEED MICRO-ENERGY SWITCHING by C. D.

Simmons (Philco); Solid State Journal, Vol. 1, pp. 31-38, Sept.-Oct. 1960

The device limitations that make mandatory the present high power level of operation of high-speed circuits, and circuit and device changes which permit high-speed operation at much lower power levels are discussed. It is shown that at present it is possible to fabricate micro-energy switches which permit the transistorization of high-speed equipment operating at about 1/10 of the power consumption of those presently in use. From observations of devices that switch in the low current region and from a general treatment of the switching speed parameters it is concluded that very low power transistorized circuits will be feasible in the near future.

7485 ELECTRICAL SWITCHING CIRCUIT by G. Abraham, U. S. Pat. 2,964,654, Issued Dec. 13, 1960

A bistable circuit consisting of a dynamic B+ which controls a variable resistance is described. The variable resistance is, for example, a piece of semiconductor material which changes its resistance upon the injection of minority carriers. This piece of semiconductor is connected in push-pull injection relationship with the dynamic B+ in such a way that the B+ controls the resistance of the semiconductor. In the case presented the dynamic B+ is a square wave. Due to the recombination of carriers an S resistance curve is formed for which there are two or more stable states when the load line falls correctly on the S curve. This bistable circuit has many advantages including small power consumption, small size and a range of stable states from zero to breakdown voltage. The circuit may also be operated as an astable or monostable device.

Cryotron Switches - See 7446

SIGNAL CONVERTERS

7486 VOLTAGE TO PULSE-WIDTH CONVERSION DEVICE by W. B. Guggi (Westinghouse); U.S. Pat. 2,965,766, Issued Dec. 20, 1960

A voltage to pulse-width conversion device which permits linear pulse-width modulation between zero and 100 percent modulation as a function of control voltage or control current magnitude is described. A pair of constant current devices are connected in series across a dc bias source. One is gated with a reference voltage and the other with a sawtooth voltage. The voltage waveforms produced across the individual constant current devices are rectangular waves in phase opposition which are oppositely variable in pulse width. The time duration of the rectangular waves is controlled by varying the reference voltage to the first constant current device. This varies the time at which it begins current limiting.

7487 TRUE RMS VOLTAGE DISCRIMINATOR by F. A. Galindo (Texas Instr.); IRE Trans., Vol. SET-6, pp. 157-159, Sept.-Dec. 1960

The circuitry, the electrical specifications, the environmental specifications, and the method of calibration of a completely transistorized true root-mean-square voltage discriminator are discussed. The circuitry is broken into four separate operational circuits, each of which is considered in relation to what it does and what its relationship to the other configurations is. The specifications of the discriminator are discussed along with a detailed explanation of the method employed in calibration of the module with nonsinusoidal waveforms.

7488 PHASE-SENSITIVE DETECTION WITH MULTIPLE FREQUENCIES by B. O. Pedersen (Nat'l. Res. Council of Can.); IRE Trans., Vol. I-9, pp. 349-355, Dec. 1960

The multiple-frequency type of phase-sensitive detector differs from the conventional detector in that the signal frequency is a multiple of the reference frequency. Conventional phase-sensitive detectors may be readily adapted for multiple-frequency operation. Two detector circuits employing diodes are analyzed and discussed in detail. The circuit configuration required for even harmonic signals differs slightly from that required for odd harmonic signals. The multiple-frequency phase-sensitive detector may be designed to discriminate against higher-order harmonics contained in the signal. As a practical application, the use of a second harmonic phase-sensitive detector in a flux-gate magnetometer which leads to a simplification of the magnetometer circuit is described.

7489 A GENERALIZED APPROACH TO THE EVALUATION OF N-FREQUENCY PARAMETRIC MIXERS by C. R. Boyd (GE); Proc. 1960 Natl. Electronics Conf., pp. 472-479

Reactance mixers using more than three frequencies have been proposed as a method of combining the low noise of upper sideband systems with the high gain of lower sideband systems. In this paper a transmission line model of a simple parametric mixer under small-signal conditions is developed and applied to the n-frequency case. The variable reactance element used as a model is the semiconductor diode-capacitor. A topological description of the frequency coupling for such a capacitor is presented, in terms of the coefficients of the usual Fourier expansion of the nonlinearity as a function of time under pumped conditions. The mixer system is viewed as a multiport junction, with each port in general at a different frequency. Matrix methods are used to describe the operation of the mixer. A technique for determining the scattering matrix, gain, and noise figure of an n-frequency mixer is outlined.

7490 A HARMONIC GENERATOR AND DETECTOR FOR THE SHORT MILLIMETER WAVE REGION by H. W. De Wijn (U. Amsterdam); Appl. Sci. Res., Vol. 8B, No. 4, pp. 261-264, 1960

A millimeter wave harmonic generator and detector in which improved operation is achieved by utilizing an unencapsulated semiconductor point contact diode is described. The crystal and a fine tungsten wire are introduced separately from opposite sides of the millimeter waveguide and contact is made by means of a mechanical system. At a wavelength of 5 mm an unencapsulated crystal detector is more than 10 times as sensitive as a detector with a commercial IN53 cartridge crystal; at 4mm about 50 times as sensitive.

7491 GAIN OPTIMIZATION IN LOW-FREQUENCY PARAMETRIC UP-CONVERTERS BY MULTIDIODE OPERATION by A. K. Kamal and M. Subramanian (Purdue U.); Proc. IRE, Vol. 48, pp. 2020-2021 (L), Dec. 1960

The use of more than one variable capacitance diode at the same point for the purpose of optimizing the gain of low-frequency parametric up-converters is described. A first order analysis, utilizing two diodes, is demonstrated along with experimental data which verifies the theoretical predictions. An

experimental twin diode circuit yielded a $G_p$max of 6.1 as compared with a single diode gain of 3.1. It is concluded that maximum possible gain can be obtained with existing diodes by means of multi-diode operation.

7492 A BROAD-BAND HYBRID COUPLED TUNNEL DIODE DOWN CONVERTER by W. J. Robertson (Ohio State U.); Proc. IRE, Vol. 48, pp. 2023-2024(L), Dec. 1960

A low-noise broad-band radio frequency mixer that provides isolation between the tunnel diode amplifier and the local oscillator is described. A pair of tunnel diodes and a balanced IF circuit are connected to two arms of a hybrid. With correct biasing of the tunnel diodes, the hybrid action isolates the input terminals from the signal source. Stable small signal conversion gains up to 10 db and a two channel noise figure of 7 db were measured at 400 Mc. Refinements that will improve the performance of the device are also suggested.

WAVEFORM GENERATORS

Tunnel Diode Pulse Generator - See 7544

Avalanche Transistor Pulse Generator - See 7425

7493 LINEAR WAVE GENERATOR by S. W. Lewinter (RCA); U.S. Pat. 2,965,770, Issued Dec. 20, 1960

A method of obtaining a linear wave of about 22 1/2 volts peak and 2-1/2 microseconds duration is described. The circuit uses two transistors connected in series, one being used as a switch and the other for its emitter follower characteristics. The capacitor across which the output is taken charges up to a quiescent level through the switch transistor. When the switch transistor is turned off the capacitor charges by a current from another capacitor which discharges through the high resistance of the emitter follower transistor, giving a linear wave. The wave is cut off when the emitter follower transistor is cut off. Since this circuit is light in weight it has applications in airborne equipment such as radar altimeters.

7494 TRANSISTOR LINEAR SWEEP GENERATOR by F. Lee (Sylvania); Electronics, Vol. 33, p. 90, Dec. 16, 1960

A linear sweep generator, using only one transistor and requiring no critical circuit values or adjustments, which generates sweeps of up to 10 sec duration is described. The input consists of two voltage levels which determine the sweep starting point and duration. A silicon diode in the collector circuit is forward or reverse-biased depending upon the input voltage level. When the diode is reverse-biased, the collector voltage is furnished by the output capacitor which also provides the collector current. Since the discharge current is relatively independent of the collector voltage, it remains nearly constant and the capacitor potential decreases in a linear fashion.

7495 DRIVING THE BEAM SWITCHING TUBE by E. J. Obelbermann and H. E. Crecraft (HRB-Singer); Electronic Ind., Vol. 19, pp. 78-80, Sept. 1960

Two circuits used to drive a Burroughs Model 6701 beam switching tube at a 1 Mc rate, a d-c coupling circuit used to drive a beam switching tube at low speeds, and a d-c coupling network used to derive a signal from the target of the 1 Mc circuit are presented. When a beam tube is operated at a high rate, it must be driven with a square wave of much higher amplitude than is needed at a slow rate. The two driver circuits for 1 M provide this high peak-to-peak square wave, one being operated by a saturated flip-flop and the other by sinusoidal or irregular wave shapes. The d-c coupled driver circuit for low spe produces a smaller amplitude wave. The d-c coupling netwo for deriving a signal from the target at 1 Mc protects the bean switching tube from overloading.

OTHER SOLID STATE DEVICE CIRCUITS

Pulse Multipliers and Dividers - See 7415

7496 A SIMPLE METHOD OF MEASURING FRACTIONAL MILLIMICROSECOND PULSE CHARACTERISTICS by O. L. Gaddy (U. Illinois); IRE Trans., Vol. I-9, pp. 326-333, Dec 1960

A method of measuring fractional millimicrosecond pulse char acteristics which is in some respects similar to the sampling os cilloscope is described. The pulse that is being measured is split into two transmission paths and applied to the two inputs of a wide-band coincidence circuit. One of the applied puls is delayed in time and the output voltage of the coincidence circuit is measured with a low bandwidth oscilloscope and plotted vs delay. The pulse characteristics can be determine from this curve even though the pulse shape is not explicitly shown. The operation of the system is analyzed for a trapezoi dal input pulse, and it is shown that all of the pulse characteristics can be determined if a diode with a nonlinear forwar characteristic is used in the coincidence circuit. Results of experimental measurements of approximately trapezoidal pulse generated by a mercury switch pulser are shown which indica that the system measures the pulse characteristics to a fairly high degree of accuracy. The bandwidth of the system is esti mated to be in the neighborhood of 4000 or 5000 Mc, and pul with rise times of the order of 0.1 mμsec have been measured.

7497 PARALLEL CONNECTION OF POWER SEMICONDUC TOR VALVES [in Czech.] by V. Maly (CKD); Elektrotech. C zor., Vol. 49, pp. 583-588, Nov. 1960

The influence of the characteristics of a semiconductor diode upon the parallel operation of diodes is explained and the three most frequently employed methods to improve the parall run, i.e. series resistance, equalizing choke coil and divisio of the valves according to the voltage drop, are analyzed. O the basis of experimental data and mathematical relations, th conclusions for the most advantageous method of improving th parallel operation are derived.

7498 EXACT DESIGN OF TRANSISTOR RC BAND-PASS FIL TERS WITH PRESCRIBED ACTIVE PARAMETER INSENSITIVITY by I. M. Horowitz (Hughes Res. Labs.); IRE Trans., Vol. CT pp. 313-320, Sept. 1960

The classical theory of the design of low-frequency band-pass filters by means of RC rejection networks in the feedback pat of active elements is extended to apply to transistors as the active element. A synthesis procedure is developed in which the finite input and output impedances and reverse transmissio

of transistors are taken into account. The freedom that exists in the synthesis procedure is used to obtain a design with a least active element. Graphs which provide the values of four of the six required network elements are presented. Two simple equations must be solved for the other two. Expressions for the sensitivity of the filter bandwidth and center frequency to the four low-frequency active parameters are developed. It is presumed that the design specifications include a statement of the extent of active parameter variation and of the tolerances on the filter response. The procedure for satisfying such specifications is an integral part of the design procedure. An example which includes all of the above features is worked out in detail.

Bandpass Filters Using Magnetostrictive Resonance Units - See 7451

7499 SIGNAL SYSTEM INCLUDING A DIODE LIMITER by A. J. Radcliffe, Jr. and A. R. Denz (Int. Tel.and Tel.); U.S. Pat. 2,964,650, Issued Dec. 13, 1960

A signal system using a diode limiter to keep incoming signals within a certain signal strength is described. A transistorized telephone signal system receiving various strengths of signals, some of which are so strong they would damage the amplifier, is cited as an example. The diode limiter is used in such a situation to cut down the high amplitude signals and not the low amplitude signals so that both may enter the system without damage. In one form the limiter consists of two diodes which have low inverse resistance at signal strengths near the threshold and high inverse resistance to stronger signals connected in series opposition. In another form two reversely connected diodes are shunted across the input.

APPLICATIONS OF SOLID STATE DEVICES

MEDICAL

7500 RADIO TRANSMITTER FOR REMOTE HEARTBEAT MEASUREMENTS by G. A. Harten and A. K. Koroncai (Philips Lab.); Electronics, Vol. 33, pp. 54-55, Dec. 23, 1960

A self-contained transistorized device which measures a patient's pulse rate continuously and transmits it to a monitoring meter or recording instrument is described. A small clip, containing a lamp in one side and a phototransistor in the other, is attached to one earlobe. Each heartbeat causes a variation in the blood stream, changing the volume of the earlobe. This changes the amount of light transmitted through the earlobe, producing a pulse in the photocell which is amplified and fed to a shaper circuit that generates a square wave signal with every beat. The pulse triggers a fixed-frequency oscillator (3 kc) that amplitude-modulates the carrier frequency (10-15 Mc) of a miniature transmitter. The complete device weighs 3 pounds and is powered by nickel-cadmium batteries.

7501 A TRANSISTORIZED PULSE MONITOR by D. M. Davies and R. L. Allen (Clarkson Coll.); Elec. Engrg., Vol. 79, pp. 915-918, Nov. 1960

An instrument that continuously monitors the pulse rate of an individual on the operating table, providing both visual and aural indication of the average pulse rate, is described. The signal, which may be picked up with either a sensitive microphone or electrocardiograph electrodes, is amplified through a three-stage audio amplifier and displayed on an ink graph recorder. Average pulse rate is obtained by averaging the output of a fixed pulse width multivibrator which is triggered by the heart beat signal.

7502 NEW THERMOLUMINESCENT DOSIMETER by J. H. Schulman, F. H. Attic, E. J. West and R. J. Ginther (U.S. Naval Res. Lab.); Rev. Sci. Instr., Vol. 31, pp. 1263-1269, Dec. 1960

A simple dosimeter design is described in which a thermoluminescent phosphor is mounted on an electrically heatable support in an evacuated or gas-filled envelope. With CaF_2:Mn as the phosphor, the device detects gamma-ray doses in the milliroentgen range and is linear in response up to at least 2×10^5r. Dose readings can be made in less than a minute with simple instrumentation requiring no darkroom facilities. The dosimeter may be reused many times. The response is independent of dose rate at least over the range 10 mr/min to 7000 r/min. With suitable tin shields the response is independent of energy over the range 40 kev to 1.25 Mev. The advantages of this device for monitoring of personnel in health physics operations are pointed out.

RADIO

7503 A PERSONAL TWO-WAY VHF RADIO COMMUNICATION SYSTEM FEATURING MODULAR CONSTRUCTION by T. H. Yaffe (Bendix); IRE Trans., Vol. VC-9, pp. 44-47, Dec. 1960; 1960 IRE WESCON Conv. Rec., Part 7, pp. 74-77

A transistorized VHF "personal" communication receiver assembled entirely from individual circuit modules is described. The modules are constructed with standard, commercially available subminiature components and defective modules can be rapidly replaced. The receiver features include 1 μv sensitivity, double conversion, a crystal filter selectivity package at the high i-f frequency and a novel squelch gating circuit. A companion subminiature transmitter features a 1 watt power output, a transistorized modulator, and a DC-DC converter type of power supply with rechangeable nickel cadmium batteries. The shirt pocket size receiver and transmitter occupy a combined volume of less than 85 cubic inches and together weigh less than 4-1/2 pounds.

Testing Device for Transistor Radio Circuits - See 7541

TELEVISION

7504 A TRANSISTORIZED VIDICON CAMERA FOR INDUSTRIAL USE by M. H. Diehl (GE); J. Soc. Mot. Pict. TV Engrs.,

Vol. 69, pp. 795-800, Nov. 1960

A transistorized vidicon camera designed for closed circuit television applications is described. The camera is completely transistorized except for one miniature tube and the vidicon. The design of the sweep and power supply circuits, the sync generator, and the video circuit are discussed. The optical accessories for the camera and its mechanical design are described. Performance characteristics of the camera under conditions of shock and vibration, temperature extremes and high acoustical noise level are given.

TELEPHONY

7505 THE E6 TELEPHONE REPEATER BACKGROUND, DESCRIPTION AND THEORY OF OPERATION by E. J. Doyle and T. J. Talley (ATT), L. Hochgraf, L. Pedersen and J. O. Smethurst (Bell Labs.); Commun. and Electronics, pp. 525-542, Nov. 1960

The LBO network, converter circuits, testing equipment, design and installation of a transistorized telephone repeater are described.

Avalanche Diode Telephone Repeater - See 7409

7506 A TRANSISTORIZED CHANNEL CONVERTER FOR CARRIER FREQUENCY TELEPHONE SYSTEMS [in German] by K. Bode, H. Kopp and R. Theus (Siemens and Halske); Nachrichtentech. Z., Vol. 13, pp. 465-469, Oct. 1960

Following a discussion of the advantages of transistors, a new transistorized channel converter in which the signal channel can accommodate a c.w. signal outside the speech channel is described. Printed circuits and light weight construction are characteristic features of the design. The unit weighs 40% and the power consumption is 15% of a vacuum tube unit.

Diode Limiter for a Transistorized Telephone System - See 7499

TELEMETRY

7507 ELECTRONIC COMMUTATOR by R. K. Page (N.A. Aviation); U.S. Pat. 2,964,657, Issued Dec. 13, 1960

A transistorized commutator or multiplexer comprising a number of gates for sequentially transmitting a plurality of information signals and a sequential pulse generator for operating the gates individually in sequence and repetitively as a group is described. The device is designed to provide one gating pulse of unique duration each frame to serve as a reference pulse and to ensure the automatic setting of a counter to a selected initial condition. A fixed reference level of output is obtained by clamping the gate outputs for a selected fractional portion of the operating time of each gate.

Zener Diode Bridge Gating Circuit for Commutators - See 7480

Heartbeat Telemetry - See 7500

HEARING AIDS

See 7542

COMPUTERS

Cryotron Switching Cricuits for Computers - See 7447

Photoelectric Binary Counter and Punched Card Reading System See 7435

7508 ELECTRONIC LOGIC CIRCUIT by I. Haas (Sperry Rand); U.S. Pat. 2,966,599, Issued Dec. 27, 1960

A half-adder utilizing positive-gap diodes as the switching elements is described. The fast rise time characteristic of positive-gap diodes, as low as 2 nsec makes possible a high pulse repetition rate, reducing the time necessary for computation by several orders of magnitude. Two circuits employing alternate biasing techniques are described. The device may be cascaded to form a full adder.

7509 MICROCIRCUIT BINARY FULL ADDER USES UNIPOLAR TRANSISTORS by M. E. Szekely, J. T. Wallmark and S. M. Marcus (RCA); Electronics, Vol. 33, pp. 48-49, Dec. 23, 1960

A microcircuit binary full adder, using unipolar field-effect transistors as its active and passive elements, with a volume of 1/400 cubic inch and power dissipation of 20 mw is described. The clock rate is 40 kc. Properly dimensioned field-effect transistors are used as resistors and metallic connections between adjacent units are replaced by semiconductor bridges. A ZERO is represented by a voltage level of -15 volts and a ONE by a voltage level of -5 volts. When a ZERO is fed into a gate, the transistor is pinched-off and presents an open circuit. With a ONE fed into a gate, the transistor presents a moderately low resistance. Further work is expected to increase the clock frequency by a factor of ten.

7510 AN ELECTRICALLY ALTERABLE NONDESTRUCTIVE TWISTOR MEMORY by R. L. Gray (Burroughs); IRE Trans., Vol. EC-9, pp. 451-455, Dec. 1960

The basic principles of twistor operation are discussed and a method of fabricating the twistor into a memory is shown. A nondestructive method of reading a twistor memory by the use of multiple solenoids is described. A typical configuration of a twistor memory which, by the use of a nondestructive reading method, may be operated either in a destructive mode or in a nondestructive mode, is presented.

7511 CRYOTRON STORAGE, ARITHMETIC AND LOGICAL CIRCUITS by M. K. Haynes (IBM); Solid-State Electronics, Vol. 1, pp. 399-408, Sept. 1960

A general discussion of the characteristics of cryotron elements and their employment in computer storage, arithmetic, and logical circuits is presented. Two-dimensional persistent-supercurrent storage, persistent-current storage with register-to-register transfer, and triple access storage systems are described. The operation of counters, shift registers, a binary full adder, and several basic circuits of three variables is described. The

cryotron supercurrent element is said to be the first electronic device capable of a d-c indication of state without a steady state dissipation of power

7512 THIN-FILM CRYOTRON CATALOG MEMORY by A. E. Slade and C. R. Smallman (A. D. Little); Solid-State Electronics, Vol. 1, pp. 357-362, Sept. 1960

A catalog memory circuit employing low gain cryotrons is described. The device is essentially a comparator where all the words in a catalog can be compared simultaneously with any other word. The memory consists of an output gate network and persistent-current memory cells, each of which consists of an enable cryotron used in the write cycle and an output cryotron used in the read cycle. Interrogation time for a memory containing 4000 twenty-five bit words is estimated at 2×10^{-8} sec. The utilization of the catalog memory as a storage and retrieval system is also described.

Cryogenic Memory Plane - See 7543

Crowe Cell Memories - See 7450

7513 A NEW, SOLID-STATE, NONLINEAR ANALOG COMPONENT by L. D. Kovach and W. Comley (Douglas Aircraft); IRE Trans., Vol. EC-9, pp. 496-503, Dec. 1960

A varistor squaring unit which is capable of providing many of the basic nonlinear functions required for analog computation is described. The unit has been compensated for the various types of errors inherent in the varistor itself, resulting in a high degree of accuracy and reliability.

7514 APPLICATION OF THE MAGNETORESISTANCE EFFECT TO ANALOG MULTIPLICATION by J. M. Hunt (Genl. Precision); Proc. 1960 Natl. Electronics Conf., pp. 619-628

Use of magnetoresistive devices as the control elements in modulators or electronic multipliers for analog computation is discussed. The simple and inexpensive magnetoresistance multiplier is most directly competitive with the widely used servo multiplier, but offers the very important advantage of complete freedom from the objectionable nonlinear effects of the servo multiplier which result from backlash, static friction, wire-to-wire resolution, etc. The magnetoresistance multiplier is unusually adaptable to design compromise to permit exchange of one desirable characteristic for another (for example, sacrifice of static accuracy to obtain improved frequency response). Factors underlying the optimum choice of magnetoresistance materials are described and possible methods of extending currently attainable performance of the device are outlined.

Ferroelectric Control Configurations for Electroluminescent Display Devices - See 7445

POWER

7515 STATIC CONTROL FOR A MECHANICALLY REGULATED D-C SUPPLY by H. J. Abrams (Norbatrol Electronics) and J. F. Brubaker (Westinghouse); Commun. and Electronics, pp. 426-430, Sept. 1960

A static control for a mechanically regulated d-c supply which operates at the dc output is described. Although the circuit is used to change the ac voltage input of the supply system, it senses the dc voltage at the output instead of the ac input. This circuit has the advantage of having no need to compensate for the conversion circuit. The sensing circuit takes the dc voltage from the output by means of a bleeder bank of resistors and uses a varistor-detector biased at its null point in conjunction with bistable amplifiers. The sensing circuit has fast response, adjustable bandwidth, a low drift level with respect to temperature, and can operate on dc outputs from 10 to 300 kv.

7516 A CONTROLLED RECTIFIER REGULATOR FOR AIRCRAFT D-C GENERATORS IN 120 C APPLICATIONS by A. L. Wellford (GE); Applic. and Industr., pp. 411-416, Nov. 1960

A controlled rectifier regulator for aircraft D-C generators in 120°C applications is described. Silicon-controlled rectifiers operated in a switching mode were found to meet the necessary qualifications of carrying 8-a average current in temperatures in excess of 120°C. A magnetic-controlled-rectifier switching circuit is used to achieve reliable turn-off of the SCR. This circuit uses the error current from a Zener diode to control the gain of the magnetic amplifier and thereby the switching frequency. The steady state rating for the regulator is 7-a at 120°C and it can supply 8-a at 120°C for one hour.

Tunnel Diode Pulse Power Supply - See 7544

7517 A HIGH-SPEED VOLTAGE-REGULATING AND STATIC EXCITATION SYSTEM FOR A-C AIRCRAFT GENERATORS by H. W. Gayek and A. C. Hupp (GE); Applic. and Industr., pp. 422-426, Nov. 1960

A high-speed voltage-regulating and static excitation system for a 40-kva a-c aircraft generator is described. The excitation power for the generator is derived from the machine itself by means of a current-potential transformer. This excitation is controlled by three magnetic amplifiers connected between the output winding of the CPT and the generator field. The voltage regulator consists of a sensing circuit which produces a direct voltage proportional to the average value of the three line voltages, a transistor preamplifier stage and a magnetic amplifier stage. The system, its principle of operation and performance data are described. The regulator has a notably quick recovery.

7518 CONSTANT CURRENT SUPPLY FOR VERY HIGH RESISTANCE LOADS by R. W. Haisty (Texas Instr.); Rev. Sci. Instr., Vol. 31, pp. 1297-1298, Dec. 1960

A solid-state constant current supply which operates in the current range of 1 to 100 μa with load resistances up to several hundred megohms is described. The system is battery operated, and allows one side of the load resistance to be grounded. The current is controlled by a gallium arsenide photoresistor in series with the load. The load current is balanced against a standard current and the difference is fed to a chopper-amplifier which drives a small lamp focused on the photoresistor. The gain of the amplifier is sufficiently high that a very small unbalance in current will drive the lamp to full output; thus, the photoresistor keeps the load current very near the standard current for any value of load resistance from zero up to the dark resistance of the photoresistor, typically about 8×10^8 ohms.

7519 PRECISE-FREQUENCY POWER GENERATION FROM AN UNREGULATED SHAFT by K. M. Chirgwin, L. J. Stratton and

J.R. Toth (Jack and Heintz); Elect. Engrg., Vol. 79, pp. 1005-1012, Dec. 1960

A system designed to provide precise-frequency power for loads of any power factor from an unregulated generator is described. The system employs a brushless Secsyn generator whose output is formed into the desired wave by a frequency changer employing 18 silicon p-n-p-n switches. Frequencies of 60, 400, 1,600, and possibly 3,200 are feasible with the frequency accuracy the same as that of the reference frequency. System ratings of 20 kva are possible with shaft speeds up to approximately 50,000 rpm, thus allowing the use of light-weight, high-speed generators.

7520 OVERLOAD PROTECTION FOR TRANSISTOR VOLTAGE REGULATORS by A.G. Lloyd (Daven); Electronics, Vol. 33, pp. 56-59, Dec. 23, 1960

Transistorized overload protective circuits for series voltage regulators are described. An extra shut-off transistor reduces output current to zero when the voltage across the series transistor rises above a selected value. The increased series transistor drop triggers a Zener diode and the shut-off transistor saturates, shorting out the series transistor base drive. The circuit remains in this condition until a manual reset switch is thrown. Another method uses automatic pulsing-type short-circuit protection. A constant current prelimiting circuit of resistors and diodes is used. A unijunction transistor pulses continuously. When the unijunction transistor fires, the shut-off transistor is biased off and current-limited output current flows. The low duty cycle of the output current results in low average power dissipation within the supply.

7521 SOME APPLICATIONS OF A TRANSISTOR INVERTOR TO LIGHTING SYSTEM AND SIGNAL UNIT [in Japanese] by T. Kobagashi and D. Suemitsu (Matsushuta Electric Ind.); National Tech. Rep., Vol. 6, pp. 391-396, Dec. 1960

A H-F fluorescent lighting system and a Xenon lamp flashing unit employing transistorized invertors are described. It was found that the H-F lighting system has a higher overall efficiency than that obtainable from operation at commercial frequencies. The application of transistorized converters to Xenon lamp flashing units resulted in reliable operation, easy maintenance, and reduced power dissipation. High lumen output and high light intensity of a flashing signal lamp utilizing Xenon tube promise a wide variety of uses in signalling equipment.

CONTROL

7522 APPLICATIONS OF TRANSFLUXORS TO AN ELECTROMECHANICAL CONTROL SYSTEM by P. Pargas (Log E-tronics); IRE Trans., Vol. IE-7, pp. 1-6, Dec. 1960

A control system which uses multiaperture magnetic cores of the transfluxor type to provide a reliable method of commanding paper advance and auxiliary functions in a photographic printer is described. The transfluxors are operated in a mode which permits larger variations in drive control pulses and which is less sensitive to extraneous signals. Coupling to the mechanical system is done via thyratrons to clutches and relays. Advantages over a purely relay or flip-flop logic for this control purpose are discussed briefly.

Phototransistor Relays - See 7437

Photovoltaic Moiré Fringe System for Machine Tool Control - See 7435

INSTRUMENTATION

7523 A TRANSISTOR-OSCILLATOR LIMIT SWITCH FOR INDICATING AND RECORDING INSTRUMENTS by J.T. Wintermute and S.G. Hayter (Westinghouse); Commun. and Electronics, pp. 518-519, Nov. 1960

A limit switch for indicating and recording instruments which will not restrict the normal operation of the measuring unit is described. The limit switch relay is controlled by the change in current from a transistor-oscillator when a vane connected to the pointer rotates between the mutual inductance coils of the oscillator and thereby turns it off.

7524 DESIGN OF A HIGH ACCURACY EXPANDED SCALE METER USING ZENER DIODES by P.D. King (Pacific Semicon.); Semicon. Prod., pp. 26-28, Nov. 1960

A method of compensating for the nonlinearity of a Zener diode in an expanded scale d-c meter by using an additional series diode is described. Two of these combinations are placed in parallel and are adjusted mechanically to give a linear scale reading. An accuracy of 1.25% has been achieved at both ends of the scale and greater accuracy can be achieved by matching components. The design for an expanded scale a-c meter is also presented.

Measurement of Fractional Nanosecond Pulse Characteristics - See 7496

7525 A TRANSISTOR FREQUENCY METER by F.R. Bretemps and S. Saito (NBS); Electronic Ind., Vol. 19, pp. 196-198, Oct. 1960

A portable transistor frequency meter providing a useful frequency range from 20 kc to 70 Mc is described. A fundamental frequency of 1 Mc is provided from a Pierce Crystal Oscillator. Six transistors are used; they operate from a 1.34v mercury cell. A 1 Mc signal input of 1 millivolt provides a strong tone. The beat frequency of the output for the oscilloscope is about 10 mv and an average of 5 mv is available from 200 kc to 20 Mc.

7526 THE PIONEER I, EXPLORER VI AND PIONEER V HIGH-SENSITIVITY TRANSISTORIZED SEARCH COIL MAGNETOMETER by D.L. Judge, M.G. McLeod and A.R. Sims (Space Tech. Labs.); IRE Trans., Vol. SET-6, pp. 114-121, Sept. - Dec. 1960

A magnetometer designed for the purpose of measuring the distant geomagnetic and interplanetary magnetic fields is described. The sensing element is a coil fixed in the frame of a spinning vehicle. The associated nonlinear amplifier has a dynamic range of approximately three decades and an equivalent noise threshold of 6.0 microgauss. This system has been flown in the Pioneer I, Explorer VI and Pioneer V payloads to detect both absolute magnitude and directional changes in the magnetic field intensity at great distances. The complete unit enclosed in RF shielded container weighs one pound.

7527 MAGNETIC FLUX PATTERN INSTRUMENTATION USING HALL PROBES by H. Hollitscher (GE); Power Appar. Sys.,

No. 5, pp. 915-920, Dec. 1960

Use of the Hall effect to measure magnetic fields at several points at once by maintaining a constant current through the probe is described. This method is of great advantage in that it can measure the magnetic field without integration and both d-c and a-c fields can be measured simultaneously.

Use of a Second Harmonic Phase-Sensitive Detector in a Flux-Gate Magnetometer - See 7488

7528 A SILICON γ-RAY SPECTROMETER by P. E. Gibbons and D. C. Northrop (SERL); Nature, Vol. 188, p. 803(L), Dec. 3, 1960

The performance of spectrometers fabricated by applying ohmic contacts to high resistivity (5,000 ohm cm) p-type silicon is discussed. The ohmic contacts are applied by alloying gold-gallium wire to a boron-diffused surface layer. Devices which detect gamma rays from Co-60 with pulses up to 2 mv and a signal-to-noise ratio greater than 50 at liquid air temperatures have been produced. Often devices have detected 1 Mev γ-radiation and 4 Mev alpha rays at room temperature. Several factors are being investigated in order to produce more uniform devices.

7529 RADIATION TRACKING TRANSDUCER by D. Allen, I. Weiman and J. Winslow (Electro-Optical Sys.); IRE Trans., Vol. I-9, pp. 336-341, Dec. 1960

The photovoltages which result when a semiconductor junction is illuminated by a spot of radiation can be used to produce a radiation tracking transducer capable of detecting the angular position of a light- or radiation-emitting target. The theory is presented, together with results on experimental models, and suggestions for possible uses are given.

7530 REDUCTION OF NOISE IN THERMAL CONDUCTIVITY DETECTORS FOR GAS CHROMATOGRAPHY by R. Kieselbach (du Pont); Analyt. Chem., Vol. 32, pp. 1749-1754, Dec. 1960

The signal from conventional thermistor thermal conductivity detectors in gas chromatographs frequently shows a noise level on the order of 10-20 μv, while the electrical noise level inherent in the (8000-ohm) thermistors is usually about 0.3 μv peak-to-peak. The higher observed noise results from convective heat transfer from the thermistor, from ambient-temperature changes, and from bridge power-supply variations. Techniques for the elimination of noise from these sources are described. Application of these techniques results in a detector whose noise level (0.3 μv) corresponds to about 2×10^{-8} mole of organic vapor per mole of helium ($pQ_0 = 8.7$). A brief description of the electrical measurement circuit is given.

7531 AN IMPROVED SING-AROUND SYSTEM FOR ULTRASONIC VELOCITY MEASUREMENTS by R. L. Forgacs (Ford Motor); IRE Trans., Vol. I-9, pp. 359-367, Dec. 1960

A sing-around system for making measurements of very small changes (few parts in 10^7) in the velocity of ultrasound in samples is described. Fast precision-gating circuitry is employed to select a particular cycle of a particular echo to trigger the transmitter. The time required for precisely 10^3, 10^4, 10^5, or 10^6 sing-around cycles is measured by a unique electronic counting and timing system, with a few parts in 10^7 having been observed. The primary limitation to detecting minute velocity changes is expected to be the accuracy with which compensation may be effected for environmentally induced variation in indicated transit time, other than that due to sample velocity changes. For instance, a sample temperature change of a few tenthousandths degree K produces detectable velocity changes under some conditions.

7532 TRANSISTORIZED BLOCKING OSCILLATOR DISCRIMINATOR AND COINCIDENCE CIRCUIT by M. Feldman (Cornell U.); Rev. Sci. Inst., Vol. 31, pp. 1356-1358, Dec. 1960

A transistorized blocking oscillator discriminator and coincidence circuit for a high counting rate is described. The blocking oscillator discriminator produces a 2-volt pulse into a 100-ohm load and has a sharp and stable threshold. The time jitter for marginal pulses is about 7 nsec and the dead time is about 25 nsec. The discriminator can make pulses of 16 nsec and 0.1 sec duration. The pulses from several blocking oscillator units enter a Rossi coincidence circuit which has several saturated transistors holding the last one off. Only when they all go off together will the last one turn on.

Miniature Transistorized Crystal-Controlled Precision Oscillators - See 7478

OTHER APPLICATIONS OF SOLID STATE DEVICES

7533 SEMICONDUCTOR-MAGNETIC OVERVOLTAGE AND UNDERFREQUENCY PROTECTION CIRCUITS by R. R. Secunde (Jack and Heintz); Applic. and Industr., No. 5, pp. 373-379, Nov. 1960

A 3-phase 400-cycle a-c overvoltage protection circuit and a 3-phase 400-cycle a-c underfrequency protection circuit are described. These two circuits are entirely independent, but can be combined in integrated protection systems. Both circuits consist of a saturable core reactor, Zener diodes and other solid state devices. The overvoltage device isolates the damageable parts of the system when there is overvoltage for a certain time which is inversely proportional to the overvoltage. The underfrequency device isolates damageable parts of the system when the frequency drops below a set minimum. Both of these circuits were designed for aircraft and have a sense of limits condition within ±1 or 2% over temperature ranges from -55 to +120 C and up to 70,000 feet of altitude.

Analysis of Radiation-Powered Thermoelectric Generators - See 7440

NEW PRODUCTS

7534 SODIUM FLUORIDE SINGLE CRYSTALS (Semi-Elements, Inc., Saxonburg Boulevard, Saxonburg, Pa.)

The availability of sodium fluoride single crystals is announced. The crystals transmit in about the same region as calcium fluoride and lithium fluoride and are of considerable value in cases

where an extremely low refractive index is needed. The material may be easily evaporated as a thin film and can be used for reflection reducing coatings.

7535 TEMPERATURE COMPENSATED ZENER DIODE (Motorola Semiconductor Products Inc., 5005 E. McDowell Rd., Phoenix, Arizona)

An extremely low dyanamic impedance 6.2 volt temperature-compensated zener diode, type 1N821A, is announced. The low dynamic impedance of the device, typically 8 ohms, minimizes voltage fluctuations due to changes in current. The device is designed for ultra-stable reference applications in digital voltmeters, precision high-stability oscillators, analog to digital converters, and similar industrial applications. Two 8.4 volt temperature-compensated diodes, types 1N3154 and 1N3154A are also available. Both series of units are housed in small axial lead 400 mw glass package.

7536 SILICON POWER TRANSISTOR (Westinghouse Electric Corp., Semiconductor Dept., Youngwood, Pa.)

A family of developmental n-p-n silicon power transistors is announced. The devices have a maximum collector current of 30 a, maximum collector to emitter voltage of 200 v, and a maximum power dissipation of 250 w. The devices, which are packaged in a hermetically sealed double-ended case of ceramic construction, exhibit extremely low saturation resistance and low thermal impedance.

7537 SILICON CONTROLLED SWITCH (Solid State Products, Inc., 1 Pingree St., Salem, Mass.)

High sensitivity silicon controlled switch series 2N884-2N889 is announced. The devices offer precise firing control (within ±0.08 v), ultra-high sensitivity (20 μa firing), and surge capability to 10 a. The devices make possible miniaturization of squib firing circuits with no sacrifice in design margin. Their low 1 ma holding current level makes them particularly useful in programming, control, and logic applications. The units are available in the miniature TO-18 case.

7538 FERRITE ISOLATOR (Sylvania Electric Products Inc., Mountain View, Calif.)

The type FD-1537 coaxial ferrite isolator is announced. In the frequency range 1.0 to 2.0 kMc the unit provides minimum isolation of 10 db, maximum insertion loss of 1.2 db, and maximum VSWR (input and output) of 1.2. The broadband, high-performance isolator is employed primarily for test bench applications. It can be used to reduce the VSWR presented by a load or antenna and to eliminate anomalies in oscillator output caused by long line effects.

7539 MECHANICAL FILTERS WITH FERRITE TRANSDUCERS (Collins Radio Co., 2700 W. Olive, Burbank, Calif.)

Filters which feature a reduction of transmission loss to 4-5 db and passband ripple to 1.5 db or less are announced. The filters utilize ferrite magnetostrictive transducers rather than the usual nickel alloy rods. The filters can be used in missle guidance and telemetering systems and in other applications which encounter severe environmental conditions such as shock and vibration.

7540 LASERS (International Business Machines Corp., 590 Madison Ave., New York 22, N.Y.)

Optical masers which can continuously generate coherent light both in the visible and the infrared regions with about 1/500 th the amount of power required by the ruby optical maser are announced. Both masers utilize calcium fluoride. In the maser which emits red light at 0.708 microns, one-tenth of one per cent of the calcium ions are replaced by divalent samarium ions. In the other, which emits infrared radiation at 2.5 microns, trivalent uranium ions replace one-tenth of one per cent of the calcium ions. The uranium and samarium ions permit the continuous generation of coherent light because they overcome the limitations of ruby as an optical maser material.

7541 TRANSISTOR RADIO CIRCUIT TESTER (Philco Corp., Tioga and "C" Streets, Philadelphia 34, Pa.)

TRACE, a testing device which automatically guides a radio serviceman in pinpointing faulty circuits and components in a transistor radio, is announced. The device is a rigid plastic panel, a facsimile of the actual radio circuitry, that aligns with the radio printed circuit chassis panel. With the TRACE panel in place over the circuit to be tested, a technician uses a signal generator to inject a signal of the correct frequency at indicated test points. The frequency and type of signal to be used is indicated by color-coded signal paths on the panel. A faulty stage is determined by a change of the sound emitted by the speaker.

7542 HEARING AID (Otarion Listener Corp., Ossining, N.Y.)

A subminiature transistorized hearing aid is announced. The aid fits flush with the ear, is invisible on the wearer from front or back, has no external parts, and weighs only 3/8 ounces. The unit has sufficient gain and power to help those with a hearing loss as high as 50 db.

7543 CRYOGENIC MEMORY PLANE (International Business Machines Corp., 590 Madison Ave., New York 22, N.Y.)

A cryogenic thin film memory plane the size of a postage stamp is announced. The memory, which consists of 135 cryotrons in 19 layers of material, is automatically fabricated. Three crossed-film cryotrons in combination with a persistent current loop make up a basic storage cell. Since this cell combines storage with logic, sophisticated operations not previously possible can be realized. For example, an "associative memory" which simultaneously searches all memory compartments and consequently speeds access to stored information is possible.

7544 TUNNEL DIODE GENERATOR SUPPLY (Straza Industries, Greenfield Dr., El Cajon, Calif.)

The model PS-2001, a compact tunnel diode generator supply which provides pulsed outputs in a variety of pulse and regulated d-c combinations, is announced. The power supply can be used for programming tunnel diode or parametron logic networks as well as for general power supply applications. The output pulses are phase locked to either an external or internal clock which is variable from 500 kc to 2 Mc. Pulse amplitudes can be varied simultaneously from 0 to 1 volt at 100 ma.

SUBJECT INDEX

CONFERENCE PROGRAMS ABSTRACTED

in SOLID STATE ABSTRACTS, Vol. I, No. 5

Properties of Elemental and Compound Semiconductors Conference, Boston, Mass., Aug. 31 - Sept. 2, 1959 (Properties of Elemental and Compound Semicon. Conf.)

Sixth Conference on Magnetism and Magnetic Materials, Nov. 14-17, 1960, New York, N.Y. (Sixth Conf. Magnetism and Magnetic Materials)

1960 National Electronics Conference, Chicago, Ill., Oct. 10-12, 1960 (Proc. 1960 Natl. Electronics Conf.)

1960 Thanksgiving Meeting of the American Physical Society, Chicago, Ill., Nov. 25-26, 1960 (Bull. Am. Phys. Soc., Ser. II, Vol. 5, Nov. 25, 1960)

AUTHOR INDEX

FOR SURFACE STUDIES

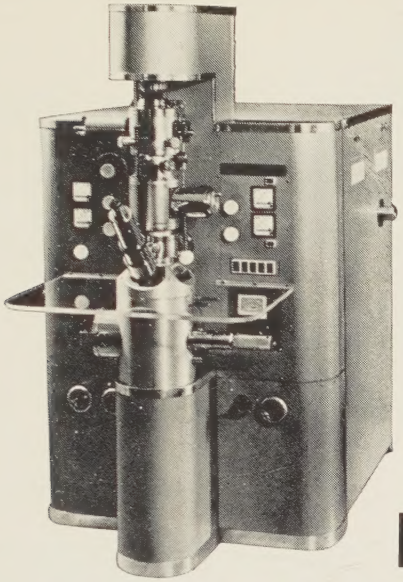

KE1

Trüb, Täuber Secondary Electron Emission Microscope

for direct viewing of metallic and semiconducting specimens by means of secondary electrons released from ion bombardment of the surface — featuring . . .

- Images free of distortion and deformation
- Enlargement up to 1500 X electronoptically
- Resolution 500–600Å
- Object temperature 150°–800° C
- Observable surface of the object 25 mm square
- Differentiation of the material

The Instrument Includes . . .

Electrostatic immersion objective
Ion beam system
Revolving contrast diaphragms
2 electromagnetic projectors
Observation chamber with fluorescent image screen
Recording chamber with plate cassette
High-intensity optical microscope
All-metal housing with vacuum equipment including diffusion pump
High-voltage equipment for 45 kV
Measuring instruments and control equipment

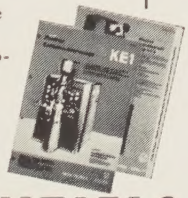

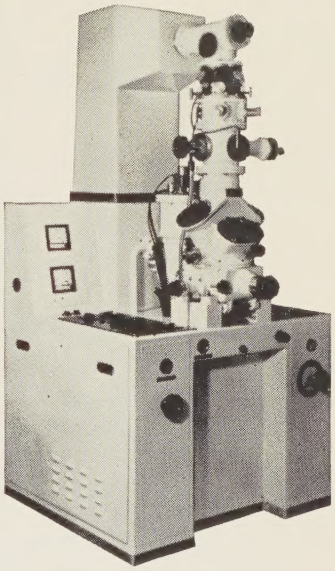

KD3

Trüb, Täuber Electron Diffractograph

for determining the crystalline structure of surfaces, thin layers, and extremely small quantities of material, including dynamic processes — featuring . . .

- Cold-cathode electron gun with practically unlimited life
- Simple design — dependable operation, extreme flexibility
- Balanced optical system
- High resolving power
- Large variety of specimen holders for various methods of investigation
- Devices for heating and cooling the test specimens (from liquid nitrogen to 1000°C)
- Devices for discharging, etching, surface evaporating
- Various cameras for photographic recording on plates and films
- Unique kinematic recorder

Specifications

Acceleration Voltage —	
continuously adjustable:	10 to 50 kV
ripple (fractional):	$\approx 10^{-4}$
stability:	$\pm 0.1\%$
Final vacuum:	approx. 2×10^{-5} mm Hg
Magnification with electronic lens:	75X
Minimum line width:	0.001 mm
Minimum diameter of beam for focussing on specimen, without additional diaphragms:	4μ

Distributed by:

NEW ENGLAND SCIENTIFIC INSTRUMENTS CO.

238 MAIN STREET • CAMBRIDGE 42, MASSACHUSETTS • KIrkland 7-1997

Electron Microscopes • Nuclear Induction Spectrographs • High Voltage Oscillographs • Precision Laboratory Instruments • Nuclear Track Microscopes